DISSERTATION

FROM THE OVINE TO HUMAN ROTATOR CUFF;

TENOCYTE AS TO MSC DERIVED EXOSOMES FOR TENDON HEALING

Submitted by

Devin P. von Stade

Department of Microbiology, Immunology and Pathology

In partial fulfillment of the requirements

For the Degree of Doctor of Philosophy

Colorado State University

Fort Collins, Colorado

Summer 2024

Doctoral Committee:

Advisor: Daniel Regan
Co-Advisor: Kirk McGilvray

Kelly Santangelo
Fiona Hollinshead

ABSTRACT

FROM THE OVINE TO HUMAN ROTATOR CUFF;
TENOCYTE AS TO MSC DERIVED EXOSOMES FOR TENDON HEALING

Tendinopathies comprise one of the most widespread and economically significant diseases in developed nations. The societal value of rotator cuff tear surgical intervention alone has been estimated at greater than 3.4 billion US dollars despite frequent repair failures (30-79%). This drives great interest in adjunct therapies; however, research is complicated by a limited understanding of the underlying pathogenesis. Recent data suggests that the primary driver is cell-to-cell communication during the acute and chronic stages of rotator cuff tears. Most notably, the paracrine signaling of macrophages, which are preferentially recruited earlier and persist longer than other immune cells, may direct the structural function of injured tendons. Extracellular vesicles (EVs) are the primary contributors to the paracrine signaling responsible for many successful cell therapy studies. Investigations into mesenchymal stromal cell (MSC) derived EVs have served as a launching point toward this end, however, cell origin can dramatically change the effect of EVs on target cells. To explore the effects of exosomes as a function of cell source on tendon healing, we have developed in vitro models in human and ovine cell lines to test the effects of tissue native, tenocyte derived EVs as they compare to MSC derived EVs on key effectors of rotator cuff tears, tenocytes and macrophages. The goal of this work is to (a) describe the direct effect of EV education, as a function of cell source, MSC vs tenocyte, on macrophage gene regulation and cytokine production and tenocyte bioactivity; (b) to then assess the indirect effects of such EV educated macrophages on tenocyte bioactivity. (c) Additionally, the underlying pathogenesis of tendinopathy and the animal models of rotator cuff tears we use will be explored and further defined in the context of contemporary histologic and biomechanical methods.

ACKNOWLEDGEMENTS

I must give thanks for my loving family, especially my wonderful wife who has been my rock through this since the beginning. Also, my son and daughter who helped motivate me to finish this endeavor, and our loving dog who solidified my sanity through it all. My parents, siblings, and their families for accepting that I wanted to go to school for an indeterminable amount of time, and especially my mother for always lending an ear when needed.

For my primary advisors: Kirk, I will be forever grateful that you were willing to take on an interdisciplinary endeavor like this, mentoring someone from another department entirely. Your guidance and mentorship were invaluable. Dan you not only served as a mentor in terms of making it through a program of study like this, but as an example of how to balance one's family life with it showing me what more I can do.

My mentors and committee, Gary, Kelly, and Fiona: you all supported me on this journey, be it through advice, kind words or needed critiques. Thank you.

The many fellow students that helped me along the way, especially Jimmy, for spending 2 years on call for samples with me, the late nights of dissection and all the other times. Also, Sam, for looping me into fun studies and joining me in the wild pursuit of 3d printed microscope mods.

Cecily and Tia, you were both invaluable in your histology and general practical expertise. You were also great friends. Thank you for all the parenting guidance you didn't realize you had passed along Cecily and Tia for joining me in my pursuit of new microscopy techniques.

There are many more I should thank, like Ben for your industry insights, and another Ben for sharing an approach to residency and life/family-work balance in addition to the many peers and students… but I will leave it there. In the words of my father:

"Learn Lots"

TABLE OF CONTENTS

CHAPTER 1: ROTATOR CUFF TENDINOPATHY AND THE OVINE MODEL

1.1: Overview

The rotator cuff is a group of four tendons, the supraspinatus, infraspinatus, teres minor and subscapularis, that insert onto the humeral head and are contiguous with the glenohumeral joint capsule (Figure 1.1). These tendons are responsible for both stability and mobility of the shoulder joint and injury to these tendons is common, with 18.5% of the general population demonstrating at least partial tears at post-mortem screening to 54% of those over 60 years old having tears on magnetic resonance imaging [1,2]. These injuries result in joint instability, loss of mobility and pain. Tendinopathy is the degenerative condition of these tendons in response to single or repeat injury resulting in irrevocable damage. The pathogenesis of this disease has not been fully elucidated; however, many recent advancements have been made as a new gold standard large animal model has allowed for increased translatability of the experimental condition. The overarching goals of this chapter are to: (1) characterize tendon from the molecular to functional length scales as it (2) relates back to the diseased state and (3) the ovine model of rotator cuff tendinopathy. (4) Exosomes as they relate to this disease and its treatment will also be characterized and discussed. This background information not only establishes the rationale for the global hypothesis that tissue-native, tenocyte derived exosomes will preferentially stimulate positive metrics of tendon healing as compared to MSC derived, but also why we use an ovine invitro model in Chapter 2. This background information is also critical to contextualize the results of

Chapter 2 and 3 in the deceptively complex process of tendon repair, and how this can be further elucidated using the future directions discussed in Chapter 4.

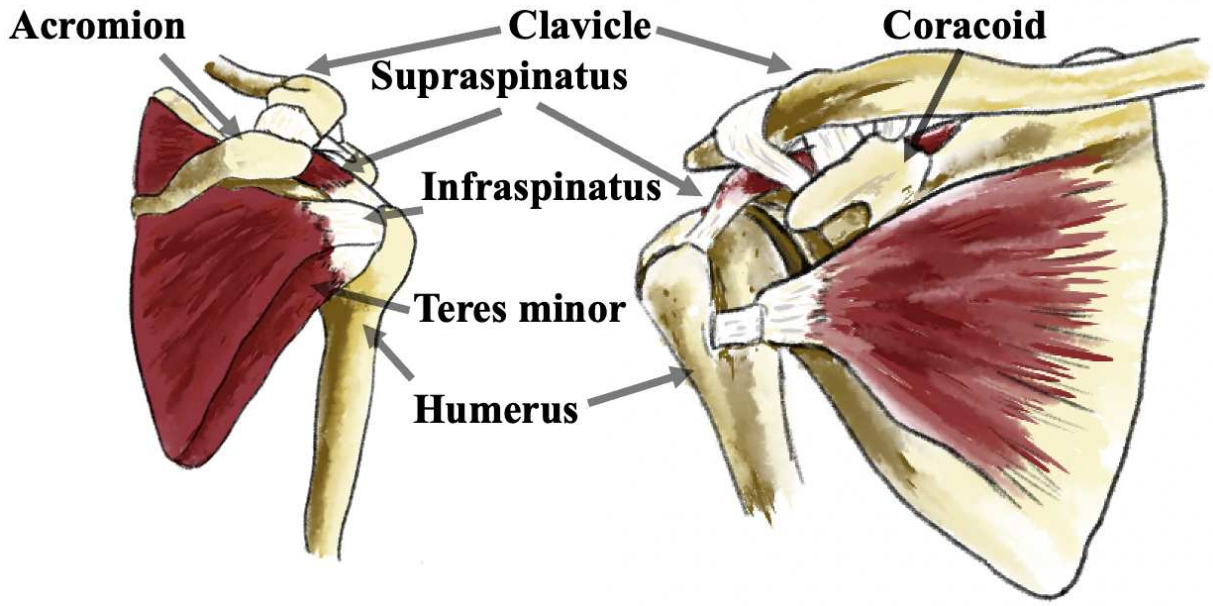

Figure 1.1. The human rotator cuff is defined by 4 tendons coming from the supraspinatus, infraspinatus, teres minor and subscapular muscles, all inserting onto the humerus in some ways contiguous with the glenohumeral joint capsule. These tendons, especially the supraspinatus pass through ligamentous and boney restrictive spaces, including by the acromion and coracoid processes, especially when the full range of motion of the shoulder is considered.

1.2: Introduction

At the societal level, the value of rotator cuff tear (RCT) surgical intervention alone has been estimated at greater than 3.4 billion US dollars (USD). This socioeconomic value is despite frequent repair failures (30-79%) resulting in greater than 430 million USD in annual costs in the United States[1,3-6]. Though one may think of rotator cuff tears as a disease of professional athletes, people are at greater risk of it in their daily lives than many realize. Some intrinsic risk factors include age, obesity, osteoporosis, diabetes, and family history, while extrinsic factors can include common spontaneous activities such as spring cleaning, painting a wall or starting a new sport, or overuse through repetitive movements or poor workplace ergonomics [1,7,8]. These tears can then

progress into rotator cuff tendinopathy, the degenerative cascade that represents a scarred tissue incapable of complete remodeling (Figure 1.3)[9].

Though the pathogenesis of rotator cuff tendinopathy has not been fully elucidated, current research is rapidly expanding our understanding of this multifactorial process. The crux of tendinopathy is that mature tendons do not heal, they scar[9]. This is thought to hinge on the fundamental organizational hierarchy of tendon and its lack of substantial remodeling under normal physiologic conditions. Once individual collagen fibers mature, they have been found to span the full length of the tendon to effectively confer their strength and resilience and being comprised of >95% type 1 collagen, they are expected to last the life of the individual, with minimal to no molecular turnover [10-12].

Additionally, at sites of injury, the majority cell type is rapidly shifted from native tendon fibroblasts (tenocytes) to infiltrating cells, especially macrophages, but also other inflammatory cells (neutrophils, and lymphocytes primarily), and stromal fibroblasts in the acute phases, and progression to include neovascularization and neoinnervation in the chronic condition [7,9,13,14]. This significant shift in cell population dynamics in the tendon microenvironment and the resulted intercellular communication is thought to drive tendinopathy [9,15,16].

Because the functional unit of the tendon extends its full length, and its study requires ex-vivo methods, we are limited in our study of human tendon to biopsies of sub-function-unit size, primarily of severely disease tendon, when injury and tendinopathy has progressed to the point indicating surgical intervention, or after death, driving a strict need for animal models. While many small animal models exist, the translatability of these models is severely limited by their size and physiology. This is especially true for the investigation of surgical interventions and subsequent

adjunct therapies. Thus, the ovine model of rotator cuff tendinopathy fills a much-needed niche and has arisen as the gold standard large animal model of the human condition[17,18].

1.3 Tendon, Structure to Function

Tendon is a paucicellular, variably elastic tissue that transmits force from muscle to bone. In health it is primarily comprised of collagen type 1 (col1) arranged into a highly organized hierarchy of fibrils within fibers within fascicles or bundles (Figure 1.2)[19]. These molecules are arranged in a triple helix, the chirality of which is mirrored at subsequent length scale from the trimeric col1 to fibril and sometimes extending to the fiber level, going from right- to left-handed etc., similar to traditional rope making[12,20,21]. This not only confers great tensile resilience, but great molecular stability[12,20,21]. Once incorporated into a fibril, their break down necessitates enzymatic access that is not available while molecules are in this counter-wound conformation, and indeed, the ability for enzymatic access is further decreased under tension, which reduces potential pore sizes in the fibril[10,20]. This contrasts with the interfascicular col1 for which there is more ready access due to the lack of fibrillar incorporation and tensile strain[10,20]. This is in part due to col1's self-assembling tendency, as well as extensive enzymatic and non-enzymatic post translational modifications[19,20,22].

At translation, Col1 molecules are in their pre-pro-α-polypeptide chain form, at which point they undergo hydroxylation of the proline and lysine residues[22]. Then, disulfide bonds are formed to assemble the initial triple helix of the pro-collagen molecule within a vesicle for transported to the ECM[22]. In the ECM, the C- and N- terminals are enzymatically cleaved to form tropocollagen which undergoes further hydroxylation, forming reactive aldehyde species that spontaneously cross link with those of other collagen molecules, such as collagen types 4 and 5, to organize, form or expand upon collagen fibrils[20,22,23]. When a third residue, generally from

another collagen molecule, is additionally bound at this site, the chemical crosslink matures, forming a trivalent bond[22]. Col1 is the molecular foundation of tendon's tensile strength as these fibrils span the full length of the tendon and under mechanical load demonstrate stretching at the molecular level (Figure 1.2)[12,22,24]. These mechanical properties are further modified by other intra and inter fibrillar matrix compounds, including other collagens, elastin, decorin, aggrecan and other proteoglycans. These generally act to manage fibrillar organization and arrangement, to add elasticity and or modulate compressive forces, which are particularly high where tendon arcs over bone, acting as a pulley.

This matrix is most striking at the enthesis, where the tendon inserts into the bone (Figure 1.6). This is perhaps the most mechanically fine-tuned portion of the tendon interfascicular matrix as it is the most abrupt transition from an elastic tissue (tendon) to a relatively stiff tissue (bone) [25,26]. If this transition did not provide a mechanical gradient, it would culminate too much strain and form a weak point, ready for rupture, especially given the dynamic nature of the joint and thus the various angles of the force that pass through the enthesis[25,26]. Here the continuous fibers of the tendon extend into the humeral bone, often as what are called Sharpey fibers, anchoring the tissues together and finalizing this transfer of force[27]. The enthesial matrix is considered to undergo a gradual transition from tendon to non-mineralized fibrocartilage, to mineralized fibrocartilage and finally to mature bone[25,28]. Within the enthesis there are a specialized set of embryologically distinct, tenocyte like cells that maintain the ECM. These cells are morphologically distinct, having more cytoplasm, their profile being more rounded and often are within lacunae, similar to chondrocytes and reflective of their function and origin, as they maintain and matrix with more proteoglycan content than the main tendon body, and progresses to a mineralized state[25,27,28].

In the tendon body, the fibrous bundles or fascicles are joined by an interfascicular matrix, which is a looser matrix of reticular fibers, proteoglycans, and other compounds that allow for sliding between bundles and for the trace vessels, nerves and telocytes to maintain tendon reflexes and homeostasis[29,30]. This is also where resident tendon stem cells are found, including at the epitenon, the outer lining of the tendon where they may be most abundant [31]. The interfascicular matrix is further maintained by a network of tenocytes, with long reaching processes that form tight junctions, which allow for direct, cell-cell communication and thus, coordinated maintenance of the ECM[15,16]. Mature tenocytes are characterized by expression of tenomodulin (TNMD), Col1, Thrombospondin 4 (THSB4), tenascin C (TNC) and early growth response protein 2 (EGR2), that in culture may additionally express scleraxis (SCX)[31].

In health, these tenocytes are peripheral circadian cells and over the course of the day will modify the intrafascicular matrix resulting in very small levels of col1 turnover contributing to a continuous maintenance and maturation of the tendon's core mechanical function[10,11]. While <5% of col1 is expected to undergo molecular turnover throughout an individual's life, the over time this maturation of the tendon is characterized by thickening of some fibers leading to fiber diameter heterogeneity as well as gradual loss of tenocyte-tenocyte processes[15,16]. This maturation is thought to contribute to the susceptibility of tendons to tendinopathy[10,32].

The interfascicular tenocytes and their production of non-col1 components of the interfascicular matrix are accompanied influenced by other resident cells, especially macrophages, to aid in the maintenance of this instructive tissue[33]. This matrix informs the tendon fibril arrangement, elasticity and dynamic mechanical functions by altering hydration and friction[20]. Some examples include collagen type 3 (col3), the second most abundant collagen in tendon, which aides in defining fibril size and providing a reticular framework for the interfascicular matrix

[20,23]. Collagen type 2 may be present in parts of the tendon that undergo significant sheer and compressive forces, such as discrete parts of the enthesis[23,28]. Collagen type 5 is a smaller collagen that is thought to aid in fibrillogenesis along with collagen type 4 and is often located at the core of col1 fibrils[20,23]. Collagen type 6 tends to be in the pericellular matrix and may play a role in col1 post translational modification[20,23]. Collagen types 12 and 14 may act as bridges between col1 and other parts of the matrix further guiding fiber formation[20,23].

Non-fibrous proteins also play a significant role in this matrix, the most abundant of which are proteoglycans, especially small leucine rich proteoglycans (SLRPs), such as decorin, fibromodulin, lumican and biglycan[20,28]. These SLRPs are a subclass of glycoproteins, which have negatively charged, hydrophilic, polysaccharide side chains attached to a leucine rich protein core. This chemical quality has long provided a unique histologic staining character, which has defined several metrics of histologic tendon evaluation[14]. Physiologically these SLRPs can bind to collagen fibrils at specific sites and play a role in both early and late fibrillogenesis and in fibril crosslinking and sliding[20,24]. Similar to these, glycoproteins are characterized by hydrophilic carbohydrate groups attached to their polypeptide core. Of note cartilage oligomeric matrix protein (COMP) is found within the fibrillar matrix only, can bind up to 5 collagen molecules and is associated with fibrillar maturity[20,23].

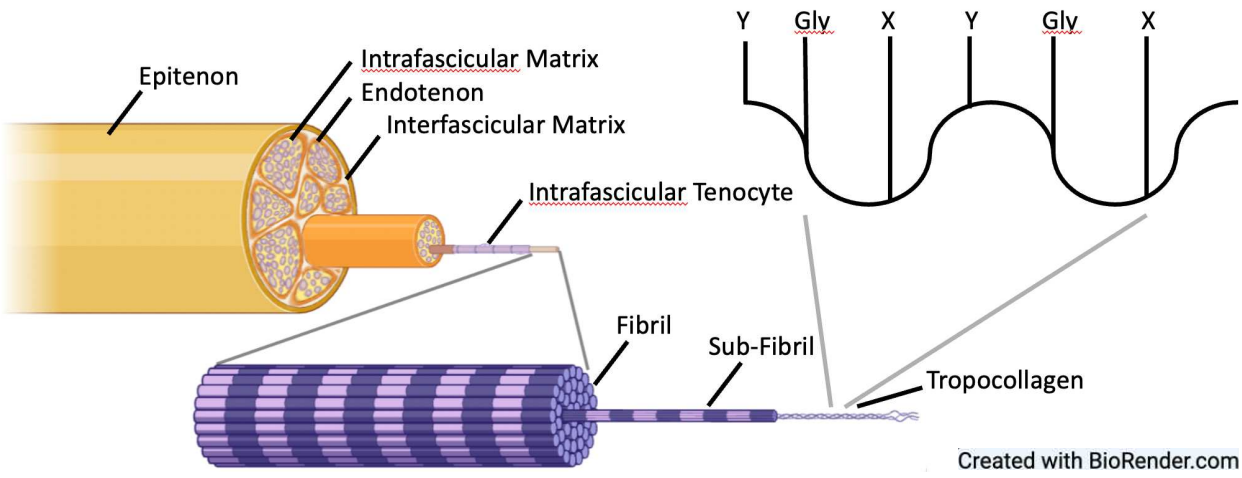

Figure 1.2. A diagram of the basic levels of Col1 organization of the tendon. At the outermost layer of the tendon is the epitenon (scale mm to cm). This is a specialized part of the interfascicular matrix that interacts with the tendon sheath and surrounding fascia. It is often vascularized and has an abundance of tendon stem cells. The Interfascicular matrix supports the fascicles, allowing for gliding, directing organization, and supplying vasculature and neural input. The fascicles are surrounded by the endotenon, acting similar to the epitenon, this fascicular lining houses numerous stem cells and interacts directly with the interfascicular matrix (these are at the um to mm scale). These spaces are filled with the specialized intrafascicular matrix and its supporting intrafascicular tenocytes which maintain the fibrils that span the length of the tendon and convey its mechanical resilience (10s to 100s of nm in diameter). These fibrils may be made up of fibrillar subunits which are in turn comprised of tropocollagen, triple helical molecules arranged in regularly spaced series of five molecules whose rotation is contrary to the individual tropocollagens and where the molecular spacing forms regular banding on transmission electron microscopy due to 5 vs 4 overlapping in a given cross section. Each alpha helix of the tropocollagen is arranged in a simple helix thanks to the repeating amino acid motif of glycine-X-Y, where X and Y are often proline or hydroxyproline, and glycine, the smallest of the amino acids, acts a pivot point and internal hub or backbone of the helical structure as it matures into tropocollagen.

1.4 Tendinopathy

While the collagen fibrils of a tendon are anticipated to last a lifetime, they undergo a mechanically dynamic existence. When running, it is estimated that the Achilles tendon undergoes forces of up to 12.5 (9kN) times an individual's body weight[34]. It's in these more extreme examples of tendon loading that the function of the tendon to elastically store and return energy, be it into a stride or into a pitch, is truly realized; however, it is also why certain tendons are at such great risk

of injury. Of the over 600 tendons in the human body, the rotator cuff is the most often affected by tendinopathy (Figure 1.3)[7].

While the discrete pathogenesis of tendinopathy remains obfuscated, there are well established metrics that are used at different length scales to characterize and define the disease state. Many of these features are also consistent with acute and chronic tears, which are indeed thought to contribute to the formation and propagation of tendinopathy thus the overlap in use of these terms. Clinical assessment of rotator cuff tendinopathy is based on clinical evaluation of range of motion, strength and patient history in conjunction with diagnostic imaging[1]. Imaging may start with radiographic and ultrasonographic assessment but generally progresses to magnetic resonance imaging for refined characterization prior to and for planning of surgical intervention when indicated[1,35].

At the mechanical level, tendinopathy results in reduced strength represented by increased percent relaxation under cyclic loading and decreased stress as well as decreased maximal force before failure[7,17,36]. At the submicroscopic level this represents increased fibril fragmentation, larger numbers of small fibrils and decreased organization[12,24]. Microscopically there is decreased collagen alignment progressing to loss of distinction of fascicles from the interfascicular matrix, reflected in increased presence of type 3 collagen fibers and proteoglycan content (Figures 1.4-1.5)[13,14]. There is marked increase in cellularity including tenocyte proliferation, stromal fibroblast proliferation, inflammatory cell infiltration, neovascularization and neoinnervation[13,14]. Of the inflammatory infiltrates, macrophages tend to infiltrate early in the acute phase and preferentially persist longer than other cell types[37]. Tenocyte proliferation and associated activation can progress to metaplastic transformation to fibrocartilage and even bone[9,38]. These metaplastic changes not only worsen tissue mechanics but can drive clinical pain[26,38].

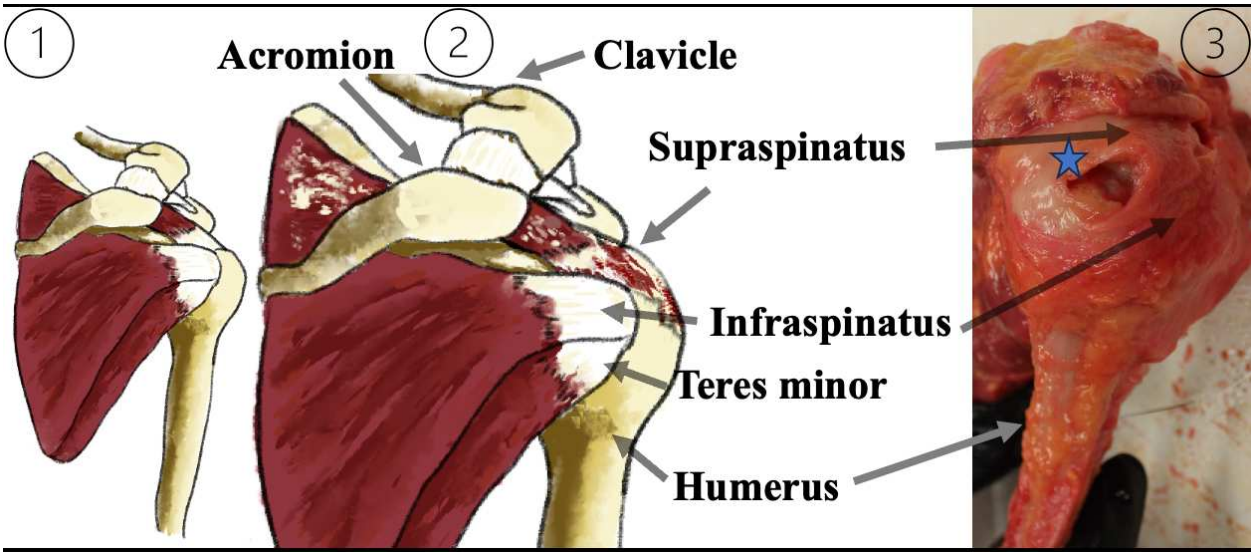

Figure 1.3. The progression of tendinopathy from (health) to disease (2&3) first results in thickening and swelling of the affected tendon. This is due to increased vascularity and disorganized matrix forming a scar tissue. This is often can often be observed extending over the enthesis as vessels spread from the joint capsule and around the periosteum, and/or from the myotendinous junction. These findings are often accompanied by fatty degeneration of the associated muscle. Through acute strain tear or gradual disease progression, tendinopathy may result in complete detachment in the case of affected supraspinatus tendon. As seen in the joint capsule defect here (blue star), where 2cm of the supraspinatus insertion has released, retracted and fibrosed over. Photo of a fresh, non-frozen cadaveric specimen[39].

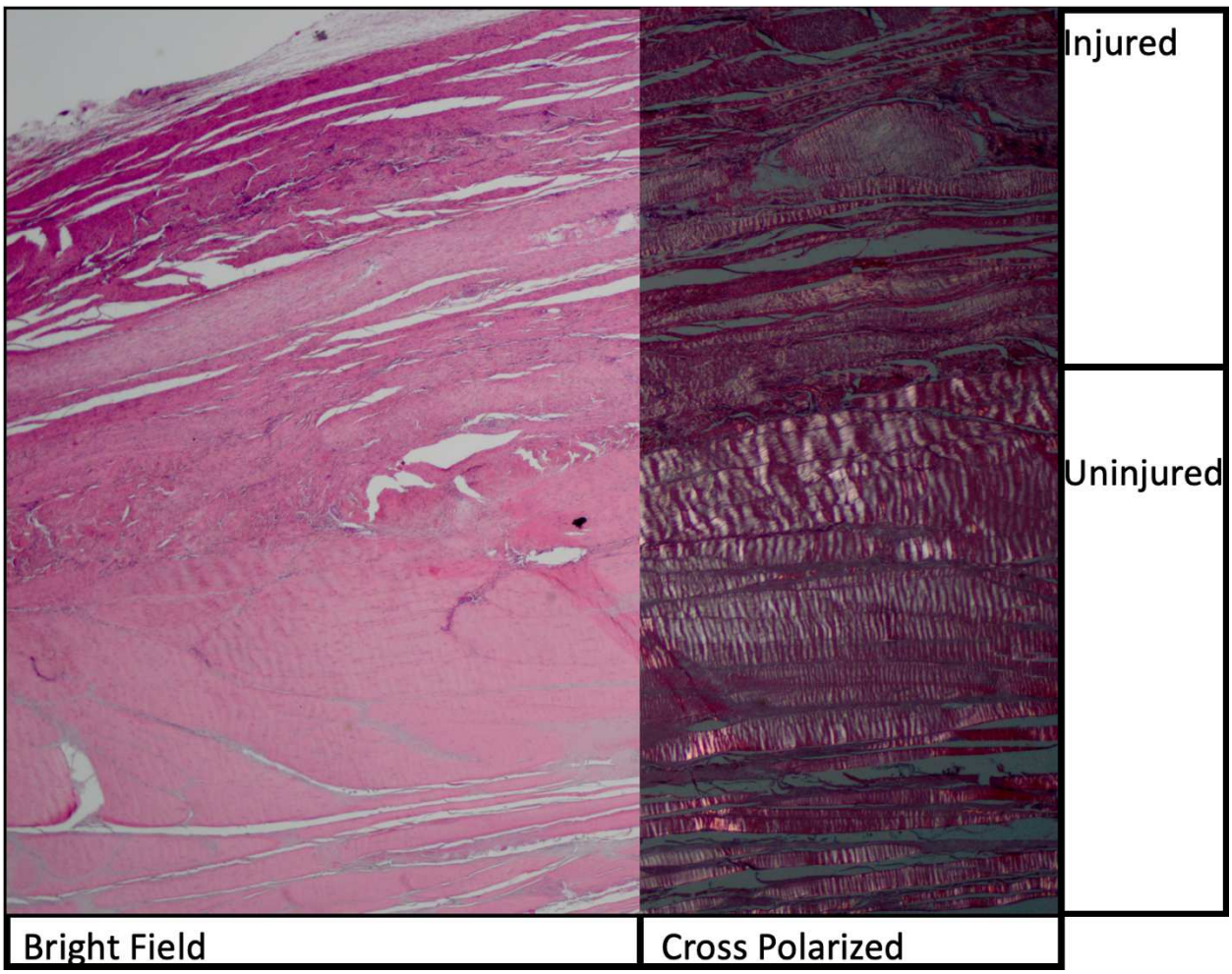

Figure 1.4. Sub-gross imaging of the ovine tendon following injury to the superficial (upper) third of the tendon as described in the sharp transection ovine model[18]. The lower 2/3 of the tendon that is uninjured demonstrates thick fascicles with scant interfascicular matrix characteristic of mature tendon. These fascicles are smaller and variably disrupted in the upper 1/3. Additionally, using cross polarized light microscopy, the regular fascicular crimping pattern is demonstrated in the alternating light and dark banding, which is finer, dimmer and much less regular in the injured 1/3. Samples are formalin fixed, demineralized, 10um sections stained with hematoxylin and eosin.

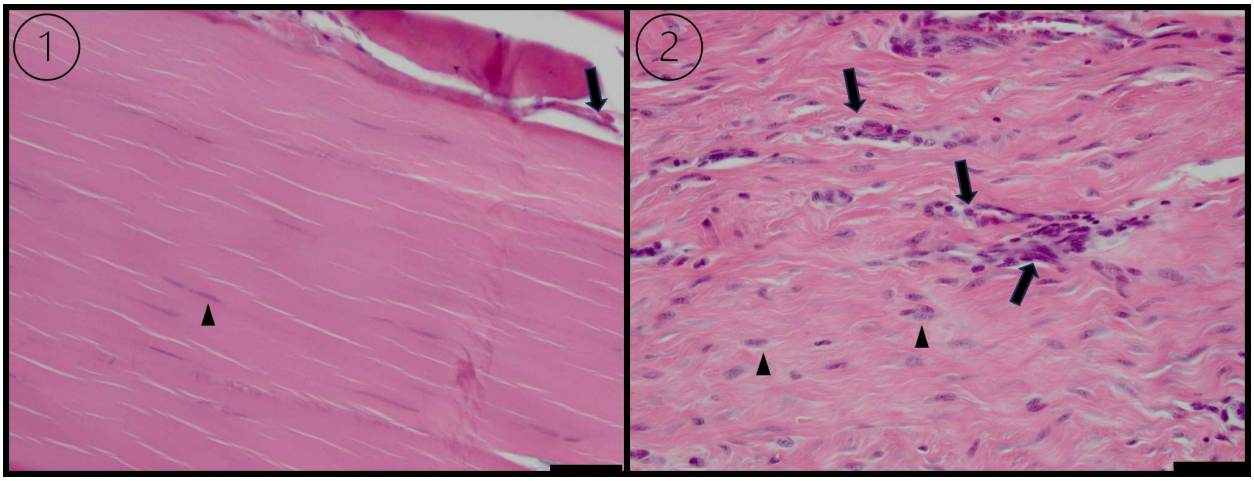

Figure 1.5. Representative photomicrographs of ovine tendon in health (1) and in the chronic model of tendinopathy (2)[17]. At this higher power we can see the organized, dense interfascicular matrix of healthy tendon with thin, ovoid tenocyte nuclei (arrowhead) barely visible within the fascicle and a complete absence of interfascicular vessels. One small vessel is appreciated at the edge of the section (arrow). This is as compared to in chronic tendinopathy (2) where numerous vessels (arrows) are appreciated within a looser, more disorganized collagenous matrix with numerous tenocytes having rounded, larger (active) nuclei, trace cytoplasm. Additionally, there is often associated increased blue-purple matrix staining of the tenocyte-adjacent ECM characteristic for increased glycosaminoglycan content. Immune cells, primarily macrophages, frequently infiltrated the peri-vascular matrix in low numbers. Samples are formalin fixed, demineralized, 10um sections stained with hematoxylin and eosin. Scale Bars represent 50um.

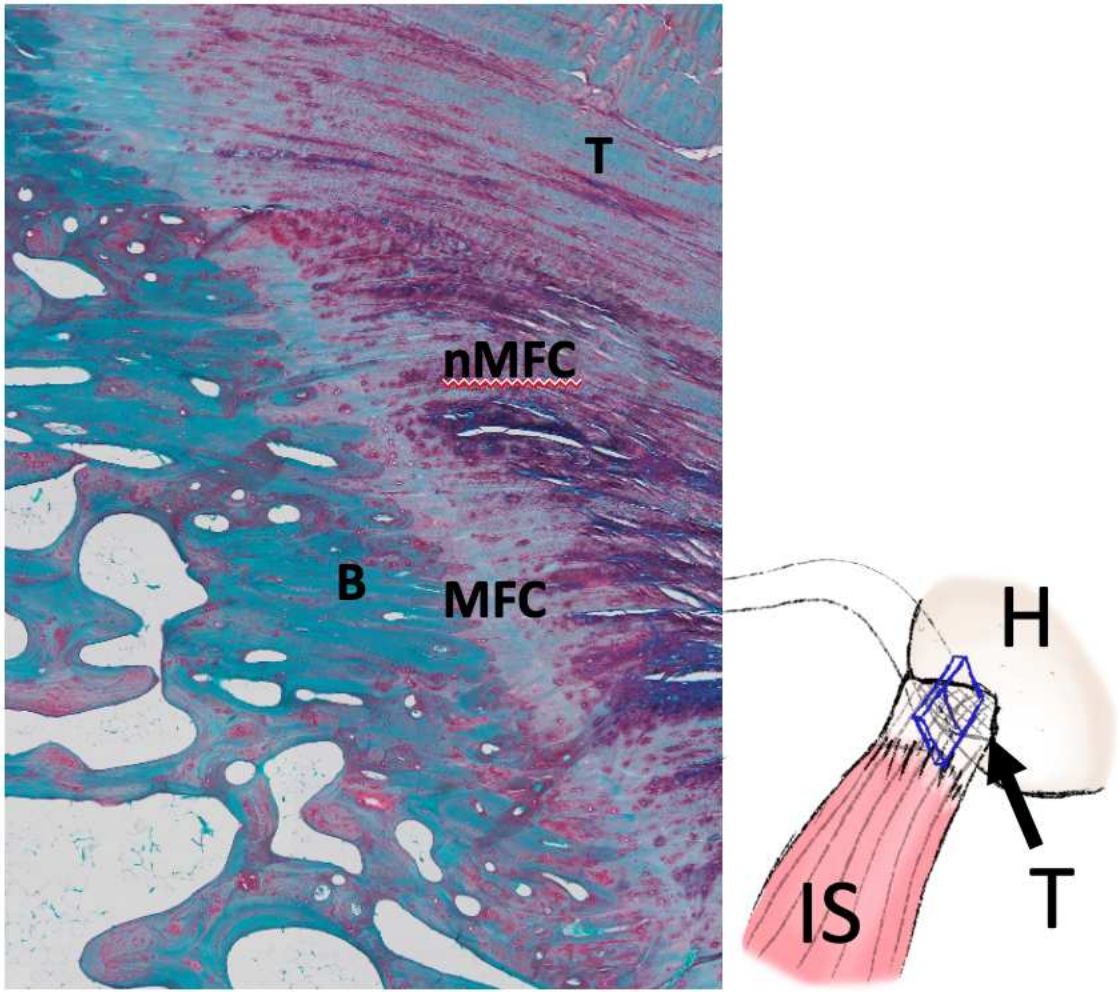

Figure 1.6. The ovine enthesis is especially well demonstrated using special stains, in this case a modified trichrome method called the RGB trichrome stain[40]. This demonstrates the delineation from bone (B) to mineralized fibrocartilage (MFC) to non-mineralized fibrocartilage (nMFC) to Tendon (T) throughout which there is prominent interdigitation. To the right is a diagram of where the tissue cross section (blue box) this represents, where the infraspinatus (IS) inserts onto the humerus (H). This is a classic orientation for histologic assessment as it tracks along the collagen fibers allowing visualization of the fascicular crimping as well as the morphologic changes present through the tendon depth. The tissue section was fixed in 10% neutral buffered formalin and demineralized in 8% trifluoroacetic acid prior to paraffin embedding and sectioning at 10um and imaged using an Olympus BX61VS at 200X.

1.5 Cell-Cell Communication

These changes to the tendon are mediated by the native and infiltrative cells, thus the healing process is directed by cell-cell communication. Tenocytes are the primary cell mediator of tendons in health and use gap junctions to direct regulation of the ECM[16,41]. As tendon-native cell-

cell communication in the tendon gets overwhelmed by non-tissue-native cell types and systemic exocrine signals, it is important to acknowledge the role of the extracellular matrix (ECM) and its contextual effect on these signals[42]. Both mature protein states and ECM breakdown products can have a significant effect on immunomodulation, be it through collagen binding leukocyte-associated immunoglobulin-like receptor-1 , promoting immunosuppressive phenotypes, hyaluronan stimulating macrophage secretion of anti-inflammatory cytokines, fibronectin, matrikines or other ECM constituents[42]. This is where the cell-cell communication begins at the instance of tendon injury for both local and infiltrating cells. There is subsequent signaling by tenocytes, neurons, telocytes and other interfascicular populations[16,43,44]. The most extreme examples are in cases of tears that extend beyond a single fascicle and thus can result in hemorrhage and supraphysiologic stretching of the interfascicular matrix[7,29,37]. Of the cell types involved macrophages are seen as key regulators of both the healing and remodeling processes[37,44].

Macrophages are recruited early during tendon injury and persist preferentially longer than other recruited immune cells[45,46]. These cells are crucial to the removal of damaged tissue(s) and cellular debris; however, if macrophage response exceeds this demand, there is increased replacement of the pre-existing tendon by scar tissue[45,46]. As in other chronic inflammatory conditions such as atherosclerosis, the preferential polarization of these macrophages toward an anti-inflammatory (M2) state over a pro-inflammatory (M1) phenotype in damaged tendons may drive effective tendon regeneration and healing[46,47]. However, regulation of this transition is critical as both phenotypic extremes have their place in tendon healing as early removal of damaged tissue relies on M1 macrophages characteristics that are thus necessary during repair, prior to remodeling[37].

There are several key regulators of macrophage phenotype that will be discussed in greater length in subsequent chapters. In brief, we will be considering cytokines and chemokines, growth factors and matrix metalloproteinases (MMP) including MMP3, MMP13, IL-1α, IL-1β, IL-4, IL-6, IL-8/CXCL8, IL-10, IL-17A, IL-36RA, IP-10, MIP-1α/CCL3, MIP-1β/CCL4, MCP-1/CCL2, TNF-α, IFN-γ, and VEGF-A. Additional individual genes and associated pathways will be discussed in the context of macrophage-macrophage and macrophage-tenocyte cross talk, including different key mediators of inflammation like IFN-γ, IFN- α, IL-8/CXCL8 and TNFα in relation to the NFkB pathway and TGFβ[48]. Macrophage phenotype will be further discussed in the context of osteoclast like behavior as it related to gene expression and tissue remodeling. Other genes discussed will be related back to improved tendon tissue healing metrics, such as CEBPB, s100B, F13A1, HLF and PROS1 or worse tendon healing like ZAP70 which has shown to increase in relation to collagen disorganization[17,49-54]. All these elements have been found to be affected by paracrine signaling, especially via exosomes, a class of extracellular vesicle (EV). As such effective means of paracrine, juxtracrine, autocrine and exocrine communication, exosomes have become of significant research interest as a means to control local microenvironments (Figure 1.7)[55,56].

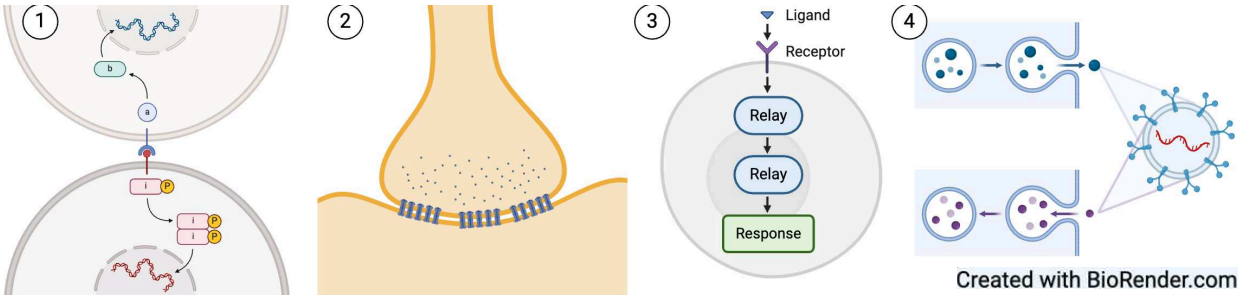

Figure 1.7. Intercellular communication may occur through (1) direct, cell membrane bound receptor-ligand interactions, (2) gap junctional exchange of signaling molecules, or juxtracrine, autocrine or exocrine signaling via excreted molecules or ECM complexes (3) or vesicles, like exosomes which may act through membrane bound receptor ligan interactions or cytoplasmic delivery of its constituents.

1.6 Exosomes

Exosomes (EVs) are a functional unit of the extracellular matrix[56]. They are 20-200nm diameter vesicles with targeting surface ligands and cargo comprised predominately of proteins, lipids and nucleic acids[31,57-59]. Most, if not all, cell types can release EVs which influence host immune response in a wide range of pathologies including cancer, cardiovascular disease, and viral infections [60-62]. These vesicles are controlled packets of communicatory cargo that have often been demonstrated to have specific target cell populations and drive specific functional outcomes[61].

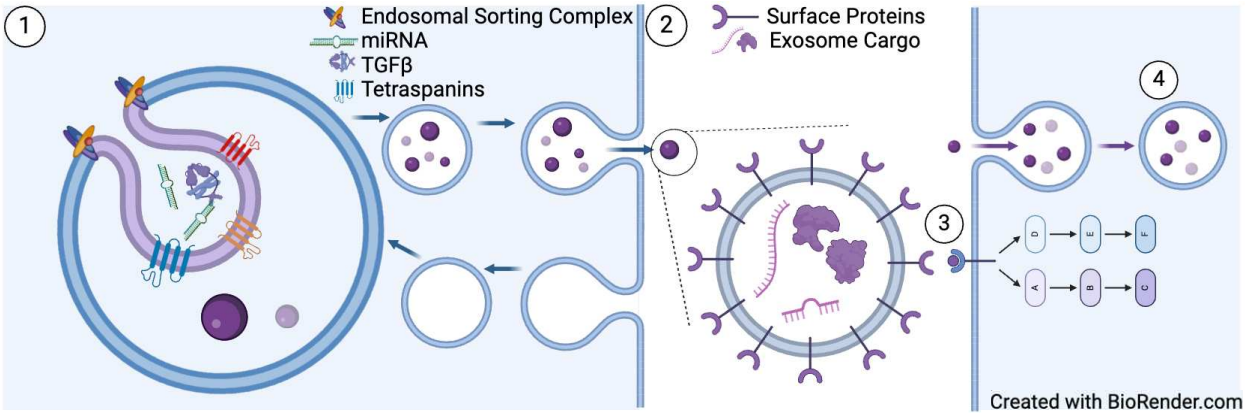

Figure 1.8. The exosome lifecycle begins (1) as an early endosome formed from the host cell membrane and containing extracellular constituents. Then, enfolding of the endosomal membrane is directed through controlled membrane sorting and inclusion of specific proteins that direct the transport and budding of the early vesicle and its constituents, such as the Endosomal Sorting Complex which concentrates at the liminal ring and tetraspanins like CD63, CD81 and CD9 which are often used as exosome surface markers. Exosome cargo is then loaded through directed and passive mechanisms as the vesicle closes and joins the endosomal compartment. This occurs repeatedly resulting in a multivesicular body that either A) is escorted to the cell membrane, which it rejoins, extravasating the mature exosomes and other content, or B) matures into a lysosome and the vesicles may be in part or whole, broken down and their constituents rejoin the cytoplasm. Those that make it to the (2) extracellular space become a component of the extracellular matrix able to migrate and diffuse, generally directed through surface receptor/ligand interactions which can direct them to specific microenvironments and or target cells. At these target cells they typically interact in two ways: (3) through cell surface receptors, directly triggering signaling cascades, or through (4) endocytosis and subsequent release of their cargo to downstream effects such as intracellular signaling via TGFβ and/or gene regulation through miRNA.

1.6.1 Exosome Isolation

Exosomes can be isolated by several different methods, each with their own benefits and potential drawbacks that make them uniquely applicable for different intended applications. In general, the considerations around the choice of isolation methods include, (1) if the method needs to be directly translated across species, (2) whether the exosomes need to be biologically active, (3) whether they will be used for in vitro or in vivo studies, (4) what the sample size and needed isolate concentrations are, and (5) equipment availability and effective budget.

Among the traditional methods, differential and density gradient ultracentrifugation have formed the foundation of much of the exosome research body[61,63]. This is in part due to it being the first methods employed as well as the low cost for institutions already employing ultracentrifuges, its translatability, and its non-specialized function, relying on particle size and density to isolate the EVs[61,63]. The major drawback of these methods is the damage to the EVs that the extreme centrifugal forces cause, which can also drive particle clumping negatively impacting experimental methodology[61]. Additionally, there are large concerns for the purity of the isolate[63,64].

Size exclusion chromatography offers an alternate means of isolating particles by size, the principle of which is a column of porous material through which smaller particles preferentially take a longer route and are eluted after larger particles[63,64]. This allows for fractionation of a sample by particle size and thus isolation of nanoparticles in the EV size range without the damaging forces applied during ultracentrifugation. Additionally, using purpose made columns, it is far faster than using ultracentrifugation, and allows a degree of standardization. This method can be further enhanced through the use of gentle EV concentrating and purifying steps prior to size exclusion chromatography, such as centrifugal removal of larger cell debris, filter concentrating and one could even employ ultracentrifugation[63,64].

There are several other methods that have been used with a variety of potential benefits and drawbacks. As in the previously discussed methods, they often rely on the physical properties of the EVs but can also act on the chemical properties. These include immunoaffinity based methods that can select for specific exosome markers and can even target specific subpopulations of EVs[63,64]. In general, these methods have great potential in the diagnostic and clinical setting, but are limited in their experimental applications by the volumes they can isolate in a cost effective manner and their direct translatability between species or exosomes from different cell sources or subpopulations there of[63,64].

1.6.2 Exosome Content

As a heterogenous population, once isolated exosomes are characterized[60,62]. At a base level, this means defining an isolated populations concentration and size distribution[62]. This can be performed using electron microscopy, primarily transmission- though scanning electron microscopy has also been employed, however this often expensive and time-consuming method has largely been replaced by nano-particle tracking analysis. Nano-particle tracking assesses the Brownian motion of particles in solution via their light scattering characteristics, and can determine individual particle diameters, volumes and counts to define a population at this level[65]. The next level of verification and characterization is defined by the presence of proteins that are concentrated in exosomes, several of which are functional in exosome biogenesis. Some examples of these include tumor susceptibility gene 101 (TSG101), apoptosis-linked gene 2-interacting protein X (ALIX), heat shock proteins (HSP) 70 and 90 as these play an integral role in exosome formation and transportation[60,63,66]. Tetraspanins are another group of consistently used markers. This family of transmembrane proteins are often enriched in EVs, especially CD9, CD63, and CD81[60,64]. Other proteins that may be enriched in certain exosome populations can include

(EpCam) and intercellular adhesion molecule 1 (ICAM1) which direct cell adhesion, Annexin A5 (ANXA5) which can direct exosome uptake, and flotillin-1 (FLOT1) which can influence exosome content[67-69]. Beyond these consistent marker proteins, exosomes can carry payloads of biologically active proteins like transforming growth factor β (TGFβ) which can have cell regulatory and immunomodulatory effects[70,71].

In addition to these protein payloads, the lipid composition of exosomes can play a significant role in their biological activity[72]. The lipid composition of the membrane is known to change based on cell origin, physiologic or culture conditions and exosome function, and is considered to be tightly controlled[72]. These lipids not only play a role in exosome biogenesis, but also in their uptake and signaling, such as through prostaglandins[72,73]. Exosome lipidomics is most often studied using mass spectrometry, and this is a rapidly growing area of exosome research, especially in the use of exosome lipid content as biomarkers of disease[72,73].

The third category of exosome content that is widely studied is the nucleic acid cargo[63,74]. While a limited number of studies have looked at DNA content in specific contexts, the importance of exosome RNA cargo is widely accepted and explored, especially messenger (mRNA) and microRNAs (miRNA), the most numerically abundant molecular cargo in exosomes[74,75]. Several studies have demonstrated the therapeutic role of gene regulatory miRNAs and that the RNA content of exosomes can be readily altered through exosome loading[74-76]. This will be discussed in greater detail in Chapter 4.

1.6.3 Exosome Labeling

Fluorescent labeling and imaging of exosomes and their uptake present a unique challenge due in no small part to their size. The size range of exosomes is below the threshold of a microscope's resolution capabilities, but, by adding a light emitting label, one can visualize the

location of exosomes in relation to cells, or use flowcytometry to study populations of EVs[62]. As antibodies are a quarter to one tenth the size of an exosome's diameter, there are not many epitopes available for binding[62]. To overcome this, there is a strong preference in the field for the use of fragment antigen binding (Fab) domains or nanobodies, which function similarly to whole antibodies, but are significantly smaller while retaining specificity[62].

Though less specific, the use of lipophilic dyes has been more widely established as a means of imaging exosome uptake and allows for direct translation across species and cell sources [62,77,78]. These dyes can be applied after exosome purification or, in some cases, to cells prior to exosome production and followed downstream in the experimental pipeline[77,78]. A more specific approach, that is particularly useful to study biodistribution, is the use of genetically encoded reporters[77]. These can tag specific exosome associated proteins of interest with a fluorescent or bioluminescent marker[77]. This technique can be coupled with other advanced application of genetic labeling, like adding specific photoactivating condition dependence[77].

1.6.4 Exosomes for Tendon Healing

In several musculoskeletal disorders, adipose-derived mesenchymal stromal cell (AdMSC) EVs are a primary paracrine effector of improvements in tissue healing[47,79-82]. Recently, AdMSC-derived EVs (MSCdEV) have improved tendon mechanical resilience, tissue organization, and M2 macrophage phenotype predominance in response to tendon injury[47]. Similarly, in rat models, exosomes from tendon-derived mesenchymal stromal cells have improved tendon healing by several metrics, from reduced inflammation and apoptosis to increased collagen organization and increased collagen fiber diameter[83].

While the underlying mechanism of EV-mediated repair is not fully understood, data suggests both a direct effect on tenocyte bioactivity and an indirect impact through

immunomodulatory effects on cytokine expression particularly via macrophage phenotypic shift (i.e., macrophage 'education')[46,47,84]. For example, in a rat model of Achilles tendon injury, treatment with EV educated macrophages decreased granulation tissue in injured tendons and improved biomechanics[46]. As these EVs can have a wide range of effects in different pathologies, the cell-source and the microenvironment thereof can influence both the biological cargo of EVs and surface signals that dictate their target cellular tropism[61]. While MSCdEVs and tendon-stem cell derived exosomes have been reported to improve tendon healing in animal models, the underlying mechanisms mediating this healing are not fully understood[47,83]. There has been some evidence to suggest that these effects could be macrophage mediated, as not only can exosomes increase the M2 phenotype, but direct application of exosome educated macrophages in a mouse model of tendon injury demonstrated significant improvements in line with those observed in other studies[46,85].

In the subsequent chapters we will further explore how tenocyte derived as compared to MSC derived exosomes may acts through different mechanisms to direct tendon healing, focusing on their effects on macrophage and tenocyte bioactivity and intercellular communication.

1.7 The Ovine Model of Rotator Cuff Tendinopathy

The work in the subsequent chapters will investigate the effect of exosomes as a function of cell source on key effector cells of tendinopathy, tenocytes and macrophages. These studies were performed in both ovine and human cell lines to establish these findings in the context of a model that can be further studied in the context of the gold standard large animal model. Since a targeted goal of exosome therapy is as an adjunct to surgical intervention, this will allow for future in vivo studies that will not only be physiologically relevant, but will be practical for testing in conjunction with contemporary gold-standards and novel treatments[58].

While many species have a rotator cuff, none are used in similar fashion to nor undergo the same natural disease course as humans. Though the nearest comparative anatomy may be in non-human primates, especially baboons, due to expense, difficulty as a model animal and ethical concerns surrounding their use non-human primates are not ideal candidates for studying this disease process [86,87]. There are many benefits to using smaller animal models such as rats and rabbits, as these have low associated costs, ready ancillary testing materials such as species-specific antibodies and established experimental models. However, these models preclude the testing of surgical techniques and biological devices that may be employed in humans due to the limitations of their size [36,86]. Additionally, their size can limit sample volume, complicating mechanical testing and limiting histologic assessment (Figure 1.9).

These limitations are largely overcome in the ovine model[86,88]. Sheep are relatively inexpensive and easily reared and handled. Given their shoulder anatomy, their infraspinatus tendon provides a suitable representation of the human supraspinatus, inserting onto the humeral head as part of the joint capsule and overlaying a bursa which allows for synovial fluid exposure in surgical models similar to the human supraspinatus which extends within the joint capsule[88]. Additionally, sheep readily tolerate surgical induction of one and sometimes both shoulders depending on the extent of the surgery[86,88]. Two experimental methods for the induction of the ovine model have become a gold-standard in the field and stand out in their recent adoption for the testing of biological devices in the pursuit of FDA approval. These are the combed-fenestration (CF) and sharp-transection (ST) models[17,18]. These models not only mimic the mechanical changes observed in the human condition but allow for non-destructive mechanical testing and histologic assessment of the same tissue for direct correlation of findings across length scale. They represent

a functional model at multiple length scales for the assessment of tendon healing in repone to surgical intervention and associated adjunct therapy.

Thus, the ovine model of rotator cuff tendinopathy is the ideal candidate to pursue research in exosome therapies. The primary short comings of the model are balanced by its benefits. These drawbacks include the larger amounts of exosomes needed to test in vivo therapies due to scale and the lack of species-specific antibodies for ancillary testing, however many of the limitations are being overcome with contemporary techniques. The use of filter centrifugal concentration of cell enriched fluids and subsequent size exclusion chromatography allows for faster, purer isolation of exosomes, the methods for which are outlined in Chapter 2. These methods, paired with the ready availability of ovine primary or immortalized cell sources help overcome this limitation. Some antibody based assays, such as cell phenotyping of formalin fixed paraffin embedded tissue sections and matrix characterization can be overcome by using methods that include using DNA barcodes for direct detection and quantification of RNA, or by using label free imaging techniques as those discussed in Chapter 4 [89] [90-92].

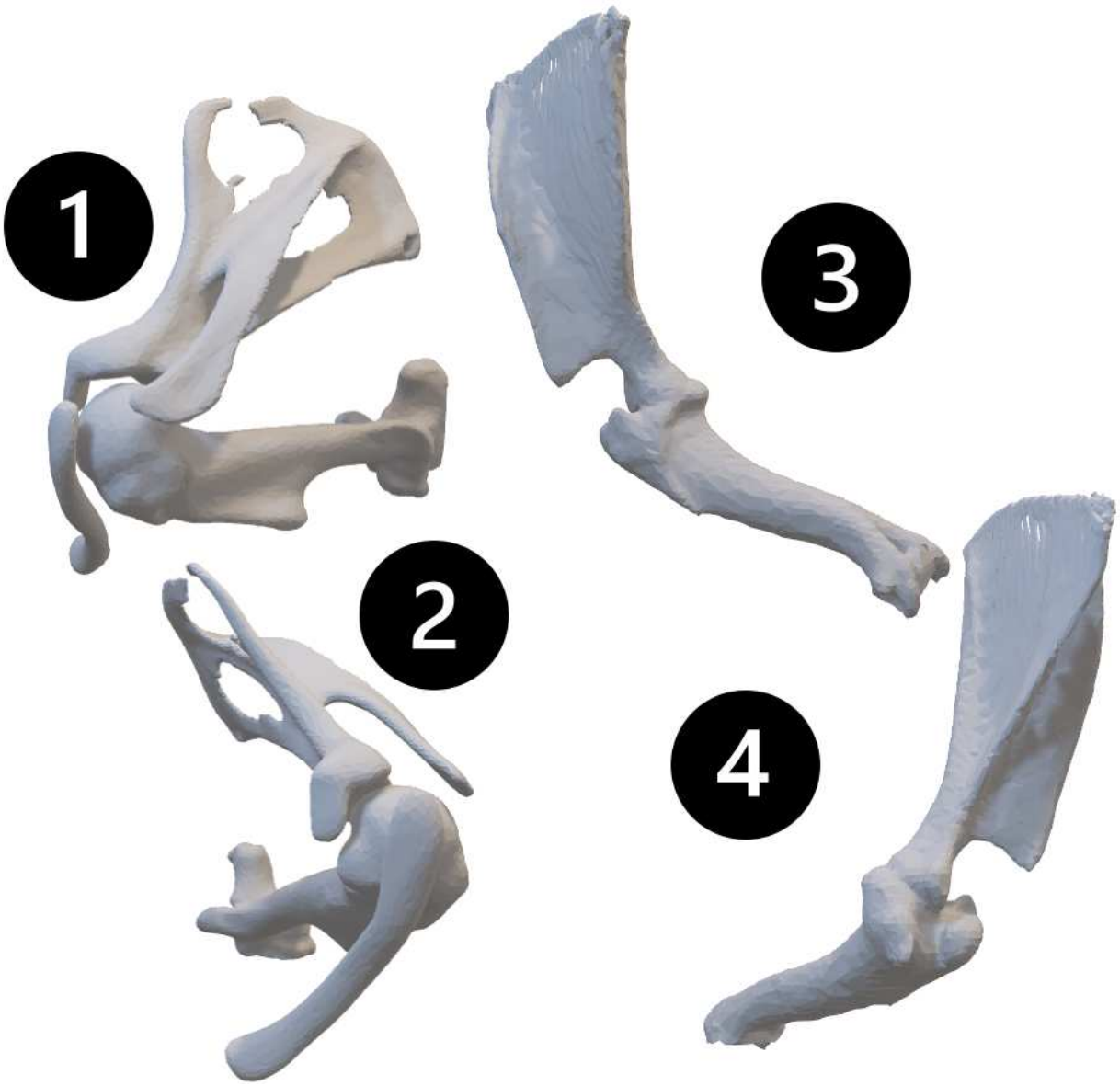

Figure 1.9. Comparative skeletal anatomy of the rat (1-2) and ovine (3-4) shoulders. Computed tomography (CT) (ovine) and micro-CT (Rat) scans reconstructed as 3d models of the skeletally radio-opaque window. These allow visualization of the increased complexity of the rat shoulder space as compared to the ovine shoulder. Images are not to scale. Rat shoulder is in flexion as compared to the ovine shoulder in extension due to limits of the imaging modalities.

1.8: Conclusions and Project Introductions

The ovine model of rotator cuff tendinopathy is well suited to investigations of multiple length scales, which will be necessary to determine the effects of exosome therapy in vivo. Though the pathogenesis of tendinopathy is not well elucidated currently, there are some key aspects of the

pathology that allow us to study it. First, we know that force is transmitted in the tendon along continuous collagen fibrils and fibers and that the extent to which these become discontinuous or disrupted in their movements is a metric of the severity of mechanical and thus physiologic disfunction. Next, we know that these fibers rely on an assortment of accessory molecules to support their order and function. This is most obvious in the interfascicular matrix, which can be viewed histologically, but extends to the fibrillar level as well. Lastly, we know that these functional elements of the biomechanical tendon unit are created and maintained by native tenocytes and infiltrating macrophages in the diseased state and that these cells are responsive to exosomes in a way that drives improved tendon mechanics.

These conclusions drove the hypothesis that native tenocyte derived exosomes, as compared to MSC derived, will preferentially drive tenocyte bioactivity, and promote macrophage to tenocyte communication toward a more tenogenic phenotype. In Chapter 2 we investigate the effect of exosomes as a function of cell source in ovine primary cells on tenocyte in vitro wound healing and macrophage cytokine, chemokine and growth factor secretion. This demonstrates that in this in vitro ovine model, tenocyte as compared to MSC derived exosomes drive increased tenocyte bioactivity and push macrophage communication toward a tenogenic phenotype. Then in Chapter 3 we explore these effects in primary human cell lines, and additionally investigate the MMP, chemokine, cytokine and growth factor secretion of the tenocytes, the RNA expression of the macrophages and the indirect effect of exosome education of macrophages on tenocyte bioactivity. Here, again, we see that tenocyte derived as compared to MSC derived exosomes drive a more tenogenic behavior in these cell lines. The methods employed for exosome isolation, characterization, and cell line preparation were intentionally replicated in the human and ovine study, as were the overlap in methods of investigating cell response. This sets a foundation for

exosome research in the gold standard, large animal model of rotator cuff tendinopathy. In Chapter 4 we will explore some of the future directions of in vivo exosome work that can be explored in this model using this foundational data, and the methods that could be used to answer these questions at multiple length scales.

CHAPTER 2: INVITRO MODELING OF OVINE EXOSOME AFFECT PER CELL SOURCE ON EFFECTOR CELLS OF ROTATOR CUFF TENDINOPATHY

2.1 Overview

Tendon injuries and disease are resistant to surgical repair; thus, adjunct therapies are widely investigated, especially mesenchymal stromal cells (MSCs) and, more recently, their extracellular vesicles (MSCdEVs), e.g., exosomes. Thought to act on resident and infiltrating immune cells, the role of MSCdEVs in paracrine signaling is of great interest. This study investigated how MSCdEVs differ from analogs derived from resident (tenocyte) populations (TdEV). As macrophages play a significant role in tendon maintenance and repair, macrophage signaling was compared by cytokine quantification using a multiplexed immunoassay and tenocyte migration by *in vitro* scratch-wound analysis. TdEV treated macrophages decreased IL-1 and increased MIP-1 and CXCL8 expression. Additionally, macrophage signaling favored collagen synthesis and tenocyte bioactivity while reducing pro-angiogenic signaling when TdEVs were used in place of MSCdEV. These *in vitro* data demonstrate a differential influence of exosomes on macrophage signaling, according to cell source, supporting that local cell-derived exosomes may preferentially drive healing by different means with possible different outcomes compared to MSCdEVs. This chapter establishes methodology that can be applied for exosome work in the context of the gold-standard large animal model of RCT and acts as a basis for comparison to the human *in vitro* model demonstrated and discussed in Chapter 3.

2.2 Introduction

Rotator cuff tendinopathy (RCT) is a chronic, debilitating disease resistant to classic interventions, including surgical and non-surgical treatments/repairs[93,94]. The underlying pathogenesis is a combination of intrinsic and extrinsic factors, including anatomic predisposition

to trauma and poor circulation, combined with cumulative degenerative changes related to age, genetics, and use[93,95]. RCT manifests as tissue changes, including alterations to tendon fiber arrangement, tendon-bone composition, and changes in tendon microenvironment, cell composition, and cytokine expression[13,95]. Recent data suggest that cell-to-cell communication during the acute and chronic stages of RCT drives the severity of tendon changes.

In health, tendon fibrocytes (tenocytes) form neatly organized arrays; networks of cell-cell junctions with low levels of connexins allowing for controlled, direct cell-to-cell communication[25,96]. When cell-cell junctions are lost and/or disrupted in injury, cells that have maintained cell-cell junctions move in cohesive aggregates to fill and 'heal' the wound[97]. While this method of collective cell migration has been studied in greater detail in epithelial cells, cancer, and *in vitro* cultures of mesenchymal stromal cells, less is known about the role of direct, contact-based cell communication, and loss thereof, in the pathogenesis of paucicellular tissue degeneration like RCT. It is thought that loss of cell-to-cell communication increases the extrinsic influence of paracrine signaling from non-tenocyte resident and recruited cells of the degenerated tendon microenvironment (e.g., macrophage paracrine signaling), particularly in adult tendons where tenocyte-tenocyte junctions are less frequent[15,96]. Additionally, in the setting of acute injury such as rotator cuff tears, an inevitable sequela of RCT, the sparsely cellular and poorly vascular tendon tissue is further remodeled by a rapid influx of cells due to hemorrhage, immune cell infiltration, and angiogenesis[98].

Macrophages are recruited early during tendon injury and persist preferentially longer than other recruited immune cells[45,46]. These cells are crucial to the removal of damaged tissue(s) and cellular debris; however, if macrophage response exceeds this demand, there is increased replacement of the pre-existing tendon by scar tissue[45,46]. As in other chronic inflammatory

conditions such as atherosclerosis, the preferential polarization of these macrophages toward an anti-inflammatory (M2) state over a pro-inflammatory (M1) phenotype in damaged tendons may drive effective tendon regeneration and healing[46,99]. The role of paracrine signaling from immune cells, such as macrophages, in the structural function of injured tendons, has driven interest in the complex heterogeneity of cell-cell interactions that may drive the progression of RCT. Extracellular vesicles (EVs) are such a means of communication and thus have become of significant research interest as a means to control local microenvironments[55].

Extracellular vesicles (EVs) have recently emerged as critical regulators of intercellular communication due to their ability to influence target cell function via the transfer of significant payloads of biological cargo, including protein and nucleic acid[60,79]. Most, if not all, cell types can release EVs which influence host immune response in a wide range of pathologies including cancer, cardiovascular disease, and viral infections[60,61]. In several musculoskeletal disorders, adipose-derived mesenchymal stromal cell (AdMSC) EVs are a primary paracrine effector of improvements in tissue healing[79-81,99,100]. Recently, AdMSC-derived EVs have improved tendon mechanical resilience, tissue organization, and M2 macrophage phenotype predominance in response to tendon injury[99]. Similarly, in rat models, exosomes from tendon-derived mesenchymal stromal cells have improved tendon healing[101].

While the underlying mechanism of EV-mediated repair is not fully understood, data suggests both a direct effect on tenocyte bioactivity and an indirect impact through immunomodulatory effects on cytokine expression particularly via macrophage phenotypic shift (i.e., macrophage ‘education’)[46,84,99]. For example, in a rat model of Achilles tendon injury, treatment with EV educated macrophages decreased granulation tissue in injured tendons and improved biomechanics[46]. As these EVs can have a wide range of effects in different pathologies,

the cell-source and the microenvironment thereof can influence both the biological cargo of EVs and surface signals that dictate their target cellular tropism[61]. While AdMSC-derived exosomes (MSCdEV) and tendon-stem cell derived exosomes have been reported to improve tendon healing in animal models, the underlying mechanisms mediating this healing are not fully understood[99,101]. Likewise, the potential differences between these mechanisms and that of fully differentiated tenocyte derived exosomes (TdEV) are not yet known.

As tendon healing is driven by a balance between the clearing of damaged tissue by macrophages and tissue deposition by tenocytes, it is logical that there is a controlled form of communication between resident tenocytes and macrophages. We hypothesize that TdEVs, as compared to MSCdEVs, will preferentially drive paracrine, pro- and anti-inflammatory, collagen modulating and angiogenic cytokine expression of macrophages toward a tenogenic phenotype as well as directly increase tenocyte migration. Thus, TdEVs may preferentially drive tendon healing through their autocrine and paracrine effects.

2.3 Material and Methods

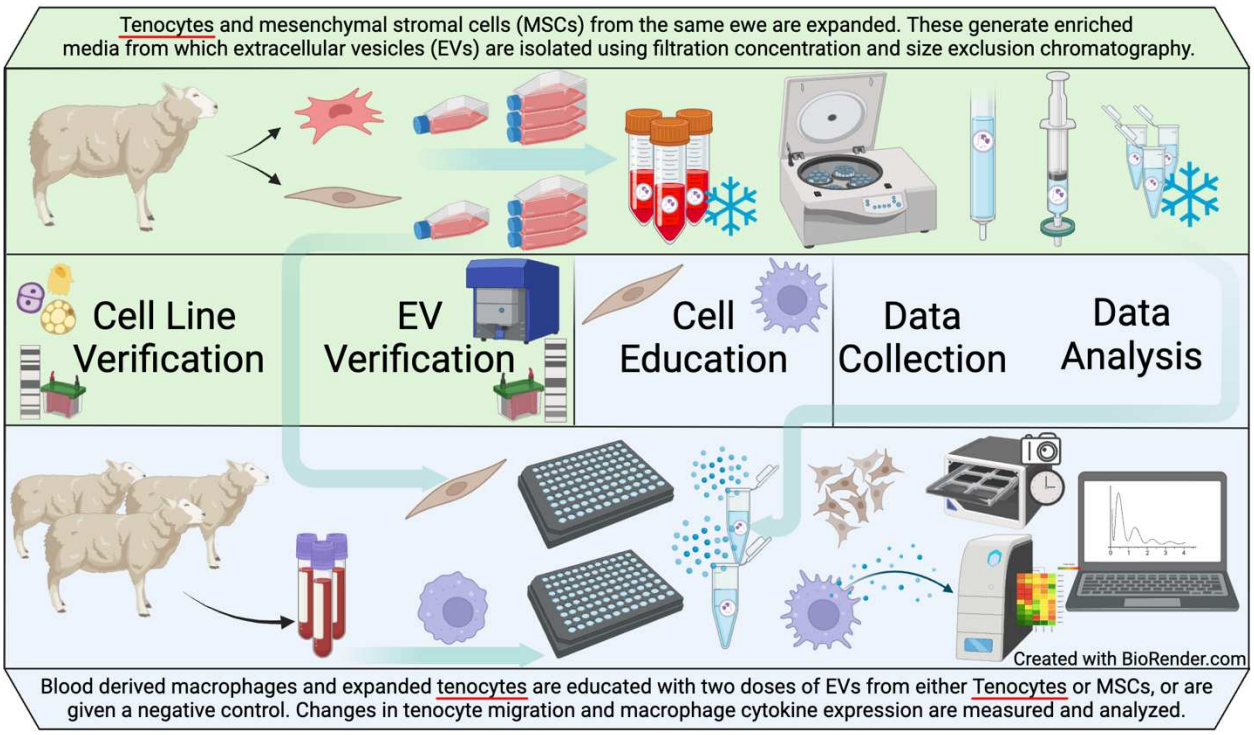

Figure 2.1. Graphical abstract of the experimental design. The top, green portion contains the workflow for exosome generation, while the bottom, blue portion contains the workflow for macrophage isolation and experimentation. In the top portion, left to right. Tenocyte and AdMSC isolation from a donor ewe for cell propagation and characterization followed by cell enriched media pooling and storage at -20°C which is then filter concentrated for size exclusion chromatography to isolate concentrated, pure exosomes. These aliquots are then filter sterilized prior to characterization and storage at -20°C. In the bottom portion from left to right, blood was collected from three adult ewes, mononuclear cells are selected by Ficoll separation prior to selection of adherent monocytes. These monocytes are then plated prior to maturation and negative control or exosome education after which end point analyses were performed. These steps were similarly performed from the cell education phase forward for tenocytes for the wound closure assessment.

2.3.1 Animals

Paired isolations of tenocytes and AdMSCs were harvested (postmortem interval <2 hours) from a skeletally mature adult (n=1; 3-4 years old; *Ovis aries*) ewe with no known clinical comorbidities that was euthanized for an unrelated research study. Peripheral blood-derived monocytes were isolated from blood drawn from ewes (n=3) during routine intake screening with no known comorbidities, collected in EDTA coated 10mL tubes. Collection and use of blood from

ewes was approved by the Colorado State University Research Integrity & Compliance Review Office, Institutional Animal Care and Use Committee (IACUC; #1503).

2.3.2 Isolation and Culture of Tenocytes and AdMSCs

Subcuticular adipose tissue (2-3 cm^3) was collected from the shoulder. The infraspinatus tendon was carefully isolated, and a 10x5x5 mm section of the central tendon body core was aseptically collected. The same procedure was then used to isolate cells from each tissue. These tissue sections were digested in 35mL of 1:1 Dulbecco's Modified Eagle's Medium with Nutrient Mixture F-12 Ham with 15mM HEPES and sodium bicarbonate (DMEM:F12, D6421, Sigma-Aldrich) with 200 units penicillin, 0.2mg/mL streptomycin and 0.5mg/mL amphotericin B (Abx, A5955, Sigma-Aldrich) and 1mg/mL of type 1 collagenase (BP2649, Fisher Bioreagents) for 24 hours at 37°C with 5% CO_2 under constant agitation as a modification of traditional enzymatic cell isolation[102,103]. This digesta was then filtered at 100 μm (Cell Strainer, Z742101, Sigma-Aldrich), and the flow through was diluted to 50 mL with Dulbecco's phosphate buffered saline (PBS; D1408, Sigma-Aldrich), centrifuged at 400xG for 10 min and the cell pellet was resuspended in and washed twice in 10mL of PBS. The resulting cell pellet was resuspended in DMEM:F12 with 10% Fetal Bovine Serum (97068-085, Avantor) and Abx (complete DMEM; CD) and grown to confluence in a 75cm^2 culture flask (156499, Thermo Fisher Scientific) before passage. Cells in passages 2-3 were used for EV purification to limit the phenotypic shift of the isolated cells and thus ensure minimal variability in exosome content[104,105]. Tenocytes were characterized by visual assessment for spindle morphology, and western blot analysis of 20 ug of cell lysate derived protein for tenomodulin (TNMD, SAB2108237, Sigma-Aldrich) and Tenascin C (TNC, sc-25328, Santa Cruz Biotechnology). AdMSC were characterized by trilineage differentiation using Mesenchymal Stem Cell Chondrogenic, Osteogenic and Adipogenic Differentiation Media's (C-28012, C-28013,

and C-28016, Millipore Sigma) the results of which were assessed using Alcian blue, Von Kossa and Oil Red O staining for cartilage, bone, and adipose respectively.

2.3.3 EV Purification

Both cell lines were amplified in passages 2 and 3 into 225cm^2 culture flasks (159934, Thermo Fisher Scientific). While at 80-100% confluence, culture media was aspirated, cells were washed with 5mL of PBS, and flasks were filled with 15mL of serum free DMEM:F12 with Abx. After 24 hours, cell enriched culture media was collected, cell debris was removed by centrifugation at 700xG for 10 min, and supernatants were stored at -20C. Cultures were then 'rested' for 24 hours in CD. After reaching 100% confluence for at least 24 hours, cultures were split and passaged.

Cell enriched media was pooled within individual cell lines and filter concentrated (Centricon 70; UFC710008, Millipore Sigma). Then, EVs were isolated by size exclusion chromatography (qEV columns; QiZON, qEVoriginal). Fraction 3, the fraction of the highest particle density per EV quantification, was used for all experimentation unless otherwise noted.

2.3.4 EV Quantification

The ZetaView QUATT 4 nanoparticle tracking analysis instrument (NTA) (ZetaVIEW software ver. 8.05.12 SP1; Particle Metrix GmbH) was used to determine the size and concentration of the isolated EVs before use. Utilizing the scatter mode of the NTA, the concentration of all EVs was measured. Assessment of the Brownian motion determined individual particle size and concentration. Sample aliquots were diluted in PBS to an average count per frame of 50-500 particles. Based on these measurements, EV concentrations were standardized using PBS as a diluent to 1x10^7 particles/ 30µL.

2.3.5 Western Blot

EVs were concentrated from fraction 2 using ultracentrifugation at 110KxG for 90 minutes, supernatants were aspirated, and EV pellets were resuspended in radioimmunoprecipitation assay (RIPA) lysis buffer (89901, Thermo Fisher Scientific) with protease inhibitor cocktail (78415, Thermo Fisher Scientific). Protein quantification was performed using the Pierce™ BCA Protein Assay (23225 and 23227, Thermo Fisher Scientific). Mini-Protean®TGC™ wells were loaded with 5ug of EV protein in Laemmli Sample Buffer (1610747, Bio Rad) or 10µL of the Precision Plus Protein Kaleidoscope prestained standards (1610375, BioRad). Gel electrophoresis was run, samples and standards were transferred to a nitrocellulose membrane, and the membrane was labeled for heat shock protein 70 (HSP70) or tumor susceptibility gene 101 (TSG101) (EXOAB-Hsp70A-1 and EXOAB-TSG101-1, System Biosciences). Appropriate secondary antibody was applied and stained using SuperSignal™ West Pico Plus Chemiluminescent Substrate (34580, Thermo Fisher Scientific). Images were taken with ChemiDoc™ XRS+ with Image Lab™ Software (BioRad).

2.3.6 Isolation of peripheral blood-derived monocytes

Whole blood was mixed 1:1 with PBS and separated by density gradient centrifugation (Ficoll® Paque Plus, 17-1440-02, Cytiva Life Sciences). The mononuclear cell layer was then collected, washed twice with PBS and plated in a 96 well plate (167008, Fisher ThermoScientific) at $1x10^6$ cells/well in 200 µL RPMI-1640 for 2 hours. Media containing non-adherent cells were removed to select for adherent monocytes, and the remaining cells were gently washed with 100µL PBS twice to remove additional non-adherent cells. Adherent cells were cultured in RPMI-1640 with Abx and 10% FBS (complete RPMI) with 10ng/mL ovine macrophage colony stimulating

factor 1 (MCSF-1, RP1640G, KingFisher Biotech Inc.) for seven days with media refreshed on day 4. From day seven onward peripheral blood-derived monocytes were considered macrophages[106,107]. Macrophage phenotype was confirmed by flow cytometry using established markers for CD205 (MCA2450PE), CD11b (MCA1425A647), CD45 (MCA2220B) or MHC class II (MCA2226F)[108]. All antibodies for flow cytometry were obtained from Bio-Rad. Conservative gating was performed for analysis using FlowJo software (Ashland, OR).

2.3.7 Macrophage EV Education

On day eight, macrophage culture media was replaced with 170µL of complete RPMI and 30µL of either 1) PBS, 2) MSCdEVs, or 3) TdEVs with concentrations of $1x10^7$ particles/30uL. After 24 hours, the media was again replaced with the same treatments and serum free RPMI. After an additional 24 hours, the media was collected, and cell debris was removed by centrifugation. Supernatants were aliquoted and stored at -20ºC. The cultured wells (n=24) were thus comprised of three cell lines, each derived from a different animal, that were given one of the three treatments in technical duplicate.

2.3.8 Multiplex Immunoassay of EV Educated Macrophages

Educated-macrophage enriched media was analyzed using a commercially available enzyme-linked immunosorbent assay kit (MILLIPLEX MAP KIT, ovine cytokine/chemokine and growth factor magnetic bead panel, Cat #SCYT1-91K-PXBK14, EMD Milipore Corp. Billerica, MA, USA). Frozen banked media was slowly thawed to room temperature and processed undiluted in technical duplicate. The bioassay measured concentrations of IL-1α, IL-1β, IL-4, IL-6, CXCL8, IL-10, IL-17A, IL-36RA, IP-10, MIP-1α/CCL3, MIP-1β/CCL4, TNF-α, IFN-γ, and VEGF-A. All experimental wells were run in technical duplicate. Mean fluorescent intensity of the means of

technical duplicates and experimental technical duplicates were used for statistical analysis (2 technical replicates, one from each experimental group, were trimmed due to low bead count per the manufacture's recommendations).

2.3.9 Tenocyte Migration and Bioactivation

Tenocytes from passage five were plated in a 96 well plate (ImageLock, 4379, Essen Bioscience) at a density of 20,000 cells/well and grown to confluence. The first 24 of 48 hours of this was in CD while the second 24 hours had the addition of 30µL of either PBS (negative control), MSCdEVs or TdEVs with concentrations of $1x10^7$ particles/30uL. After confluence a uniform scratch was made in each well (WoundMaker™, Essen BioScience, Ann Arbor, MI). Each well was then washed twice with 150µL PBS. Cells were then cultured in 200µL of CD (positive control) or 170µL DMEM:F12 with Abx and 30µL of either PBS (negative control), MSCdEVs or TdEVs with concentrations of $1x10^7$ particles/30uL. Serial temporal images were taken of each well using an automated plate scanner (IncuCyte™, Essen BioScience, Ann Arbor, MI) at 0, 2 hours, and every 6 hours after that for a total of 20 hours. Image analysis was used to measure the percent change in area of the decellularized scratch.[109]

2.3.10 EV Fluorescent Labeling and Uptake Imaging

Purified EVs were stained using Vybrant™ DiD (V22887, Thermo Fisher Scientific) lipophilic dye and washed twice in PBS using ultracentrifugation. PBS with 10% exosome depleted FBS (A2720801, Thermo Fisher Scientific) was treated and 'stained' in parallel as a negative control. Macrophages were differentiated and cultured on glass coverslips (C8-1.5H-N, Cellvis). Cells were dosed with 30µL of 'stained' controls or stained EVs ($1x10^7$ particles). Macrophages were then washed twice with PBS, fixed in 4% paraformaldehyde for 10 minutes,

and stained with ActinGreen™488 ReadyProbes™ reagent (R37110, Thermo Fisher Scientific), then with DAPI (EN62248, Thermo Fisher Scientific) before preservation in antifade mounting media (P36961, Thermo Fisher Scientific). Wells were then imaged using a spinning disc confocal microscope (IX83 P2ZF using cellSens Dimension v4.1, Olympus).[78]

2.3.11 Statistical analysis

Scratch-wound confluence data were evaluated using a multiple Mann-Whitney tests with significance considered for treatment and time factors where $p<0.05$ and $q<0.05$. Multiplex immunoassay mean fluorescent intensity was compared across experimental and control groups. To compare the overall difference between control and experimental groups, a 2-way ANOVA was used with significance considered when $p< 0.05$. To compare shifts in cytokine levels between experimental groups, a multiple paired t-tests analysis was performed with data paired by the donor. Significant discoveries were considered for those with q and p values <0.05.

2.4 Results

2.4.1 EV Characterization

Harvested EVs were assessed for purity and consistency. Brownian motion analysis demonstrated a median particle size of 116.5nm (StDev 72.9nm) for TdEVs, and 135.2nm (StDev 76.7nm) for MSCdEVs (Figure 2.2 A-C). These size ranges are consistent with exosomes being the predominant EV type present in these cell culture supernatants [63]. Consistent with this observation, immunoblot analysis of purified TdEVs, and MSCdEVs, for the exosome-associated proteins HSP70 and TSG101 demonstrated positive immunoreactivity for a protein band at the expected molecular weights (70 and 44 kDa, respectively; Figure 2.2 A). HSP70 has been found to preferentially localize to the surface of exosomes[110], while TSG101 is considered an exosome

marker due to its association with the endosomal sorting complex required for transport [111]. These data confirm pure populations of EVs from each cell source.

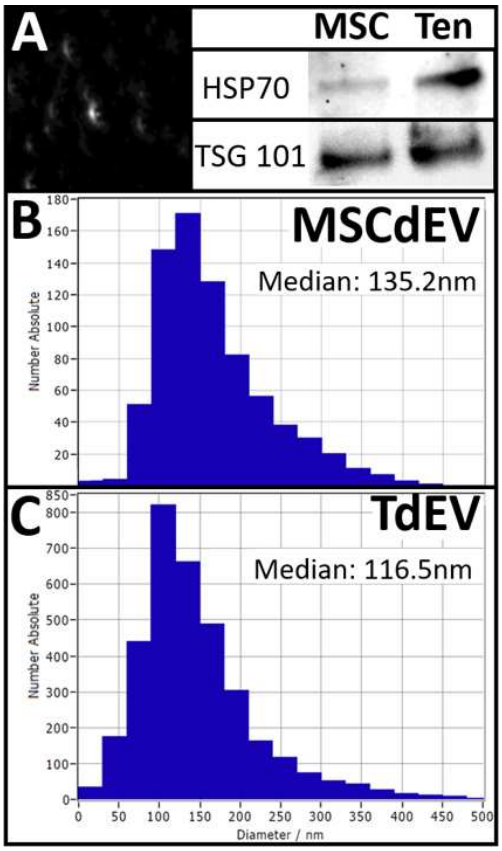

Figure 2.2. Differential protein expression in MSCdEVs compared to TdEVs of cell-enriched medium filtrates after size exclusion chromatography. **(A)** Representative photomicrograph of nanoparticles and Western blots demonstrating low, but present heat shock protein 70 (HSP70) content in EV lysates of MSCdEVs compared to greater expression in TdEVs with similar expression levels of TSG 101. **(B, C)** Histograms of the nanoparticle tracker analysis demonstrating the distribution of nanoparticles by size with median diameters reported.

2.4.2 *In Vitro* Assessment of Macrophage Uptake of EVs

Next, we sought to determine, *in vitro*, if macrophages represent a viable cellular target of endogenously released or exogenously administered EVs in the tendon microenvironment. Peripheral blood monocyte-derived macrophages were treated with fluorescently labeled EVs for 4 hours, punctate fluorescent aggregates localized within the cytoplasm, consistent with EV uptake, based on counterstaining for actin and nucleic acid (Figure 2.3 A-C).

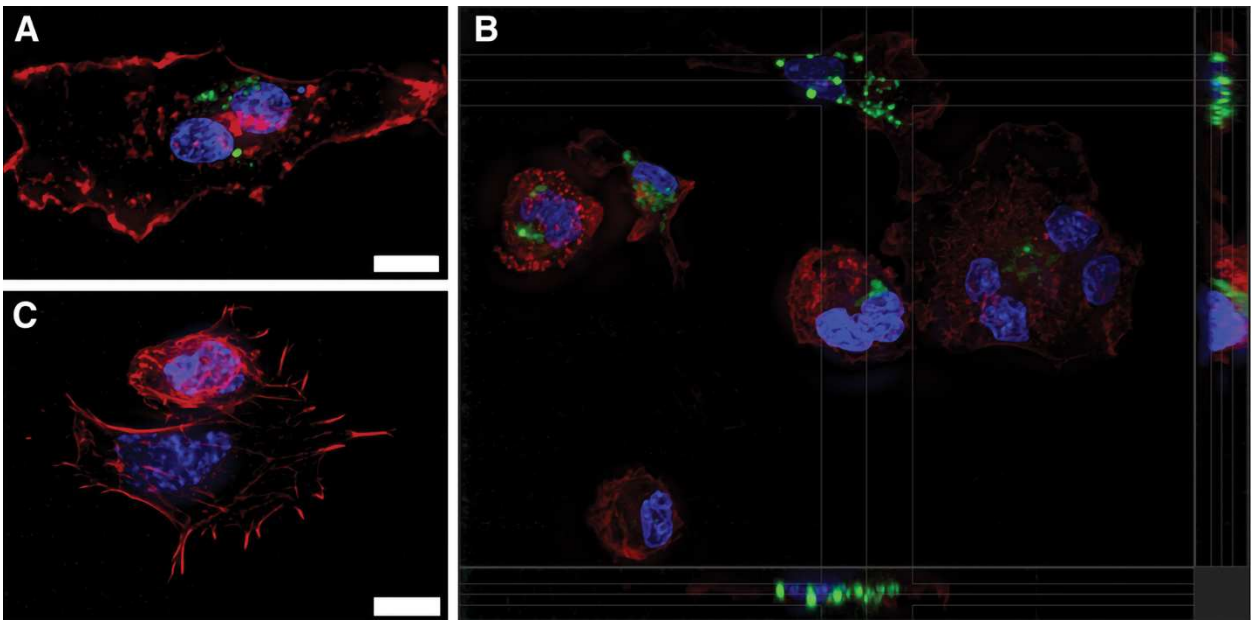

Figure 2.3. Spinning disc confocal photomicrographs of cultured macrophages stained with fluorescent markers for actin (*red*, phalloidin) and nucleic acids (*blue*, DAPI). **(A, B)** Macrophages cultured for 4 h with TdEVs that were lipid membrane labeled using DiD (*green*). **(A)** is a flattened z-stack view of a single, binucleate cell, while **(B)** is an expanded slice view of a field containing multiple macrophages with orthogonal views on the *bottom* and *right* sides of the image rendered from the z-stack and showing that the *green*, TdEVs, are within the cell body. **(C)** is a representative flattened z-stack view of control macrophages cultured for 4 h with 10% exosomes-depleted FBS in PBS that underwent the same staining process as the TdEVs used in **(A, B)**. All images are taken using a 60X oil immersion objective with synchronized exposures (*white* scale bars = 10 μm). FBS, fetal bovine serum; PBS, phosphate buffered saline.

2.4.3 Macrophage EV Education

The impact of EV uptake by macrophage cytokine expression over 24 hours was assessed. There was a significant difference in cytokine expression between both treatment groups and the negative control (p-value<0.001; 2-way ANOVA). Between the two treatment groups, there were several significant discoveries of a difference in cytokine expression (Table 1. multiple paired t-tests, $p<0.05$, $q<0.05$). Macrophages educated with MSCdEVs had higher expression of IL-1α, IL-1β, TNFα, CXCL8, and IL-36RA, whereas TdEV-educated macrophages had higher expression of MIP-1β/CCL4. These shifts in expression were relative to the negative controls and to each other

as demonstrated by mean pg/mL (Figure 2.4 A&B) and when grouped by biological function and demonstrated by fold change in mean fluorescent intensity of experimental groups compared to the control groups (Figure 2.5 A-C).

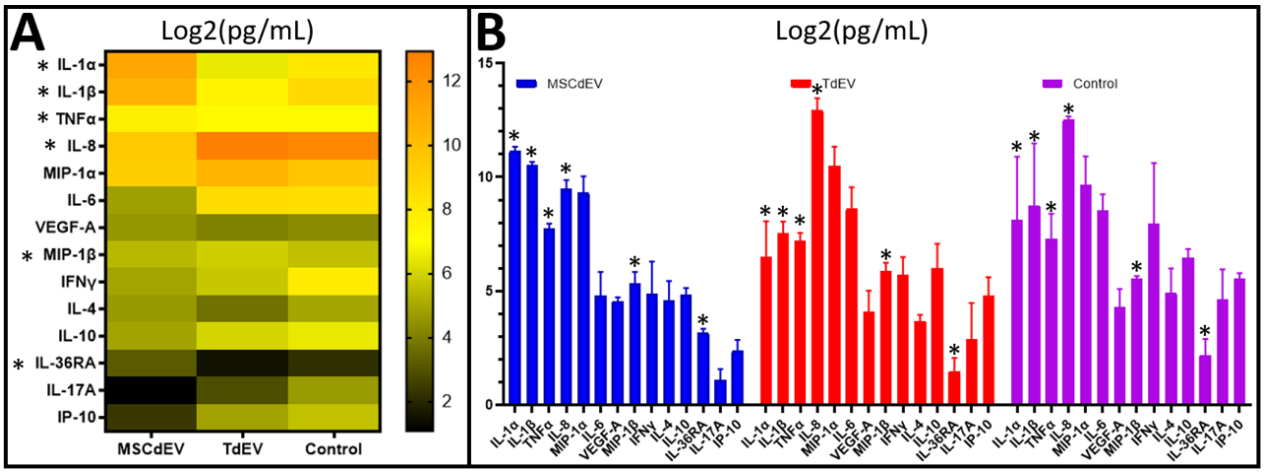

Figure 2.4. The mean accumulated cytokine levels expressed by macrophages over 24 h that were educated over 48 h by two doses of 1×10^7 particles of either TdEVs or MSCdEVs in PBS or PBS without EVs, given 24 h apart. Cytokine expression was measured by multiplex bead-based immunoassay and reported as picogram per milliliter log2 to best visualize relative shifts in each analyte on a single scale. (A) A heat map highlighting the relative differences among treatment groups. (B) Bar graphs with standard deviations to highlight trends among treatment groups. The interaction of treatment with cytokine showed a significant difference between treatment groups (two-way ANOVA: $p < 0.0001$). *Asterisks* (*) mark the cytokines that demonstrate statistically significant differences between experimental groups; Multiple paired *t*-tests of the untransformed MFI, $p < 0.05$, $q < 0.2$. ANOVA, analysis of variance; MFI, mean fluorescent intensity.

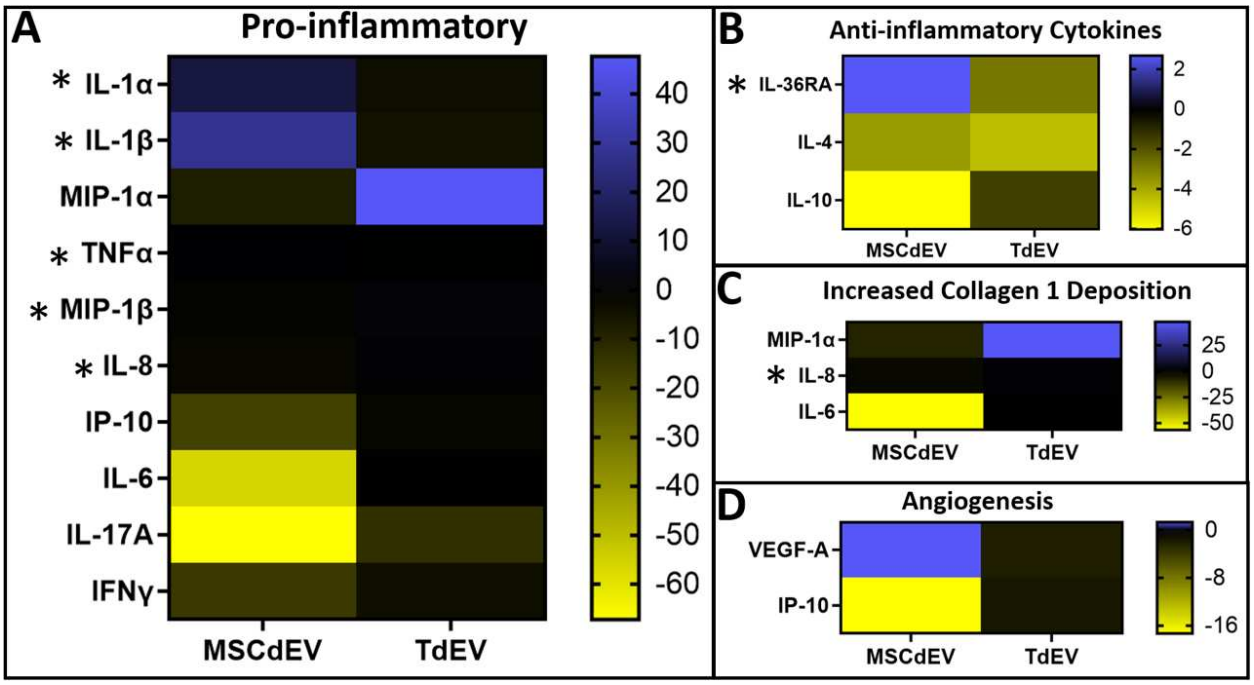

Figure 2.5. Heat map of cytokine expression as mean fluorescent intensity fold change of experimental groups relative to the control group separated by relevant functions. (A) highlights cytokines described as proinflammatory in the literature, (B) as anti-inflammatory, (C) as increasing collagen type 1 deposition, and (D) as driving angiogenesis. Statistical analysis was performed by multiple paired *t*-tests; cytokines marked by *asterisks* (*) have *p* and *q* values <0.05.

2.4.4 Tenocyte Migration

Lastly, to assess whether tenocyte bioactivity was affected by treatment with TdEVs vs. MSCdEVs, an *in vitro* scratch-wound analysis was performed to evaluate cell migration (Figure 2.6 A-C). When treated with TdEVs, scratch-wound closure was, on average, 82.5% over 20 hours. This closure rate and magnitude were significantly greater than for those tenocytes treated with either MSCdEVs (64.9%), the positive, FBS enriched controls (59.3%), or the negative, PBS controls (35.0%) (two-way ANOVA, treatment factor over 20hrs: p=0.0056) (Figure 2.6 A&B).

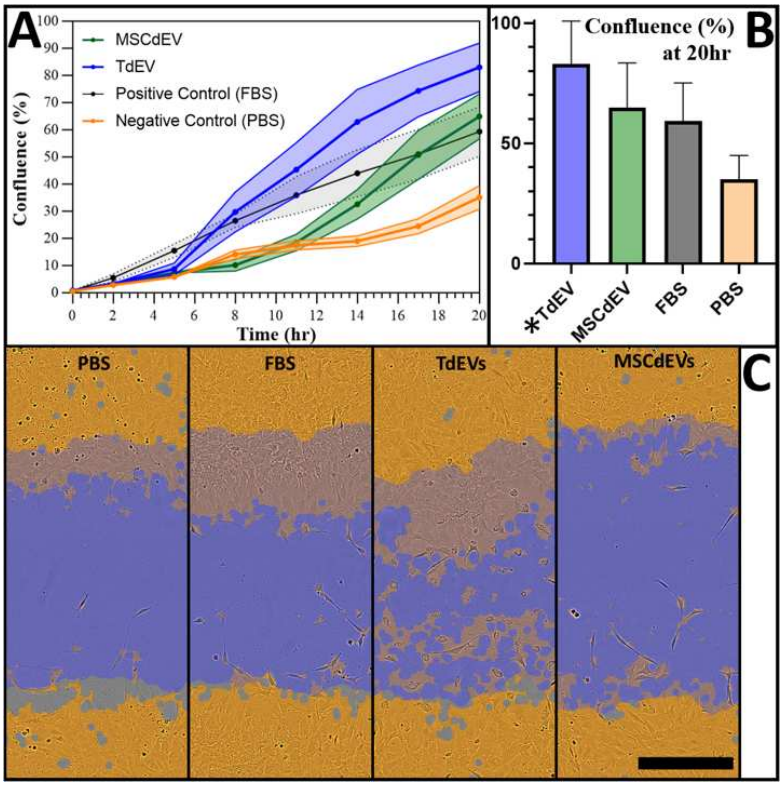

Figure 2.6. Tenocyte bioactivity measured by *in vitro* scratch-wound. Wounds were made in confluent cultures 24 h after experimental dosing with PBS, FBS, or 1×10^7 particles of TdEV or MSCdEV in PBS, with a second dose administered after scratch-wound at time zero. **(A)** Percent confluence over time of each treatment group with shaded areas accounting for standard error. **(B)** relative percent confluence at 20 h with standard error. *Asterisks* (*) denote statistical significance compared to the negative control using multiple Mann–Whitney tests. **(C)** Representative wells of tenocyte cultures at time point zero, and the reflected same region at 11 h, highlighting the time point of most significant difference among groups. *Blue* highlights the initial scratch-wound, while *orange* highlights the cell profiles, and *gray* where cell profiles were absent outside the scratch-wound.

2.5 Discussion

As previous studies have demonstrated that paracrine signaling of MSCdEVs may be responsible for the positive therapeutic effects of AdMSCs on tendon healing [99,101], we sought to determine how TdEVs may differentially effect cellular responses associated with tendon healing using donor-derived tenocyte and macrophage *in vitro* cell culture models. We successfully *ex vivo* cultured and isolated EVs from donor ovine-derived tenocytes and AdMSCs. These EVs demonstrated similar size and appropriate protein expression and are bound and taken in by

macrophages. Most notably, TdEVs increase tenocyte migration significantly more than MSCdEVs, and preferentially upregulate macrophage secretion of cytokines responsible for collagen type 1 deposition and crosslinking, favor a MIP1 and CXCL8 inflammatory profile, and decrease IL-1 secretion.

To evaluate the direct effect of MSCdEVs on tenocytes compared to TdEVs, we assessed cell migration using a scratch-wound assay. This simulates a tendon tear to resolve the cells' ability to close this "wound". We observed a significantly greater response of tenocytes to TdEVs compared to MSCdEVs, or the positive and negative controls (Figure 2.6), suggesting greater upregulation of tenocyte bioactivity from exosomes that are autologous to their target cell. Notably, TdEVs more quickly began closing the "wound" and by 11 hours had exceeded the positive control, which MSCdEVs did not match until the 17th hour. There was a delay in the EV treated groups' "wound" closure compared to the positive control of 5-8 hours for TdEVs and 12-14 hours for MSCdEVs. This could be due to the protracted but significant effect of gene regulatory signaling that vesicular cargo can play and the time for vesicular uptake and cargo integration compared to the more direct signaling of growth factors and other proteins present in FBS. It should be noted that no mitosis inhibitor, such as mitomycin C, was used, and thus, these data do not explicitly demonstrate the sole effect of EVs on migration. Additionally, while these data are compelling, the suggested 'autocrine' effect observed here does not fully recapitulate the complexity of paracrine signaling that is expected to take place *in vivo*.

As macrophages are one of the most abundant recruited cell types during early tendon injury and persist the longest in tendon repair, their phenotypic state is known to influence tendon healing. We sought to evaluate the effects of MSCdEVs compared to TdEVs on macrophage cytokine secretion. We observed differential secretion of multiple cytokines relevant to tendon

healing when comparing macrophages educated with TdEVs as compared to MSCdEVs. IFN-γ, IL-1β, and IL-1α all drive M1 macrophage polarization[112-115], and IL-1β and TNFα have been reported to be increased in animal models of tendon injury, wherein they drive elevated matrix metalloproteinase (MMP) activity and progressive tendon degeneration[112-114,116]. Our data showed 24-, 7.9- and 1.46-fold increases in IL-1α, IL-1β, and TNF α, respectively, in macrophages educated with MSCdEV as compared when educated using TdEVs (p=0.006, 0.275 & 0.012, Figures 2.4-2.5). IFN-γ showed a trend of strong downregulation of >7-fold by both EV treatments (p=0.626).

In contrast, although not statistically significant, MIP-1α/CCL3 and IL-6 increased 2.3- and 14-fold, respectively with TdEV treatment as compared to MSCdEV (p=0.32 & 0.156). MIP-1α/CCL3 not only drives fibroblast bioactivity but is crucial for collagen type 1 production, especially in early tendon healing[117,118]. Similarly, IL-6, while active in pro-inflammatory cascades in some tissues, plays multiple roles in tendon healing, including upregulation of IL-10 and suppression of TNF-β and IL-1β[119]. It also plays a crucial role in tendon healing and integrity, possibly through its effects on fibroblast recruitment and collagen type 1 synthesis[119-121].

IL-17A can further increase tenocyte expression of inflammatory cytokines while increasing collagen type III expression and apoptotic factors[122]. While not significantly different between the treatment groups, there is a greater than 3-fold reduction in expression in both treatment groups compared to the negative control, which may be favorable for tendon healing (Figure 2.5).

Cytokines such as IP-10, MIP-1β/CCL4, and CXCL8 can act directly to recruit myeloid cells such as neutrophils and monocytes. Some of these same molecules and others like VEGF-A are pro-angiogenic, increasing endothelial cell proliferation and neo-vascularization. These

changes in the local cytokine milieu can result in significant changes within the cellular composition of the injured tendon microenvironment[119,123-125]. Interestingly, we observed a trend in TdEV promoting IP-10 (5.2-fold; p=0.094) expression, concurrent with suppressing VEGF-A (0.82-fold; p=0.875) relative to MSCdEVs. Additionally, there was a significant increase in MIP-1β (1.4 fold) and CXCL8 (>10-fold) in macrophages treated with TdEVs as compared to MSCdEV treatment (p=0.007 & 0.017). Taken together, these data suggest a shift away from an angiogenic, pro-inflammatory, and collagenolytic phenotype in MSCdEV-educated macrophages towards a TdEV driven phenotype that may be more conducive to early tendon repair in TdEV-educated macrophages, characterized by cytokine secretion that would further enhance monocyte and neutrophil chemotaxis, and promote collagen type 1 deposition and some angiogenesis [119].

Anti-inflammatory cytokines IL-4 and IL-10 are both drivers of M2 polarization [126-128]. IL-10 *in vivo* data shows improved healing in the tendons of a mouse model with induced overexpression of IL-10. At the same time, increased concentrations of IL-4 correlate with increased collagen type 1 expression and cell proliferation in injured rotator cuff tendon [124,126]. Interestingly, these data show trends in IL-10 expression increasing 2.2-fold with TdEV treatment over MSCdEVs (p=0.256) while IL-4 expression is increased with MSCdEV treatment by 1.9-fold (p=0.302). Another anti-inflammatory cytokine assessed, IL-36 receptor antagonist (IL-36RA), showed a 3.2-fold increase with MSCdEV treatment compared to TdEV(p= 0.007); however, the role of this cytokine in tendon homeostasis and healing is not understood yet [129]. Some paracrine signaling may, in turn, influence exosome characteristics. IFN-γ was shown to prime mesenchymal stromal cells *in vitro* toward expression of exosomes that drive local anti-inflammatory effects in an *in vivo* mouse model[115]. The effector molecules are not known and may, in-fact, be multi-model. Current research is beginning to elucidate some of these effector molecules, such as HSP70. This

protein is preferentially expressed on exosomes where the concentration may vary. In an *in vivo* study, increased HSP70 expression on exosomes was correlated with decreased cardiac fibrosis and *in vitro* decreased fibroblast bioactivity[130]. This study was carried out using cardiac myofibroblasts, and serum-derived exosomes[130]. In our research, we see increased tenocyte migration as a metric of bioactivity in those cells treated with TdEVs, which demonstrated increased HSP70 expression (Figure 2.2). This differential role of HSP70 warrants further investigation.

Ovine cell lines were used to demonstrate *in vitro* exosome function in a translational model of rotator cuff disease, i.e., RCT[18]. While the ovine model is excellent for translatable anatomy, mechanics, and surgical approach, antibody-based assays are limited in this species, especially toward exosome specific markers[18]. This limited the analyses that could be performed at the protein level and informed the choice of protein markers. In the macrophage education and scratch-wound experiments, one biological replicate of EV source was used due to the limited, biologically paired EV sample size. This similarly limited sample size. Future work will investigate the constituent variance of EV cell source and biological source and the direct effect of educated macrophages on tenocyte bioactivity. *In vivo* experimentation in this translatable model will be investigated as the therapeutic potential of TdEVs is established.

This insight into the influence of TdEVs on macrophage signaling is exciting. It demonstrates a shift in pro-inflammatory cytokines away from the IL-1 predominance seen in MSCdEV educated macrophages and toward MIP-1 & CXCL8 predominance. Furthermore, there is an increased bias toward collagen synthesis and tenocyte bioactivity with decreased angiogenic signaling when TdEVs are used in place of MSCdEV. These *in vitro* data demonstrate a compelling reason to further investigate the differential influence of exosomes by cell source on tendon healing

and how control of exosome composition may lead to effective therapies for these difficult-to-treat tissues.

2.6 Conclusions

Adipose-derived mesenchymal stromal cell (AdMSC) exosomes (EVs) can improve tendon mechanical resilience, tissue organization, and M2 macrophage phenotype predominance in response to tendon injury. This active area of investigation drives great interest in the function of these exosomes as adjunct therapies for tendon disease, particularly rotator cuff tendinopathy. However, little is known about the effects of EVs as a function of cell source, nor regarding their efficacy in preclinical translational ovine models. Herein we demonstrated a differential effect of exosomes as a function of cell source, tenocyte as compared to AdMSC, on macrophage signaling and tenocyte migration of ovine cells. This not only sets a standard for the comparison of the human invitro model demonstrated in Chapter 3, but also sets up the methodology for generation and isolation of ovine tenocyte and AdMSC derived exosomes for use in future studies discussed in Chapter 4.

CHAPTER 3: INVITRO MODELING OF HUMAN EXOSOME AFFECT AS A FUNCTION OF CELL SOURCE ON EFFECTOR CELLS OF ROTATOR CUFF TENDINOPATHY

3.1 Overview

The high failure rate of surgical repair for tendinopathies has spurred interest in adjunct therapies including exosomes (EVs). Mesenchymal stromal cell (MSC) derived EVs (MSCdEV) have been of particular interest as they improve several metrics of tendon healing in animal models. However, research has shown that EVs derived from tissue-native cells, such as tenocytes, are functionally distinct and may better direct tendon healing. To this end, we investigated the differential regulation of human primary macrophage transcriptomic responses and cytokine secretion by tenocyte derived EVs (TdEVs) as compared to MSCdEVs. As compared to MSCdEVs, TdEVs upregulated TNFa-NFkB and TGFβ signaling, and pathways associated with osteoclast differentiation in macrophages while decreasing secretion of several pro-inflammatory cytokines. Conditioned media of these TdEV educated macrophages drove increased tenocyte migration and decreased MMP3 and MMP13 expression. In contrast, MSCdEV education of macrophages drove increased gene expression pathways related to INFa, INFg and protection against oxidative stress while increasing cytokine expression of MCP1 and IL6. These data demonstrate that EV cell source differentially impacts the function of key effector cells in tendon healing and that TdEVs, as compared to MSCdEVs, promote a more favorable tendon healing phenotype within these cells.

3.2 Introduction

Tendinopathies comprise one of the most widespread and economically significant diseases in developed nations. The societal value of rotator cuff tear (RCT) surgical intervention alone has been estimated at greater than 3.4 billion US dollars (USD) despite frequent repair failures (30-

79%) resulting in greater than 430 million USD in annual costs in the United States[3-6]. This socioeconomic burden has driven ever-increasing research interest in adjunct therapies to surgical repair of RCT, particularly into biologically active additions to graft matrixes[31,58].

Mesenchymal stromal cells (MSC) and their cell products have been of focused interest as they consistently demonstrate functional improvements at the biomechanical level in animal models[81,82]. These benefits have also been replicated using MSC derived exosomes (MSCdEVs) [46,47]. Exosomes (EVs) are 20-200nm diameter vesicles with targeting surface ligands and cargo comprised predominately of proteins, lipids and RNA[31,57-59]. They replicate the benefits of direct MSC therapy without the risks of working with live, and therefore phenotypically plastic cell lines. As research charges ahead with MSCdEVs it is important to ask if EVs derived from tissue native cells, tenocytes, may better direct tendon healing[57].

Much of the tendon pathology is thought to arise from a communication over-ride secondary to tissue degeneration and injury[57,58]. In health, tendon is primarily comprised of matrix components, > 90% of which may be collagen type 1 (Col1), maintained by a paucicellular network of tenocytes with cell-cell junctions that allow for direct communication[15,16,31]. As these junctions are lost or disrupted with injury and age, extrinsic communication can overwhelm this network, shifting guiding signals to exocrine and endocrine modalities, or juxtracrine signals from infiltrating cell types[15,131]. These changes in cell signaling are thought to direct the aberration of the native tissue reducing biomechanical strength and increasing the likelihood of tissue repair failure.

One of the principal cell types that infiltrate early and stay longest in tendon disease, contributing to the cell signaling milieu is the macrophage[33]. These innate immune cells play a large role in both the early pro-inflammatory phase of tendon healing, critical for removal of

damaged tissue and cell recruitment, as well as the later regenerative phase of matrix deposition, organization and cell population refinement[33,37,132,133]. Macrophages have thus become a focus of many research interests because of this pleomorphic role they play throughout the healing cascade especially their ability to communicate with native tenocytes. Additionally, there is ample evidence that EVs affect macrophage phenotype and behavior in tendinopathies and other conditions, such as neoplastic and infectious diseases; from shifting macrophage activation and polarization to priming regions for metastasis and directing immunotolerance[46,47,57,134]. EVs also have significant effects on tenocyte bioactivity and can direct MSCs to be more tenocyte like[57,71].

EVs have shown great potential to shape the tendon healing environment through the predominant cell types of tendon healing, macrophages and tenocytes[59,71,85]. Furthermore, animal models have demonstrated a significant effect of EV cell source on macrophage and tenocyte response[57]. Thus, we hypothesize that tenocyte derived EVs (TdEVs) as compared to MSCdEVs will drive differential expression at the RNA and protein levels in primary, human macrophages which in turn will differentially drive primary tenocyte bioactivity. In so doing, TdEVs will preferentially drive a tenogenic phenotype.

3.3 Materials and Methods

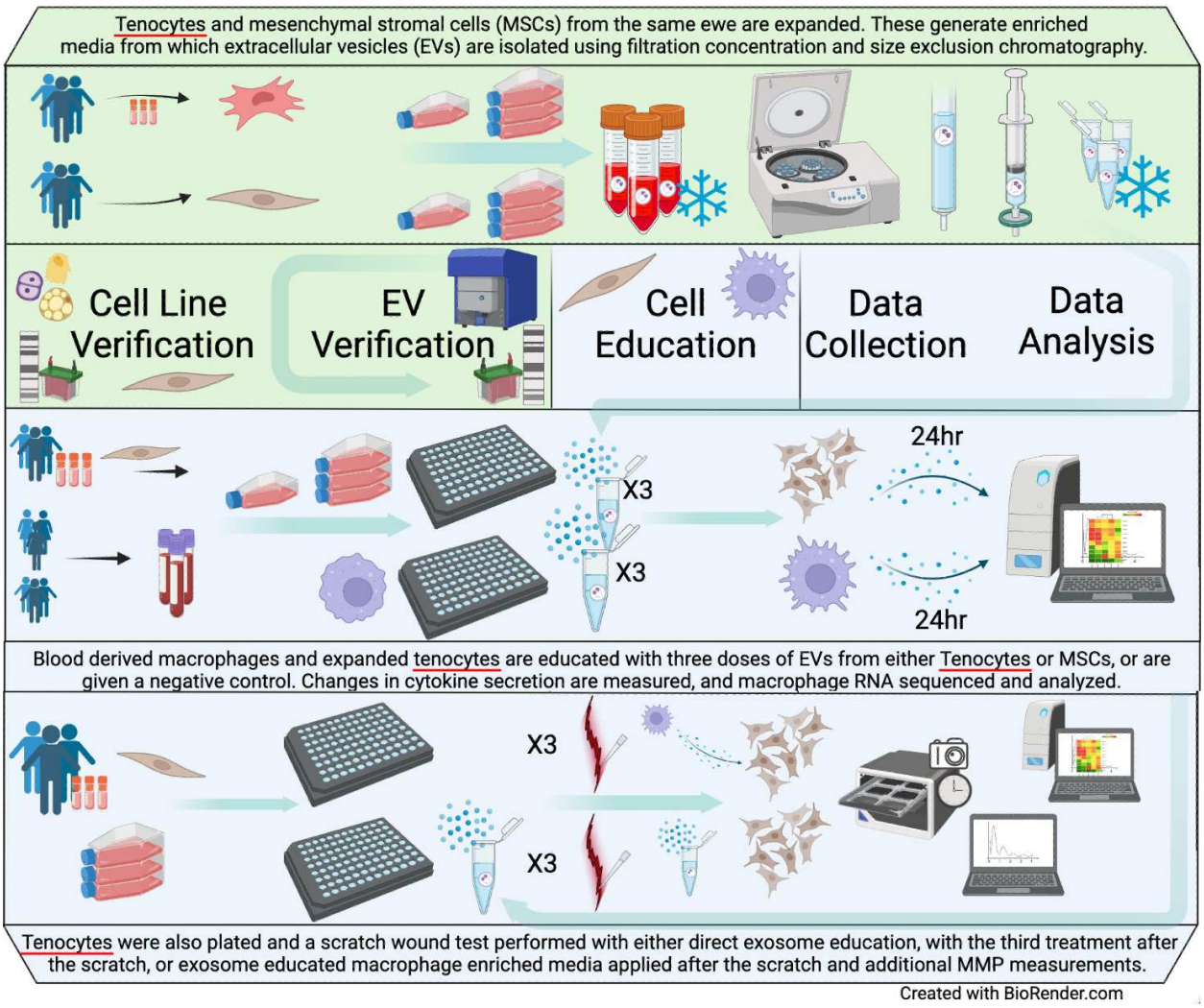

Figure 3.1. Graphical abstract of the experimental design. The top, green portion contains the workflow for exosome generation, while the bottom, blue portion contains the workflow for macrophage isolation and experimentation. In the top portion, left to right. Tenocyte isolation from a three donor males for cell propagation and characterization as well as propagation of three lines of AdMSCs from frozen stock, followed by cell enriched media pooling and storage at -20°C which is then filter concentrated for size exclusion chromatography to isolate concentrated, pure exosomes. These aliquots are then filter sterilized prior to characterization and storage at -20°C. In the middle portion from left to right, blood was collected from three adult males and three females, mononuclear cells were selected by Ficoll separation prior to selection of adherent monocytes. These monocytes are then plated prior to maturation and negative control or exosome education after which end point analyses were performed and exosome educated, macrophage enriched media aliquoted and pooled by gender and treatment group for indirect treatment of tenocyte scratch wound assays. In the bottom, blue panel, stock, frozen tenocytes from 3 adult males, biologically distinct from those of exosome generation, are thawed and propagated. Plates are prepared and tenocytes either go through direct exosome education of two doses 24hours apart prior to scratch and one dose after scratch, or just one dose of exosome educated macrophage

enriched media after the scratch. Cells are imaged over 24hours, and images analyzed for confluence of the wound closure, and indirect educated groups' media assessed for MMP secretion.

3.3.1 Cell Sources

All human donor tissues were deidentified with only age and sex as indicators (Essent Biologics). Given the tissue source, Colorado State University's Institutional Review Board (IRB) deemed approval unnecessary.

Tenocytes for EV generation were harvested from the anterior tibialis (n=2, age 41yo and 54yo) or biceps (n=1, age 35yo) tendon of skeletally mature, adult males (*Homo sapiens*) with no know clinical comorbidities. Postmortem interval to ice was <24 h, and total postmortem interval was <48hr. Work by our group, deemed that this time interval did not lead to aberrant gene expression in the tendon[135].

Tenocytes for scratch wound assays, EV uptake and cytokine assays were acquired from Angio-Proteomie (cAP-041; Boston, MA, USA, n=1, male, age 61yo) and Zen-Bio (TEN-F; Durham, NC, USA, n=2, male, ages 59yo and 87yo). These cell lines were derived from achilles tendon and expressed CD44, CD90, and CD105, were negative for CD45 and CD31 and were negative for HIV-1, HBV, HCV, and mycoplasma.

Peripheral blood-derived monocytes were isolated from blood drawn from clinically healthy, mature adults (male/female n = 3/3, ages 20-65yo) by standard protocols for SepMate (#15415; StemCell technologies, Vancouver, Canada) density gradient separation. The collection and use of blood was approved by the IRB (No. 4821).

3.3.2 Isolation and Culture of Tenocytes and MSCs for EV Production

Established methods for tenocyte isolation were followed; in brief, a 10 × 5 × 2 mm section of central tendon body core was enzymatically digested using 1mg/mL type 1 collagenase

(BP2649; Fisher Bioreagents) in 1:1 Dulbecco's Modified Eagle's Medium: Nutrient Mixture F-12 Ham with 15 mM HEPES and sodium bicarbonate (DMEM:F12, D6421; Sigma-Aldrich) with 200 units penicillin, 0.2mg/mL streptomycin, and 0.5mg/mL amphotericin B (Abx, A5955; Sigma-Aldrich). This was then filtered (100um, Cell Strainer, Z742101; Sigma-Aldrich), and washed, prior to resuspending and culturing the cells in DMEM:F12 with 10% Fetal Bovine Serum (97068-085, Avantor) and Abx (complete DMEM [CD]). Tenocytes were characterized by spindle morphology and light microscopic analysis and a positive Western blot for tenomodulin (TNMD; SAB2108237; Sigma-Aldrich), Col1, Tetraspanin-4 and Tenascin C (TNC; sc-25328; Santa Cruz Biotechnology). MSCs were purchased from Essent Biologics (ADMSCN001; Centennial, CO, USA) where they were isolated from mature adult adipose tissue (*Homo sapiens*) and verified for trilineage differentiation (chondrogenic, osteogenic and adipogenic) and immunoassayed for the presence of positive markers CD90, CD73, CD105, and CD44, and absence of negative markers of CD34, CD45, CD79, CD14, and HLA-DR. MSCs were cultured in identical conditions to Tenocytes.

3.3.3 EV Purification

Tenocyte and MSC were used to produce and isolate EVs using previously published protocols[57]. In brief, while at 80–100% confluence during passage 2-3, culture media were aspirated, cells washed with 5 mL of Dulbecco's phosphate buffered saline (PBS; D1408; Sigma-Aldrich), and flasks were filled with serum-free DMEM:F12 with Abx. After 24h, cell-enriched culture media were collected, cell debris was removed by centrifugation and supernatants were stored at −20°C. Cultures were then “rested” for 24h in CD prior to repeating wash and serum free media enrichment steps. After reaching 100% confluence for at least 24h, cultures were split and passaged.

Pooled within individual cell lines, cell-enriched media was filter concentrated (Centricon 70; UFC710008; Millipore Sigma) and EVs were isolated by size exclusion chromatography (qEV columns; QiZON, qEVoriginal). The fractions of the highest particle density (fractions 1-3) per EV quantification, were pooled and used for all experiments, unless otherwise noted.

3.3.4 EV Characterization

The size and concentration of EVs by isolated fraction was measured using the ZetaView QUATT 4 nanoparticle tracking analysis instrument (NTA) (ZetaVIEW software ver. 8.05.12 SP1; Particle Metrix GmbH). As per previously published methods, in brief, the overall concentration of each fraction of EVs was determined using the scatter mode of the NTA and counting of particles by size through Brownian motion analysis. Exosome content of EV isolates was then verified using Exo-Check™ Exosome antibody array (EXORAY210B-8; System Biosciences, Palo Alto, CA, USA) which confirms concentrated exosome related proteins CD63, EpCam, ANXA5, TSG101, FLOT1, ICAM1, ALIX, CD81 and compares to cell contamination marker GM130. Then EV concentrations were standardized using PBS as a diluent to pooled fractions (1:1:1 by particle count) to a final particle count of 2×10^7 particles/30 μL for use in cell education experiments.

3.3.5 Isolation of Peripheral Blood-Derived Monocytes

Isolated mononuclear cells were plated in technical and biological triplicate for each sex (n=54) in a 96-well plate (167008; Fisher ThermoScientific) at 1×10^6 cells/well in 200ul of a 1:1 solution of RPMI-1640 (10-041-CV; Mediatech, Manassas, VA, USA) with Abx and 10% fetal bovine serum (FBS; complete RPMI): 2%FBS in PBS (transport media) for 2h. The media was then syphoned, and the wells were washed twice with 100ul PBS to remove non-adherent cells, selecting for the adherent peripheral blood derived monocytes (PBMCs). PBMCs were cultured in

complete RPMI-1640 with 10 ng/mL human macrophage colony-stimulating factor 1 (MCSF-1; 300-25-10UG; PeproTech, Cranbury, NJ, USA) for 7 days, with media refreshed on day 3. From day 7 onward, PBMCs were considered macrophages [57,136,137].

3.3.6 EV Fluorescent Labeling and Uptake Imaging

Purified EVs were stained using PKH26 (MINI26-1KT, Sigma-Aldrich) lipophilic dye, quenched using 5% dextrose in water and washed twice in PBS using ultracentrifugation. PBS was treated and "stained" in parallel as a negative control. Macrophages were differentiated and cultured in parallel to those already described, under the same conditions in 75cm2 culture flask (156499, Thermo Fisher Scientific). On day 7 these cells were passaged to glass cover slips in a 12 well plate. Tenocytes (passage 5) were similarly plated on cover slips. Each well was dosed with 50 µL of "stained" controls or stained EVs (2×10^7 particles). Cells were then washed twice with PBS, fixed in 4% paraformaldehyde for 10 min, and counter stained with ActinGreen™488 ReadyProbes™ reagent (R37110; Thermo Fisher Scientific), and DAPI (EN62248; Thermo Fisher Scientific) before preservation in antifade mounting media (P36961; Thermo Fisher Scientific). Wells were then imaged using a spinning disc confocal microscope (IX83 P2ZF using CellSens Dimension v4.1, Olympus).[78]

3.3.7 Direct EV Education

On day 7, macrophage culture media were replaced with 170 µL of complete RPMI and 30 µL of treatment (1) PBS, (2) MSCdEVs, or (3) TdEVs with concentrations of 2×10^7 particles/30 µL. On day 8, an additional 30uL of the same treatments were added respectively. On day 9 the media were gently washed with serum-free RPMI:1640 and replaced with 170 µL of

serum-free RPMI and 30 μL of the respective treatments. After 24h, on day 10, the media were collected, and cell debris was removed by centrifugation.

Similarly, 3 cell lines of tenocytes, biologically distinct from those used for EV generation, were seeded at 3 x 10^5 cell per well in a 96 well plate in technical triplicate. These cells underwent the same treatment protocol as the macrophages replacing RPMI:1640 with DMEM:F12, receiving their first treatments on the day of seeding, and the subsequent 24h periods. Cell achieved confluence in the first 24-48h.

Supernatants were aliquoted and stored at −20°C. Thus, the cultured wells (macrophage n = 54, tenocyte n = 27) were comprised of six macrophage lines from three male and 3 female individuals, respectively, and 3 lines of tenocytes (from male donors) which were given one of three treatments in technical triplicate.

Supernatants were assessed for matrix metalloproteinase (MMP) cytokine and growth factor product by a multiplexed enzyme-linked immunosorbent assay kit (MILLIPLEX MAP KIT, Human MMP Magnetic Bead Panel 1, HMMP1MAG-55K; Human Cytokine/Chemokine/ Growth Factor Panel A, HCYTA-60K, Millipore Sigma). These bioassays measured concentrations of MMP3, MMP12, MMP13, EGF, ETXN, GCSF, GMCSF, IFNA2, IFNG, IL10, IL12, IL10, IL12p40, IL12p70, IL13, IL15, IL17A, IL1A, IL1B, IL1RA, IL2, IL3, IL4, IL5, IL6, IL7, IL8, IP10, MCP1, MIP1A, MIP1B, TNFA, TNFB and VEGFA. The mean fluorescent intensity of each set of technical triplicates was used for statistical analysis.

3.3.8 Tenocyte Migration and Bioactivity

Tenocytes from passage five were plated in a 96-well plate (ImageLock, 4379; Essen Bioscience) at a density of 3x10^5 cells/well and treated either with EVs or a PBS negative control as described above, or were cultured in CD and at the time of the third treatment were given 100ul

EV-educated-macrophage (EVedM) conditioned-media (CM): 100uL 1%FBS in DMEM:F12 with Abx. Prior to this third treatment day, or treatment with EVedM-CM, a uniform scratch (scratch-wound) was made in each well using a p200 pipette tip and each well was washed twice with 150 µL PBS. Cells were then cultured in their respective treatments and serial temporal images were taken of each well using an automated plate scanner (IncuCyte™, Essen BioScience) every 3hr for 24h. Automated image analysis was used to measure the percent change in area of the decellularized scratch. Cultures were performed in technical and biological triplicate.[138]

After this 24h period, cell supernatants of the EVedM-CM treated tenocytes were collected and processed for analysis by the Human MMP Magnetic Bead Panel 1, for production of MMP3, MMP12 and MMP13.

3.3.9 Macrophage EV Education RNA Sequencing

After removal of the EVedM-CM from the cell supernatants, macrophages were washed in PBS prior to RNA extraction using a RNeasy mini kit (Qiagen, Hilden Germany) during which technical triplicates were pooled. Isolates were stored at -80C prior to sequencing at Novogene Corp (Novogene Co., Sacramento, CA) on the Illumina platforms. Several samples were culled from the analysis pipeline due to quality control leaving two of each biological triplicate with the exception of the male macrophage lines treated with the negative, PBS, control for which only one passed quality control (n = 11). Primary Bioinformatics was performed by Novogene, including quality control, mapping to reference genome, structure analysis, gene expression quantification, differential expression analysis and enrichment analysis. Gene set enrichment analysis was further explored using GSEA (GSEA 4.2.2; Broad Institute, Inc., Massachusetts Institute of Technology, and Regents of the University of California). Protein-protein interaction analysis was further assessed using Cytoscape (Cytoscape 3.10.1) based on STRING (String Consortium, 2023,Version

12.0, https://cn.string-db.org) with the plugin cytoHubba for maximal clique centralities to further predict important nodes and subnetworks of the initial network.

3.3.10 Statistical Analysis

Statistical analyses were performed using Graphpad Prism9 software. Cytokine, growth factor and MMP assays were assessed by mean fluorescent intensity unless otherwise specified, across experimental and control groups. A two-way analysis of variance (ANOVA) was used to compare the overall difference between the experimental and control groups. Shifts in analyte levels between experimental groups was compared using a multiple paired *t*-test analysis with data paired by biological donor. Scratch-wound confluence data were evaluated for the treatment group and time factors using multiple Wilcoxon tests and collectively using indirect mixed effect analysis. Significant discoveries were considered for those with q and *p*-values <0.05 unless otherwise specified.

3.4 Results

3.4.1 EV Characterization

Purity and consistency of EV's was assessed. Median particle size of TdEVs and MSCdEVs were 90nm and 120nm respectively (Figure 3.2). Exocheck immunoblot assay

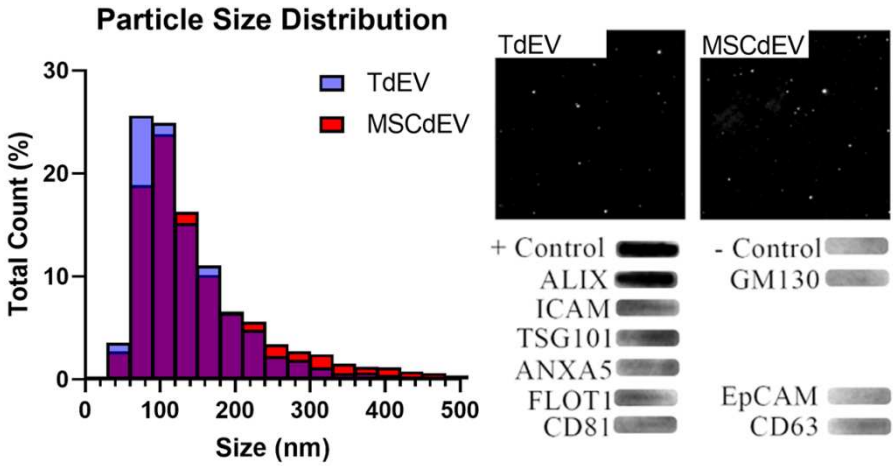

demonstrated strong positive signals for ALIX, TSG101, ICAM, FLOT1, ANXA5 and weak signals for CD81, CD63, and minimal to absent signal for EpCAM and GM103 a cell debris contamination marker (Figure 3.2). These size ranges and markers are consistent with an exosome predominant population of EVs[63].

Figure 3.2. Exosome characterization including size distribution (left; median diameters: TdEV 90nm, MSCdEV 121nm), representative photomicrographs (upper right), representative protein blot of lysed exosome concentrate. Exo-check protein blot includes exosome markers ALIX, ICAM, TSG101, ANXA5, FLOT1, CD81, EpCAM and CD63 as well as cell debris marker GM130 and positive and negative controls. Discrete blot lines are considered strongly positive for ALIX, weakly positive for ICAM, TSG101, ANXA5, FLOT1, very weak for CD81 and CD63 and negative for GM130 and EpCAM.

3.4.2 In Vitro Assessment of Tenocyte and Macrophage Uptake of EVs

Next, to confirm our target cells' ability to uptake our EVs, we observed accumulation of fluorescently labeled exosomes from both cell sources by confocal microscopy compared to negative controls. Tenocytes and macrophages were treated with fluorescently labeled EVs for 4 h prior to fixation and contrast staining, after which punctate fluorescent aggregates were observed to have localized within the cytoplasm, consistent with EV uptake (Figure 3.3).

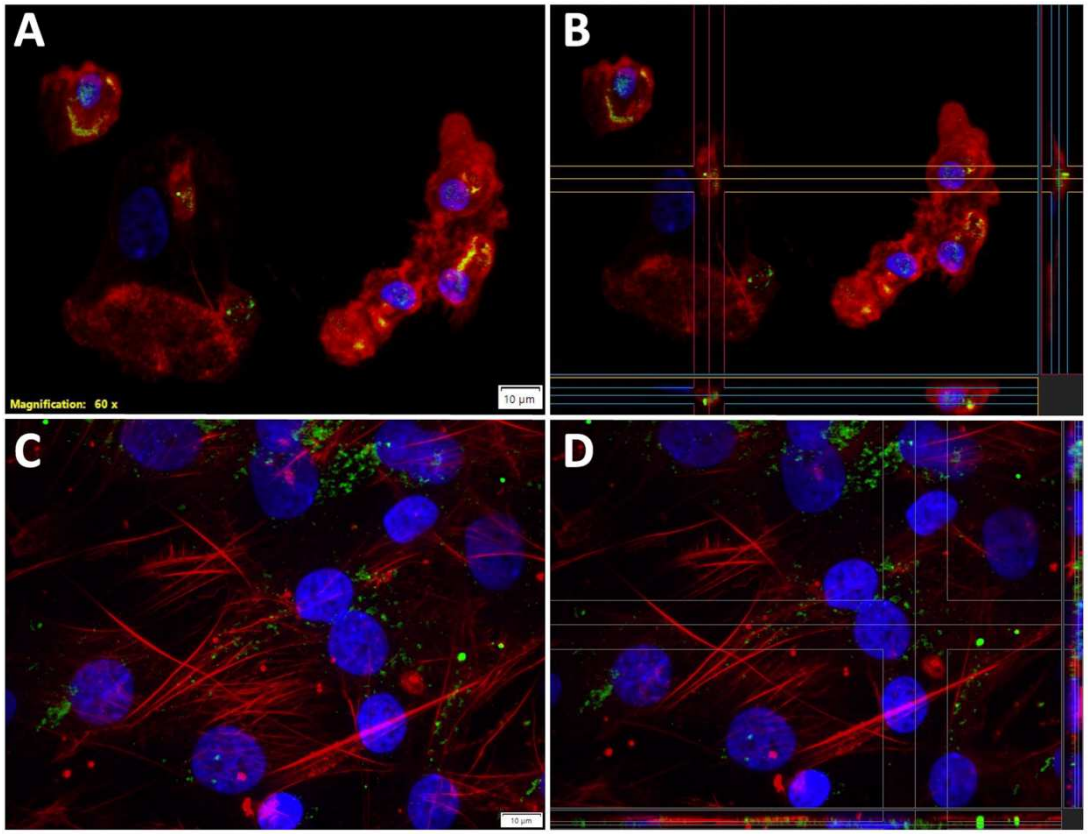

Figure 3.3. Representative confocal microscopy of exosome uptake. Intracellular accumulation of exosomes is demonstrated 4 hours post treatment with PKH26 labeled exosomes (green) within both macrophages (A-B) and tenocytes (C-D) taken using a 60x, oil emersion objective. A and C represent flattened Z stacked images, while ranged orthogonal slices of the z-stacks in B-D confirms that the punctate exosome accumulations are within the cytoplasm of the cells.

3.4.3 Macrophage and Tenocyte Protein Secretion in Response to Direct Exosome Education

The effect of EV education as a function of cell source and as compared to negative, PBS, controls was examined across 3 female and 3 male (n=6) PBMC derived primary macrophage cultures and 3 male (n=3) tenocyte cell lines all run in technical triplicate. Post education period, washed cells were given serum free media to enrich over 24h. These supernatants were then assessed using a multiplex immune assay.

Macrophages demonstrated a significant difference in protein secretion levels. While many proteins assessed were below the limit of detection, MCP1/CCL2 experienced the largest shift in secretion with a 11502.9pg/mL (93.0%) and 9230.6pg/mL (91.5%) reduction in secretion by TdEV educated macrophages as compared to MSCdEVedM and PBS-edM respectively (Figure 3.4, A). Similarly, IL8 and IL6 were also reduced by 590.7pg/mL (77.3%) and 24.8pg/mL (90.8%) respectively when compared to MSCdEVedM and 420.3pg/mL (70.7%) and 15.4pg/mL (86.0%) when compared to the negative control. Interestingly this decrease in inflammatory cytokines was inverted, though not significantly so, in directly educated tenocytes with MCP1 secretion reaching nearly 112.8pg/mL (34.2%) and 70.8pg/mL (21.5%) increases over the negative control in TdEV and MSCdEV education conditions respectively (Figure 3.4, B).

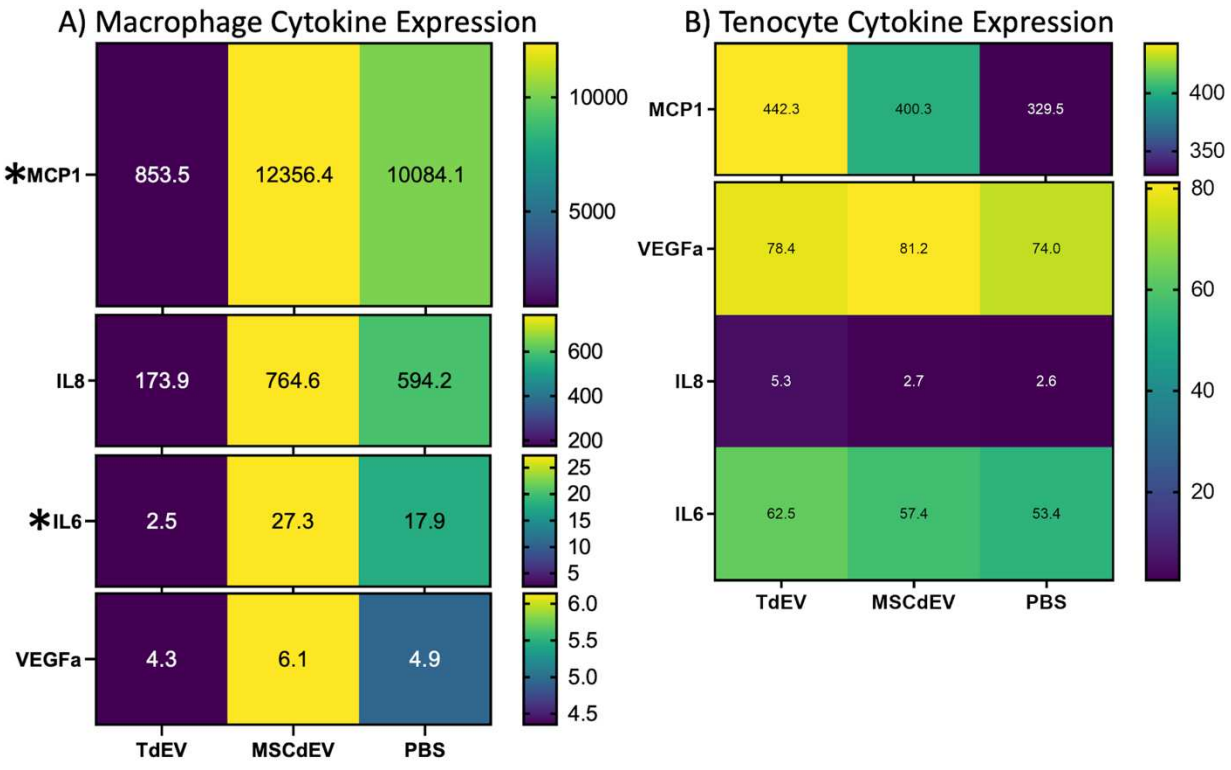

Figure 3.4. A) Cytokine expression by macrophages in response to education by TdEVs, MSCdEVs or PBS. Macrophages were dosed every 24hours for 3 doses, starting at day 7 of macrophage differentiation from PBMCs, of $2.7x10^8$ particles or a negative PBS control of equal

volume. Macrophages then conditioned serum free media over 24hours prior to cytokine measurement using a multiplex immunoassay. Mean pg/mL is displayed in a variably scaled heat map. Statical significance is indicated by * where $p<0.05$ using a multiple paired t-test. B) Cytokine expression by tenocytes in response to education by TdEVs, MSCdEVs or PBS. Tenocytes were dosed every 24hours for 3 doses of $2.7x10^8$ particles or a negative PBS control of equal volume. Tenocytes then conditioned serum free media over 24hours prior to cytokine measurement using a multiplex immunoassay. Mean pg/mL is displayed in a variably scaled heat map. Statical significance was not reached for these cytokines.

3.4.4 Macrophage Transcriptomic Profile After EV Education

Following supernatant extraction for protein analysis, RNA was extracted from the macrophages for transcriptomic analysis as a function of EV source of education and as compared to PBS controls, here technical triplicates were pooled, but biological replicates were preserved (n=6, 3 female: 3 male). There were 418 and 611 differentially expressed genes under TdEV and MSCdEV educated conditions, respectively. Among differentially expressed genes, TdEVedMs increased expression of PPARG, FOS, FOSB, SRC, JUN, MEF2C, BMP2, MAPK6, MAPK13, ITSN1, DUSP1, IL1R1, NFIL3, ADRB1, LIPG, LRFN2, GNA13, MMP8, IL6R and ANXA2 while down regulating ZAP70, IFNG, IFNAR, TLL1, ANGPTL6, CENPM, IL3RA, BIRC5, SPC24, BUB1B, IL7R, CXCL9, CCL5, LTBP4, CCL1, TNFSF13, NUP37, ZWILCH, LTBP4, CDCA8 (Figures 3.5-3.7, Table1).

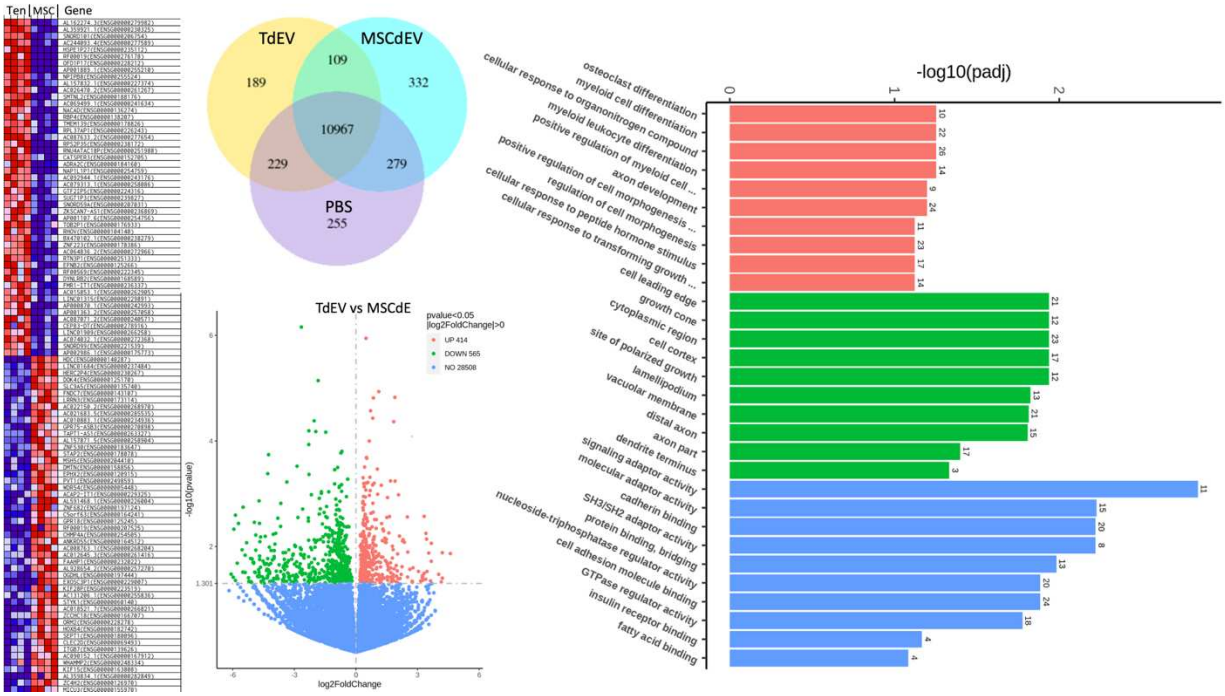

Figure 3.5. Differential gene expression of TdEV vs MSCdEV treated macrophages and analysis. Macrophages were dosed every 24hours for 3 doses, starting at day 7 of macrophage differentiation from PBMCs, of $2.7x10^8$ particles or a negative PBS control of equal volume. Macrophages then conditioned serum free media over 24hours prior to RNA isolation. Left: heat map of top differentially expressed genes, red is higher expression, blue relative repression, left 4 columns are TdEV treated macrophages, right, 4 columns are MSCdEV treated. Top Central: a vendiagram of the differentially expressed genes across all treatment groups. Lower Central: A volcano plot of differentially expressed genes, TdEVedM vs MSCdEVedM, plotting –log10 of the p value over log2fold change. Right: Gene Ontology (GO) showing the top 10 categories by –log10 of the padj score, which include Biological Processes (BP) such as osteoclast differentiation and cellular response to transforming growth factor beta; Cellular components (CC) like cell leading edge and dendrite terminus; Molecular Functions (MF) like protein binding, bridging and cell adhesion molecule binding.

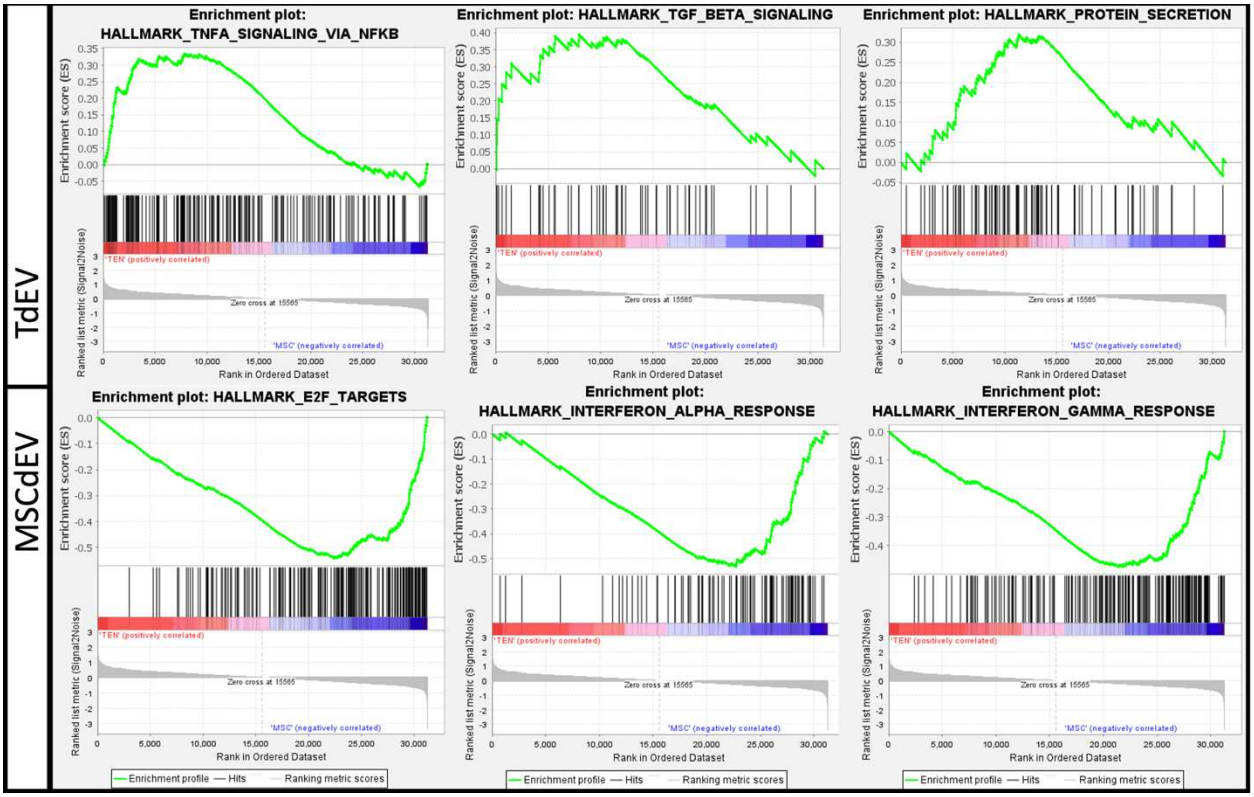

Figure 3.6. The six significantly differentiated Hallmark Gene profiles distinguished by GSEA analysis of TdEVedM as compared to MSCdEVedM gene expression. The upper three graphs demonstrate the upregulated hallmarks of TdEVedM, TNFα signaling via NF**κ**B, TGFβ Signaling and Protein Secretion while the bottom three demonstrate those upregulated in MSCdEVs, E2F targets, IFNα response and IFNγ response.

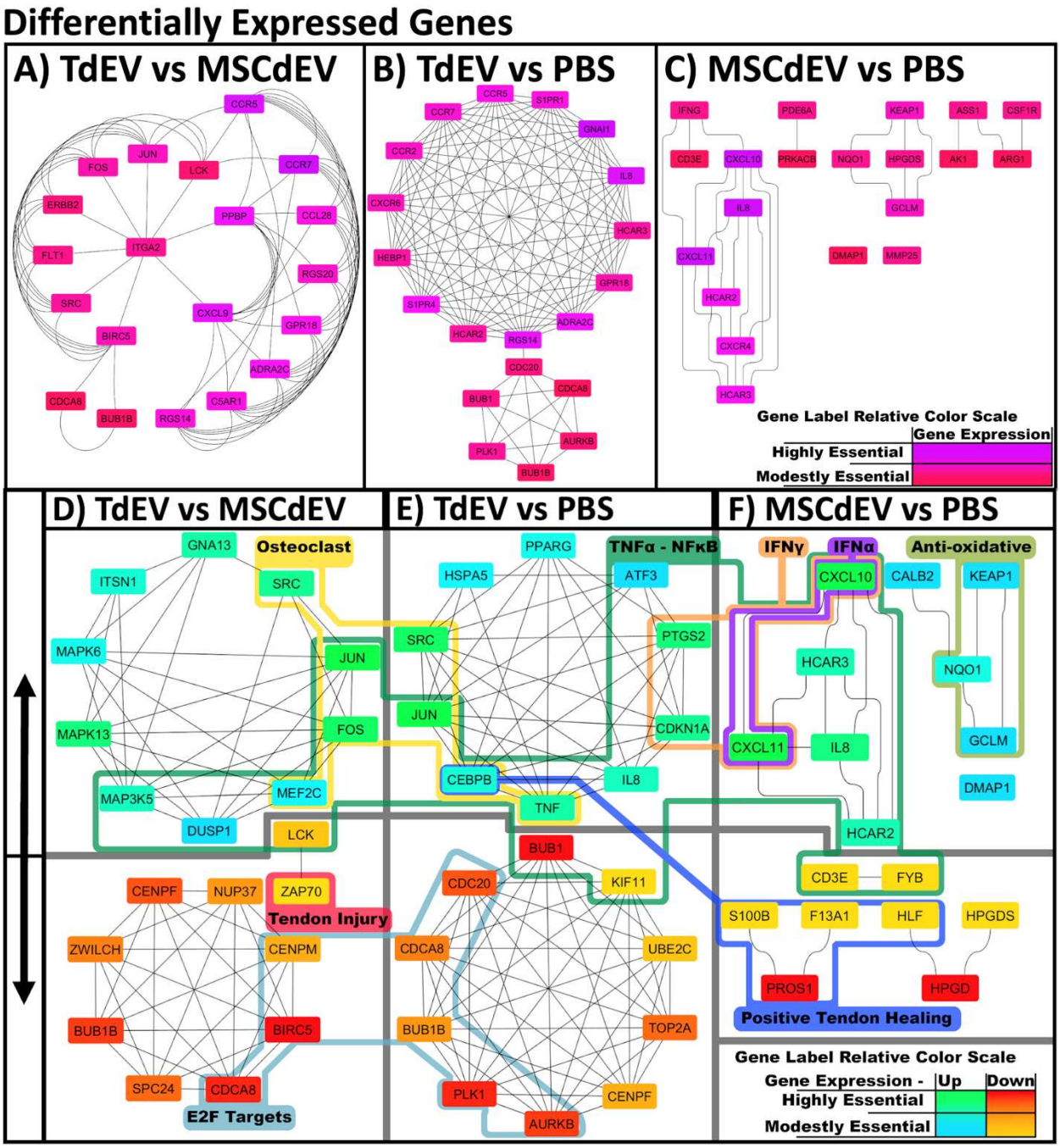

Figure 3.7. Protein-protein interaction networks are generated for all differentially expressed genes for A & D) TdEVedM vs MSCdEVedM, B & E) TdEVedM vs PBSedM and C & F) MSCdEVedM vs PBSedM. Networks A-C are based on all differentially expressed genes (ranked red to purple), while those in D-F are formed based on the up regulated genes (upper, ranked blue to green) and down regulated genes (lower, ranked red to yellow). These maps highlight the 20 (A-C) or 8-10 (D-F) maximal clique centralities of the overall networks. Cytoscape (Cytoscape version 3.0) based on STRING (String Consortium, 2023, Version 12.0, https://cn.string-db.org) protein interaction database and further simplified using Cytohubba plugin for Maximal Clique Centralities where color infers gene rank based on degree of instructiveness within the network.

Layouts were generated radially, circularly, or hierarchically based on degree of connection overlap and ease of interpretation. In panels D-F, genes linked to functional groups of the discussion and/or GSEA analysis are outlined in varying colors. These groups include osteoclast differentiation related genes, TNFα signaling via NFκB and regulators thereof, IFNα and IFNγ related signaling, antioxidant production and response to oxidative stress, indicators of tendon injury and tendon healing, and E2F targets.

Table 1. TdEV vs MSCdEV Macrophage Education Gene Expression

TdEV vs MSCdEV Macrophage Education					
Up Regulated			Down Regulated		
Gene Symbol	pValue	Log2 Fold Change	Gene Symbol	p Value	Log2 Fold Change
ADRB1	0.034	4.03	TLL1	0.046	-5.21
LIPG	0.009	3.67	CCL1	0.023	-3.52
LRFN2	0.019	3.67	IFNG	0.003	-2.31
FOSB	0.003	3.32	CENPM	0.006	-1.47
MMP8	0.003	2.50	IL3RA	0.002	-1.46
BMP2	0.006	2.12	CXCL9	0.002	-1.43
FOS	0.042	1.05	BIRC5	0.018	-1.33
DUSP1	0.005	0.98	SPC24	0.012	-1.16
IL1R1	0.012	0.56	BUB1B	0.023	-1.15
NFIL3	0.003	0.52	CDCA8	0.019	-1.09
PPARG	<0.001	0.51	ANGPTL6	0.047	-1.06
MAPK13	0.004	0.47	CCL5	0.001	-0.78
ITSN1	0.004	0.46	IL7R	0.003	-0.76

ANXA2	0.001	0.46	ZAP70	0.010	-0.74
MAP3K5	0.011	0.46	CENPF	0.024	-0.73
JUN	<0.001	0.42	LCK	0.005	-0.71
MAPK6	<0.001	0.40	LTBP4	<0.001	-0.68
IL6R	0.001	0.37	TNFSF13	0.036	-0.55
MEF2C	0.041	0.36	IFNAR	0.041	-0.54
SRC	0.029	0.26	NUP37	0.032	-0.41
GNA13	0.017	0.24	ZWILCH	0.038	0.36

Table 1. Select significantly up (left) and down (right) genes including the p-values and Lo2 Fold Change. Genes were selected based their relevance to the discussion and/or their fold change.

3.4.5 Tenocyte Response to EV Educated Macrophage Conditioned Media

Scratch wound modeling of the three tenocyte lines that were directly educated and cultured for 24h post scratch-wound, or treated post scratch-wound with EVedM-CM and cultured for 24h was assessed using automated scratch wound analysis of images taken every 3h. While there was an increase in confluence with direct EV treatment irrespective of cell source, compared to negative controls, interestingly, there was a more significant increase in wound closure in the group treated with TdEVedM-CM compared to negative controls and PBS-edM-CM as well, than that of MSCdEVedM-CM treated tenocytes (Sup.Figure 1). The 9h timepoint was dropped due to an imaging frame shift across all samples. Resulting supernatants were assessed for MMP production. While MMP12 secretion levels were often below the limits of detection, TdEVedM-CM treatment resulted in significant reduction in MMP3 and MMP13, while MSCdEVedM-CM treatment resulted in increased MMP3 and a lesser decrease in MMP13 (Figure 3.8).

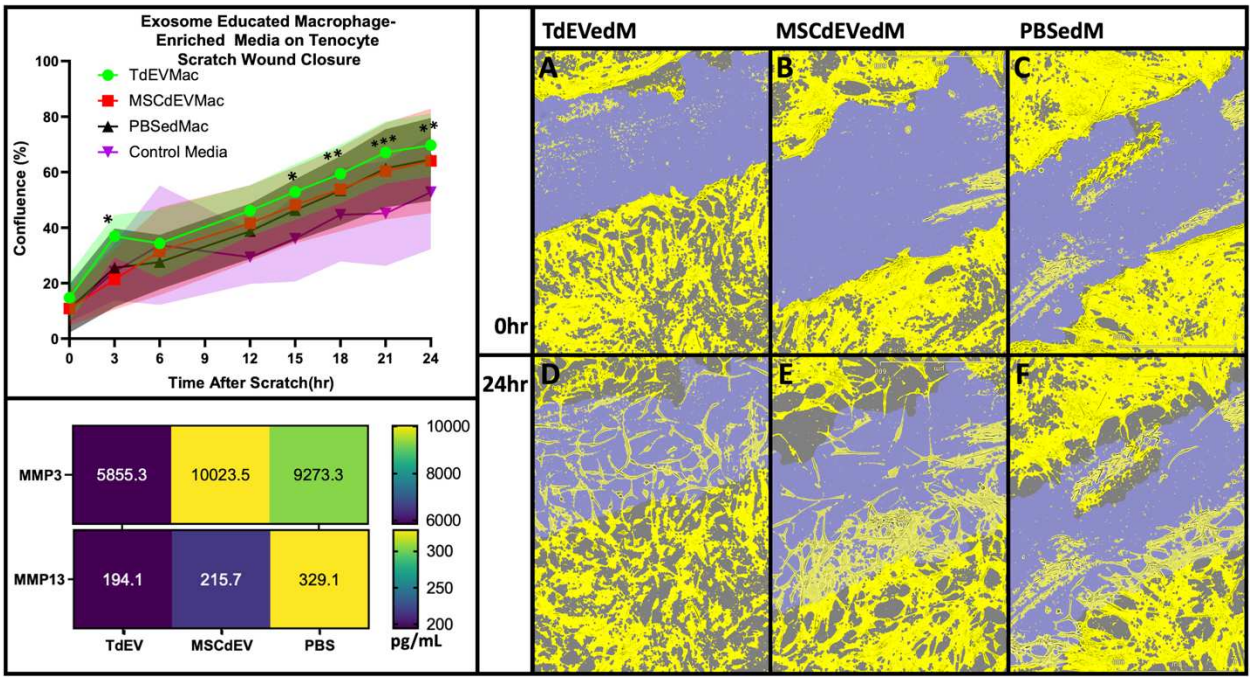

Figure 3.8. Tenocyte treatment with EV educated macrophage conditioned media (edM-CM) as compared to negative control. Top Left: There was a significant difference in percent confluence over time based on treatment (mixed effect $p<0.001$, treatment effect $p=0.002$; Indirect Mixed Effects Analysis) where TdEVedM-CM treated (top left) was consistently significantly different as compared to the control media (* p= 0.01-0.05, ** p=0.001-0.01, *** $p<0.001$; Multiple Wilcoxon). Bottom Left: MMP generation in pg/mL after 24hours of treatment. Representative images of tenocyte scratch-wound with functional masking, yellow for cell body, blue for original scratch-wound immediately after wound induction (A-C) and after 24 hours of growth (D-F). Tenocytes were either treated with TdEVs (A&D) MSCdEVs (B&E) or a negative PBS control (C&F).

3.5 Discussion

To expand on previous studies showing differences in the effect of EVs as a function of cell source and their potential for tendon healing, we sought to determine how primary, human, TdEVs as compared to MSCdEVs would drive the cellular response of the two most studied cell types of tendon disease and regeneration, tenocytes and macrophages[37,44,57]. We successfully isolated and characterized EVs from primary, donor derived tenocytes and AdMSCs in their early passages (passages 1-3). Importantly this limited passage number helps avoid cell phenotypic drift but, for tenocytes, necessitates working with direct tissue samples from healthy donors to have

sufficient productive cells, limiting biological variability (n=3 for TdEV and MSCdEV). These EVs were of the appropriate size range and demonstrated protein expression consistent with exosomes. Additionally, they were taken in by both target cell populations[59,63].

Most notably, TdEVs preferentially decreased pro-inflammatory marker secretion of macrophages, MCP1/CCL2, IL8/CXCL8 and IP10/CXCL10 and while direct education of tenocytes with TdEVs and MSCdEVs showed similar scratch wound healing rates, indirect education with TdEVedM-CM preferentially drove scratch wound healing and decreased secretion of MMP3 and MMP13 by these tenocytes, which can breakdown matrix and weaken tendons[44,133,139,140].

Inflammation plays a dynamic role in tendon healing. While inflammation may drive pain, and negative clinical measurements, in the early phases of tendon healing it is critical to initiate the tissue, and especially the matrix, turnover needed to allow for *de novo* tissue formation and return of function[132,141,142]. Macrophages play a predominant role in this, and proper healing occurs through their working in concert with local tenocytes[132]. Because of this, it is unsurprising that we find a differential effect of EVs on macrophages' proinflammatory profile. Where MSCdEVs appear to drive a IFN gamma, IFN alpha and IL-8 predominant inflammatory pattern, TdEVs drive a TNFα predominant profile through the NFkB pathway.

TdEVs additionally drive TGFβ signaling, which, acting in concert with the NFkB pathway, may be responsible for the increased tenocyte bioactivity observed as both have been found to drive tenocyte replication and recruitment[48]. Analysis of the key hub genes highlighted by the protein-protein interaction networks indicates there is a consistent appearance of genes related to NFkB pathway and TNF regulation with distinct promoting pathways in the TdEVedM including upregulation of MAP3K5, DUSP1, MEF2C, PPARG and TNF with down regulation of

LCK and BUB1, whereas MSCdEVedM demonstrated upregulation of CXCL10, CXCL11, HCAR and HCAR3 with down regulation of CD3E and FYB (Figures 3.6-3.7, Table 1).

Both treatments appear to upregulate IL8 compared to the PBS-edM controls. Notably, while TdEVs appear to upregulate TNFα-NFkB pathway, they also direct it away from proinflammatory cytokine production, possibly through BMP2, DUSP1 and MEF2C which downregulate proinflammatory and M1 related protein expression that can be driven by TNFα-NFkB and/or promote the M2 phenotype[143-145]. This is supported by the reduced expression of inflammatory cytokines, measured using the multiplex immunoassay, observed in response to TdEVed (Figure 3.4). Furthermore, TdEVs show gene set enrichment consistent with increased protein secretion suggesting that while there were lower levels of cytokines measured by the multiplex immunoassay employed here, these EVedM may be communicating or interacting with their surroundings more beyond the scope of the cytokines and growth factors this assay includes. For instance, the upregulation of IL6R by TdEV education may be consistent with reshaping of these macrophages' communication means toward a tenogenic phenotype[33].

When considering distinct pathways associated with tendon healing and mechanical performance, it is interesting that while TdEVedM upregulate CEBPB which is correlated with improved tendon mechanics, and down regulated ZAP70 which has shown to increase in relation to collagen disorganization, MSCdEVedM demonstrate downregulation of several hub genes generally associated with improved tendon outcomes (s100B, F13A1, HLF and PROS1)[17,49-54].

Additionally, several differentially regulated genes by TdEV education appear related to osteoclast differentiation (FOS, JUN, SRC, BUB1, KIF11, MEF2C)[139,146-151]. Functionally, this may correlate to Col1 predominant tissue repair/replacement, especially in light of some of the most differentially expressed genes; increased BMP2's promotion of M2 polarization and local

tenocyte activation with elevated FOSB, while decreased TLL1 levels may help damaged tissue breakdown[152-155]. Whereas MSCdEVs favored upregulation of genes associated with oxidative stress resilience and antioxidant production (KEAP1, NQO1, GCLM), which are also valuable to tissue repair[156-161].

These findings together demonstrate a significant shift in macrophage phenotype and macrophage effect on tenocytes in relation to the cell origin of EVs used to educate them. TdEVs may preferentially drive a tenogenic phenotype, as compared to MSCdEVs. The data presented here will inform future studies and contextualize past studies as to potential therapeutic implications of EVs as a function of cell source.

Of particular interest are in vivo investigations of the effects of differential EV constituents. The in vitro nature of this study limits direct inference and animal models will be necessary to see how the many facets of tendinopathies may be affected. These data, however, allow for some direct comparisons to animal models such as large, ovine, and small, mouse and rat, models[47,57,58].

To increase the ability to compare these data to past works, and control for additional variables, both tenocytes and AdMSCs used for EV generation were cultured in identical media conditions. While these conditions work well with these cell lines, these cell types may react differently under different culture conditions and thus shape their EV cargo to different effect[82]. Separately, biological variability was limited in the study due to tissue and cell line availability, limiting tenocyte and thus EV origin lines to male, where male and female macrophage lines were both employed. While AdMSC lines of both sexes were available, the use of only male lines of the same number as the tenocytes was opted for consistency. Further work to clarify potential difference by donor demographics is warranted.

Together, these data demonstrate that key cells of tendon healing, macrophages and tenocytes, are differentially affected by EVs per their cell origin, MSC as compared to tenocyte derivation. From TdEVs' TNFα and TGFβ predominate macrophage phenotypes with osteoclast like gene expression and reduced inflammatory cytokine production that increases tenocyte bioactivity to MSCdEVedM's interferon weighted response with more anti-oxidative gene expression and heightened levels of inflammatory cytokine expression that increases tenocyte MMP3 production. We know from animal models that EVs of both cell origins may benefit tendon healing. Given their differential effects, they may both serve a synergistic role in helping us reach better intervention in tendinopathies.

3.6 Comparison to Ovine Model

In both the cell lines presented here and the ovine cell lines discussed in Chapter 2 there was an effective shift in macrophage and tenocyte responses to exosome education as a function of exosome cell source. As these exosomes and their cell sources were propagated, generated, collected, isolated and characterized following the same methodology this establishes grounds for comparison between the two lines of investigation.

It is interesting to note that in both species the macrophages educated by either exosome cell source showed what could be considered a pro-inflammatory response based on the protein secretion profiles and gene expression patterns, be it through the TdEV-MIP1α vs MSCdEV-IL1β predominance in ovine or TdEV-TNFα vs MSCdEV-IFN, MCP1 and IL6 predominance in Human cell lines. This speaks to the complexity of the immunologic response and the importance of contextualizing it within the tendon microenvironment. An example being how the RNA sequencing data discussed in this chapter showed TdEVs driving macrophages toward an osteoclast like expression profile. This could reflect a pro-inflammatory like phenotype that is focused toward tissue remodeling, a needed quality in early tendon healing, and could be driven

by TNFα signaling via NFkB, in conjunction with TGFβ to trigger collagen remodeling and deposition while suppressing osteoblastic differentiation[162].

In both species, treatment with TdEVs appeared to favor a tenogenic response in macrophages through a decrease in angiogenic growth factor secretion in ovine lines and an increase secretion of cytokines linked to higher Col1 deposition. TdEVs were also consistent in demonstrating an overall decrease in secretion of most cytokines in relation to both MSCdEV treatment and PBS treated negative controls. Interestingly, in these lines there was a nominal increase in TNFα secretion in response to MSCdEV education contrasting to the human lines were TNFα signaling appeared upregulated at the RNA level in response to TdEV education. In the human cell lines, it is the increased tenocyte bioactivity, decreased MMP secretion and increased TGFβ signaling that drive the conclusion of an increased potential for Col1 secretion[33,71]. TGFβ, in particular, is used as a means of macrophage-fibroblast cross talk, promoting tenocyte activity and Col1 secretion [33,70,162].

3.7 Conclusions

Exosomes (EVs) can direct tendon cells, including tenocytes and macrophages, toward better tissue healing outcomes in humans and sheep, driving interest in their adjunct-therapeutic potential to treat tendon diseases, like rotator cuff tendinopathy. Mesenchymal stromal cell (MSC) derived EVs have served as a launching point toward this end, however, cell origin can dramatically change the effect of EVs on target cells. In animal models, tissue-native cell derived EVs have shown the potential to better direct tissue healing toward original function. Herein we demonstrated the effect of EV cell origin, tenocyte vs MSC, on macrophage protein and gene expression, and subsequent direct and indirect effects on tenocyte bioactivity. Furthermore, this work sets a grounds for comparison to the ovine cell line work demonstrated in Chapter 2, creating

a foundation for the translation of future in vivo works in the gold standard large animal model discussed in Chapter 4.

CHAPTER 4: CONCLUSIONS AND FUTURE DIRECTIONS

4.1 Overview

Where Chapter 1 set the foundation for why rotator cuff tendinopathy is a significant individual and societal problem, the basic science behind tendon healing functional outcomes and how exosomes may act upon them, Chapter 2 and 3 developed a basis for translation of these exosome effects as a function of cell source between humans and the gold standard, translational, large animal model. Here we will discuss how this informs the future directions of investigation into exosomes as potential bio-therapeutics for rotator cuff tendinopathy. This will include the augmentation of exosome content, how exosomes may be applied to in vivo studies and applications and how functional outcomes can be assessed at the tissue level in the context of current literature as well as preliminary explorations into imaging modalities.

4.2 Introduction

Exosomes transport protein, lipid, and nucleic acid cargo while specific surface receptors make them targeted mediators of intercellular communication. EVs are considered the primary paracrine effectors of MSC-mediated suppression of inflammation, and improved healing of tendons[163,164]. As covered in Chapters 2 and 3, their impact on target cells or tissues, and thus their composition changes depending on the cell source of origin. In human and ovine macrophages, TdEVs appear to preferentially decrease inflammatory cytokine expression with the exception of MIP1α and direct signaling toward and TGFβ and TNFα via NFkB predominant pathways, driving an osteoclast like phenotype at the RNA expression level. Meanwhile MSCdEVs expression demonstrated increased interferon signaling and increased inflammatory cytokine expression,

especially IL1β in ovine cells and MCP1 in human cell lines. In the context of other bodies of work, this suggests that exosomes of these cell sources may improve tendon healing and mechanics by distinct means.

Several studies have explored some of the discrete means by which exosomes may either have a specific affect or may be manipulated to do so[163,165,166]. Some methods include cell or physiologic conditioning prior to exosome collection or loading of exosomes with specific molecules or compounds of interest[163,165,166]. Of particular interest in the research community is the inclusion of miRNAs as these otherwise lack a ready means of delivery to specific targets. Other areas of research explore delivery mechanisms for exosomes from direct to systemic injection to suspension in a gel or matrix[47,163,167].

By establishing these methods of exosome generation, isolation and characterization from cells of interest for rotator cuff tendinopathy (RCT), as well as part of the basis for their biological function on the effector cells of RCT, we now have a comparative basis on which to investigate the in vivo effects of these exosomes as a function of cell source in the gold standard large animal translational model[17,18,168].

4.3 Exosome Content Shaping

4.3.1 Exosome Content Consistency

EVs are cell-derived packets that deliver various functional molecules (e.g., proteins, bioactive lipids, and messenger and micro-RNAs) to select recipient cells[169-172]. Though some variability is known to exist between exosome biological replicates, these replicates can be limited to conserve statistical power across biological replicates of treated samples or animals[173]. This practical and ethical limitation is why studies commonly limit exosome biological replicates to single cell lines[173,174]. Data also demonstrates the potential for marked variability between passages

of a given cell line [105,173]. By limiting EV purification to three passages, this variance is accounted for while staying within practical limitations[174]. To further control for variability, all samples can be standardized for a given study, ensuring similar storage conditions between experimental groups, and homogenizing any potential subpopulations of exosome isolates of respective experimental groupings prior to any functional testing. Though these are biologically stable agents once formed their constituents and content can be altered through altering the cells generating them either directly or through environmental manipulations, or even through direct loading with molecules of interest after isolation[163,164].

4.3.2 Exosome Loading Through Cell Physiology

Perhaps the easiest method to perform and most difficult to control is functional exosome loading through modification of the derivative cell's homeostatic condition. Be it through cellular aging or passaging, or through changes in culture media or environment; environmental factors can have a significant effect on exosome loading[163,165,166,174]. This can be as simple and including an abundance of a non-cytotoxic compound in the culture media with the aim of exosomes entrapping the compound during their biogenesis[63,163]. Alternately culture conditions can direct cellular phenotypes such as through the alternative activation of macrophages into an M2 phenotype which can increase peritendinous fibrosis through downstream effects of circRNA-EP400 containing exosomes, as compared to those derived from M1, classically activated macrophages[165]. An alternative, more targeted approach is through genetic manipulation of cell line, such as through a lentiviral vector[167]. In so doing you gain access to the full tool box of gene editing techniques which can be as simple as transfection for over expression of known exosome constituent, to something more involved like inclusion of pH sensitive fluorescent labels tied to exosome markers[175-177].

4.3.3 Direct Molecular Loading

One of the most common methods for exploring the effect of specific exosome constituents is to individually load them into an exosome population[163,178]. In theory, this utilizes exosomes' ability to target cell populations and deliver compounds intracellularly[163,179]. These compounds can be extra of an endogenous exosome constituent or an exogenous molecule such as a chemotherapeutic agent[179]. Some established methods for introducing or enhancing content of these molecules include incubation with membrane permeabilizers, freeze thaw cycling, electroporation, sonication and extrusion[163,178,179]. These techniques all share the basic principle of membrane disruption in a solution containing excess of the molecule of interest, subsequent reformation or healing of the vesicular membrane after concentration gradient diffusion[163,178]. These techniques are often used for inclusion of larger proteins and/or nucleic acids. Techniques that avoid membrane disruption include unassisted diffusion which relies heavily on the molecule of interest having the right charge and/or size to either be incorporated into the membrane or make its way through the membrane following its concentration gradient; or chemically attaching them to the exosome surface through using copper-catalyzed azide alkyne cycloaddition to attach small molecules to the exosome surface through covalent bonds[163,178].

4.4 In Vivo Exosome Studies

4.4.1 In Vivo Exosome Studies Overview

As biologically stable agents, which are incapable of genetic drift and unwanted trans-differentiation or proliferation, EVs avoid many of the safety concerns associated with direct MSC or tendon stem cell based treatments[180,181]; making EVs an enticing delivery vehicle to affect changes in damaged tissues with minimal risk[182-185]. We have shown that ovine exosomes can be readily generated, isolated and characterized. The utilization of our ovine tendon degeneration

model affords better predictive ability as compared to rodent models, due to the similar size, degeneration cascade, and healing rates in sheep as compared to humans[17,18,168,186]. With the model focus identified, we will discuss (1) comparative methods of delivery, such as direct injection vs incorporation into a biological scaffold, and (2) the expected outcomes and how we can measure them. Select methods will then be discussed in subsequent sections. The scale of the ovine model allows for an abundance of such methods to be used on the same sample, even following mechanical testing and/or periods of frozen and/or fixed storage or archiving.

4.4.2 Methods of Delivery

That exosomes can be readily coupled with existing and novel medical devices and therapeutic techniques has driven much of the current research into their applications in the orthopedic field[46,47,58,81-83]. In part due to their small size and vesicular composition, exosomes are uniquely stable and retain their bioavailability and bioactivity in an array of applications[163,178]. These innate qualities can be further enhanced through the introduction of scaffold or matrix binding domains, such as through the use of collagen binding domains for attachment to decellularized tendon based surgical patches[167]. However, beneficial effects have also been observed after a single, direct injection of MSCdEVs in rat models[47]. Additionally, one study has already demonstrated that exosomes can aid in tendon healing in an ovine model of acute rotator cuff injury in conjunction with a collagen scaffold[187]. This preliminary study established some of the xenogeneic effects that can be observed with exosomes' decreased immunogenicity compared to source cell therapy, as human cell line derived exosomes were used in this ovine model.

Another method of delivery is through the application of exosome educated autologous cells. As MSCdEV educated macrophages have already been demonstrated in rodent models to have a significant effect on tendon and ligament healing, and this would be a logical progression

for the work described in Chapter 2 and 3[46,188]. Though more well established in other fields, especially cancer therapy, there are well established methodologies for the harvest, alteration/conditioning and application of macrophages[46,188,189].

4.4.3 Expected Results

As exosomes of both cell sources are known to improve tendon healing through different means, their effects and that of their constituents necessitate evaluation at multiple length scales to fully elucidate functional outcomes. This has been shown in several instances where functional, mechanical changes are not explained by traditional histologic methods[8,92,190].

Fortunately, the different length scales of tendon can be assessed at the Tissue→Fiber, Fiber→Fibril and Fibril→Molecular levels using a combination of novel and traditional imaging methods paired with biomechanical testing. These techniques include quantitative imaging from the Tissue→Fibril levels under relaxed and strained conditions. Data generated using these techniques can demonstrate key extracellular matrix changes at the key levels of tissue to mechanical translation and can be directly compared to traditional imaging methods for correlation of data to preexisting studies.

We anticipate these data to replicate findings of other animal models that demonstrate MSCdEVs as improving tendon healing, as well as expand on and reinforce our in vitro data suggesting that Tenocyte derived EVs may be more appropriate for directing repair of this tissue [46,47,81,174,187,188]. This would see MSCdEVs improving tendon mechanics and decreasing inflammation and TdEVs further increasing tendon mechanics through improved tissue composition and organization of Col1 at all scale levels while reducing characteristics typical of a mechanically stable, physiologically abnormal tissue, such as may be present in chronic rotator cuff tendinopathy[47,115,191]. To assess this, traditional, contemporary and novel imaging techniques

may be used to investigate the multiple scale levels of tendon ECM changes that define the tendon's functional mechanics as has been indicated by our previous work in this animal model, where traditional techniques along do not always coincide with function, mechanical changes[8,92,190].

At the cellular level, gene sequencing data is anticipated to reflect this with TdEVs promoting greater expression of tissue regeneration and collagen organization markers while MSCdEVs may lead to increased metabolic processes as expected from their comparative increase in tissue catabolic and vessel recruitment profile in macrophage treatment[174]. In particular we anticipate that TdEV treatment will increase expression of MIP-1alpha/CCL3 and IL-6 which increase collagen type 1 production and cross linking, playing a critical role in early tendon healing, whereas MSCdEV educated macrophages may increase levels of IL-1α, IL-1β which drive matrix destruction and VEGF which drives angiogenesis[117,118,121,192,193]. At the finer scale lengths, we expect tissue mechanics to be further improved by TdEV treatment through upregulation of gene expression for Col1 and Col1 synthesis and support molecules such as scleraxis, tenomodulin, lumican and fibromodulin and tenascin-C[128,194]. To better evaluate these gene expression profiles, newer technologies allow for targeted approaches that are cost effective, work in ovine and other comparative species and applicable to samples that are normally difficult to isolate stable RNA from.

4.5 Targeted RNA sequencing

One of the primary drawbacks from working with ovine models of disease is the lack of species-specific antibodies for immunolabeling. This is especially true for the standards of macrophage phenotype characterization beyond simple M1 vs M2 polarization. While custom antibodies may be prepared these are cost inhibitive, especially when protocols are needed to

establish repeatable labeling. To further complicate this, tendon, especially at the enthesis, is notoriously difficult to work with for immunolabeling in situ as these tough tissues are prone to warping off slides a fragmentation during antigen retrieval steps. New technologies and associated techniques have circumnavigated much of this issue though.

While whole tissue RNA sequencing can be of immense value and is readily applied to a wide range of species, it requires higher sample volume and integrity than may be reproduceable in a multiscale analysis. Newer methods using NanoString technology on the nCounter platform allow for targeted, reproduceable, multiplexed, direct counting of RNA even from formalin fixed paraffin embedded tissues[195]. This technology has demonstrated the ability to characterize immune cell populations in sheep and to assess archived formalin fixed paraffin embedded orthopedic sections in equids[89,196]. Already having a basis for comparison in human rotator cuff outcomes, there is an ease of translatability that is not found using immunolabeling methods[197].

4.6 Electron Microscopy, Scanning and Transmission

Electron microscopy offers the power to image and assess structures smaller than the resolution capacity of visible light, which is theoretically around 200nm, the same reason alternate methods are needed to assess nanoparticles like exosomes[21,198,199]. Scanning electron microscopy (SEM) assess the surface characters of the tissue and is classically used to assess fibrillar organization, direction, and continuity, even allowing visualization of fibrillar crimps, splits and merges[21,198,199]. Transmission electron microscopy (TEM) allows cross sectional assessment of fibril diameter, distribution and defines their banding patterns as discussed in Chapter 1[21,198]. These methods are most powerful when used together, however, they limit the intrasample comparison to other imaging modalities due to the need for different sample preparation methods[200]. Their other primary limiting factor is the tradeoff of extreme magnification for a

limited field of view[200]. To overcome these limitations, other imaging modalities may be applied to fresh, frozen tissue sections, especially label free imaging otherwise, where indicated, separate, representative samples may be prepared in parallel.

4.7 Polarized Light Microscopy

In its simplest form, traditional, bright field microscopy may be altered through the use of perpendicularly oriented linear polarizers, one prior to the sample (generator) and one after (analyzer), which act in concert to demonstrate birefringence in a sample, where the angle of polarization is altered by the sample[201]. In so doing, light intensity becomes a measure of the degree of birefringence in a given area of the sample, and in the case of Col1, with its tightly arranged helices forms a uniaxial semicrystalline structure in line with the tissue function and demonstrates significantly more birefringence at these angles than the orthoganols[201]. This provides native contrast to the tendon fibers allowing visualization of fiber alignment, orientation and crimps[13,14]. It has also served as a means to infer relative amounts of Col1 as compared to collagen type 3 in conjunction with special stains[13,14,17,18].

One restriction of this technique is its inability to resolve multiple angles simultaneously. There have been several approaches over the years to overcome this limitation, through dynamic imaging and use of parallel analysis or photo-stacking[202]. These techniques are limited in their applications due to the lack of continuity of angle of analysis and often the inability to be as a means of direct visualization. These limitations drove our preliminary work to identify and create a means of imaging tendon during mechanical testing with the fidelity to assess fiber and even fibrillar levels of tissue organization. Thus, we prototyped a polychromatic polarized light microscope that can image sections of tendon up to 400um thick while in a mechanical tester. This method of imaging allows for real-time direct visualization through an eye-piece, indirect

visualization through a camera as well as direct image translation to light intensity by hue data via spectrometry all while the tissue is mechanically tested (Figure 4.**1**).

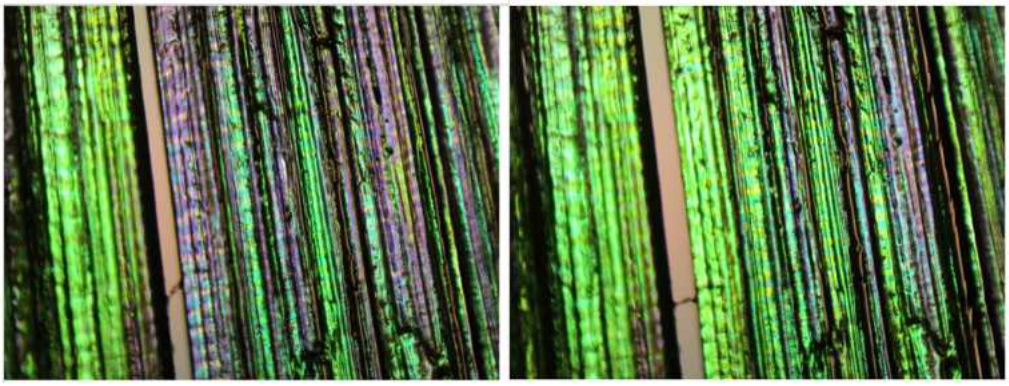

Figure 4.1. Polychromatic polarized light microscopy of tendon when relaxed (left) and loaded (right). Imaging was performed using a BX40 Olympus microscope modified with a PPM light generator and analyser, and taken at 400X magnification. Unstained sections of ovine rotator cuff tendon (paraffin-embedded fixed infraspinatus; 2x1cm and 200um thick) were deparaffinized and soaked in mineral oil prior to mounting on a mechanical tester. Samples were loaded uniaxially in the direction of the fibres. Sections of tendon demonstrate shifts in the characteristic crimping pattern of the tendon collagen bundles demonstrated by hue shifts from purple to green.

This design was based on a static polychromatic polarized light microscope adaptation where a standard linear cross-polarized optical system is modified to have a z-axis cut quartz crystal is used after the generator and an anti-chiral z-axis quartz crystal also added after the sample prior to the analyzer[203]. These quartz crystals demonstrate chiral asymmetry, and when light is passed through them in the z axis, its refractive index is altered such that it will cause the polarization angle to rotate as a function of the frequency of light, the direction will be inverted for the opposite chirality. By arranging these crystals as such, linearly polarized light is fanned out by hue or frequency, interacts with the sample, is and is collapsed by the opposing crystal prior to analysis by the cross polarizer, in so doing, the traditional assessment of birefringence is further modified by hue, where hue is angle of incidence and light intensity is the degree of anisometric birefringence[203]. This allows for direct visualization of the unstained tissue as well as spectrometric

quantitative measurement of fiber angle and organization[203]. Because all angles can be measured simultaneously this can be readily applied to dynamic imaging applications, such as during mechanical loading[202].

To verify what we are seeing with this technique we developed a means of sample preparation that is compatible with this novel imaging modality as well as second harmonic generation imaging in the transmission and epi-, 'reflectance', directions (Figure 4.2). This is accomplished through fresh-frozen sections being prepared through gradual cooling and freezing over 24 hours prior to sectioning on a cryotome, and subsequent rapid thawing which preserves tissue mechanical properties and soaking in glycerol, which prevents dehydration during handling and analysis while also increasing optical clarity [204,205] [206].

4.8 Nonlinear Spectroscopy

When light-matter interactions are interpreted through a linear relation of a single condition of light at the subject as compared to the light out of the subject we are using linear spectrometry. These techniques, while powerful, are limited in their dimensionality in that several molecular states may yield the same output at a given input. Nonlinear spectrometry seeks to overcome these limitations by increasing the dimension of the input and output readings. When recording these outputs in situ, often in conjunction with photomicrography, this is considered nonlinear spectroscopy. When these techniques assess coherence, this describes cases where the character of the outgoing signal is defined in part by its directionality, as compared to spontaneous spectrometry where the direction of the outgoing signal is non-specific. Here we will discuss transient absorption spectroscopy and second harmonic generation as both techniques are of interest to tendon research in their ability to be coupled with other techniques and as a label free translational means of studying this tissue.

4.8.1 Transient Absorption Spectroscopy

Operating on the principle of a pump-probe system, transient absorption spectroscopy (TAS) systems utilize a pump beam to induce a high energy state, causing a highly localized jump in thermodynamics, which induces distinct changes in its photodynamic response to a given probe beam[207,208]. To functionally assess a given molecule, it first needs to be modeled to define its internal vibrational redistribution, vibrational cooling and any characteristic rearrangements that may take place such as dissociation and reattachment of specific atomic bonds[208]. This has been used to spatially resolved heme proteins in their reduction vs oxidative states[208]. These methods offer a label free means of interpreting mitochondrial and therefore metabolic activity at the individual cell level. Though this technology is in an infancy, it could provide valuable insights in translational applications and basic science research into difficult to study tissues such as tendon.

4.8.2 Second Harmonic Generation

This technique is especially useful for imaging and analysis of Col1 in situ. Second harmonic generation is where two photons of a consistent, and specific to the subject, wavelength of light are absorbed and destroyed, while a new photon having twice the frequency (half the wavelength) of light is released[209]. This phenomena relies on the non-centrosymmetric crystalline molecular structure of the material, and while it was first observed in inorganic quartz, it was later found to be highly expressed in collagen[209,210]. This is in large part thanks to collagens repeating, chiral motifs. Because of the orderly hierarchy and relative abundance of Col1 in tendon, this tissue is one of the best organic generators of a second harmonic signal. This is typically at a wavelength of about 440nm (pump wavelength 880nm)[209,210]. Because the signal emitting from the collagen fibril emits from its shell, rather than from its volume, it is additionally sensitive to hydration state

of the tendon and to is mechanical load[210]. This makes it a uniquely sensitive methods for the resolution of submicron fibrillar characterization, capable of discerning fiber direction, crimping patterns and fibrillar thickness[211]. Because of the specificity of these techniques, and their ability to be coupled with more traditional confocal microscopy set ups, they can be paired with other labeled and label free imaging methods such as for the autofluorescence or chemical labeling fluorescence of elastin[212,213].

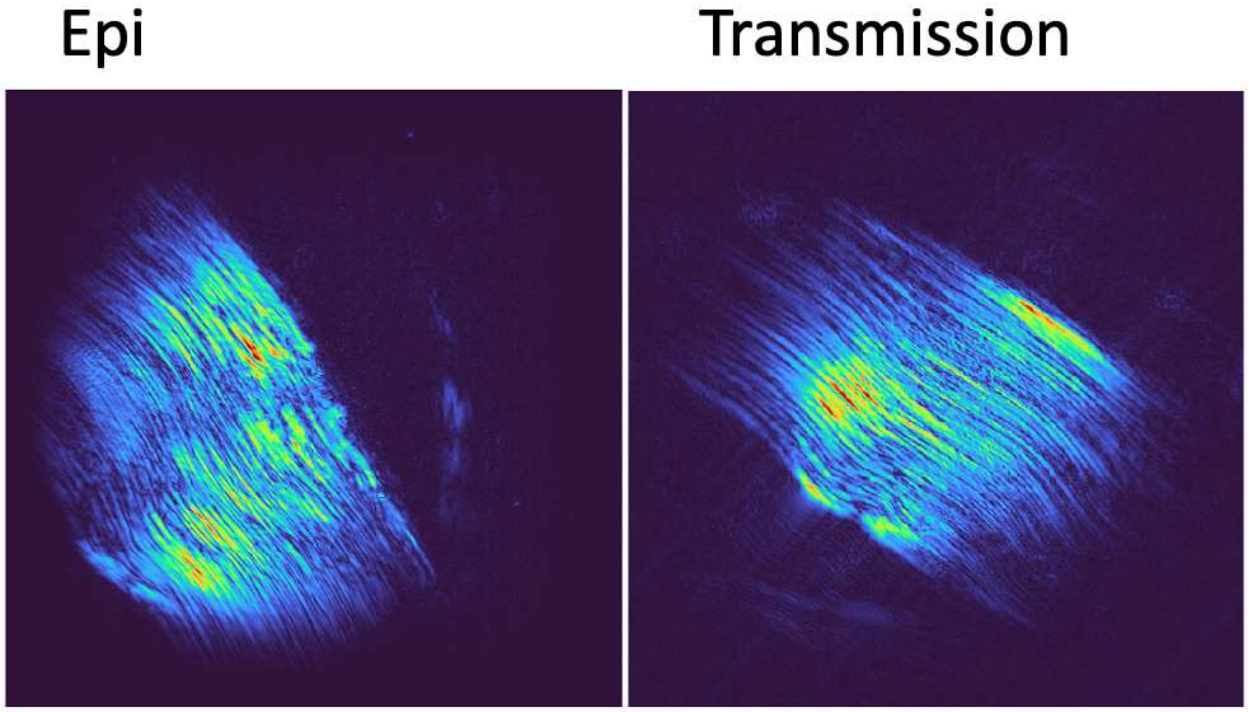

Figure 4.2. A demonstration of second harmonic generation on fresh frozen ovine tendon soaked in a solution of glycerol. Here we can see scatter of the generated photons in the epi and transmission directions. These appear to occur in line with fibrillar direction and the influence of electron shell diameter and direction on the scatter direction, this could imply localized shifts in these properties. Such shift could be explained by the fibrillar crimp regions that experience torsional direction shifts and are thought to represent areas of thinning or flattening of the collagen fibril.

4.9 Integration of Techniques

These advanced and experimental imaging techniques have the great advantage of being directly translatable between species, as they rely on chemical and physical molecular

characteristics largely independent of the species-to-species variations that can affect antibody specificity for epitope-based labeling. They can further be compared to traditional histologic and immunohistology evaluation and tendon scoring matrices. By applying these techniques to the ovine model of rotator cuff tendinopathy and in the context of exosome research, we can further our interpretation of traditional tendon evaluation methods. These functional changes can then be compared to the effector cell populations and gene sequencing to inform on how these cells affect these ECM changes.

At the cell regulatory level, Nanostring RNA sequencing techniques can be performed on fresh frozen and paraffin embedded tissue sections, allowing for assessments of targeted areas of tissue, archival sections and directly compared to gene regulatory in vitro data to establish similarities and difference between single cell, multi cell and in situ/ in vivo cellular response to exosome education of the tissue and/or target cells. These can then be contextualized through the changes in extracellular matrix composition, which can be evaluated at the Tissue→Fiber length scale using traditional light microscopy, Tissue→Fibril level using polarization resolved inmaging, second harmonic generation imaging and elastin autofluorescence and at the Fibril→Molecular level using specialized second harmonic generation imaging and/or electron microscopy. These techniques offer the unique ability to assess down to the fibrillar level during dynamic mechanical testing of cryopreserved sections and allow for the same sections to undergo multiple forms of assessment for direct comparison of given sample. Thanks to the model's size there is also the option of generating parrel sample processing from a single tissue sample or from each of its regions of interest. As many of these techniques can be used in conjunction with and without modification to current practices in orthopedic tissue assessment, their establishment in

comparison to traditional techniques, presents the unique opportunity to expand on current best practices, adding additional levels of investigatory depth when indicated.

4.10 Concluding Remarks

Exosomes demonstrate a great potential to direct tendon healing through cellular mechanisms. They can be readily isolated from primary or immortalized cell lines and can be engineered through direct or indirect augmentations to have specific effects. We have demonstrated discrete differences in how exosomes of tissue-native cell origin direct key effector cells of the tendon microenvironment, macrophages and tenocytes, toward different phenotypes of tendon healing. By using these tenocyte-derived, as compared to MSC-derived, exosomes we may better drive tendon healing. In establishing these methods in the context of the gold standard, large animal model of rotator cuff tendinopathy as well as human cell lines we set a foundation for future explorations of exosomes as direct and adjunct therapies for rotator cuff tendinopathy.

We have further discussed traditional, contemporary, and novel techniques that when used in conjunction allow for more in-depth investigations of tendon biology, disease, and response to treatment at the different length scales as outlined in Chapter 1, as each of the length scales may contribute to the overall mechanobiology and clinical functionality of the tendon. These detailed analyses will aid in differentiating the effects of exosome therapies as they are engineered more toward the function of tendon healing.

As these techniques are refined through this line of investigation, they may be applied to our understanding of exosome biology in the context of disease and improve our ability to image other tissues (e.g. ligament and bone) and to study other disease states (e.g. cartilage degeneration), broadening not only the data we can obtain from future samples, but from archived samples as well.

REFERENCES

1. Weber S, Chahal J. Management of Rotator Cuff Injuries. JAAOS - Journal of the American Academy of Orthopaedic Surgeons 2020;28(5):e193-e201, doi:10.5435/jaaos-d-19-00463
2. Sher JS, Uribe JW, Posada A, et al. Abnormal findings on magnetic resonance images of asymptomatic shoulders. JBJS 1995;77(1):10-15
3. Henry P, Wasserstein D, Park S, et al. Arthroscopic Repair for Chronic Massive Rotator Cuff Tears: A Systematic Review. Arthroscopy: The Journal of Arthroscopic & Related Surgery 2015;31(12):2472-2480, doi:https://doi.org/10.1016/j.arthro.2015.06.038
4. McCarron JA, Derwin KA, Bey MJ, et al. Failure With Continuity in Rotator Cuff Repair "Healing". The American Journal of Sports Medicine 2013;41(1):134-141, doi:10.1177/0363546512459477
5. Mather RC, Koenig L, Acevedo D, et al. The Societal and Economic Value of Rotator Cuff Repair. Journal of Bone and Joint Surgery 2013;95(22):1993-2000, doi:10.2106/jbjs.l.01495
6. Young BL, Bitzer A, Odum S, et al. Healthcare costs of failed rotator cuff repairs. JSES Reviews, Reports, and Techniques 2023;3(3):318-323, doi:10.1016/j.xrrt.2023.03.008
7. Millar NL, Silbernagel KG, Thorborg K, et al. Tendinopathy. Nature Reviews Disease Primers 2021;7(1):1, doi:10.1038/s41572-020-00234-1
8. Johnson JW, von Stade D, Gadomski B, et al. Modified Alendronate Mitigates Mechanical Degradation of the Rotator Cuff in an Osteoporotic Ovine Model. The American Journal of Sports Medicine 2022;50(13):3649-3659, doi:10.1177/03635465221125175
9. Durgam S, Stewart M. Cellular and Molecular Factors Influencing Tendon Repair. Tissue Engineering Part B: Reviews 2017;23(4):307-317, doi:10.1089/ten.teb.2016.0445
10. Saini K, Cho S, Dooling LJ, et al. Tension in fibrils suppresses their enzymatic degradation – A molecular mechanism for 'use it or lose it'. Matrix Biology 2020;85-86(34-46, doi:https://doi.org/10.1016/j.matbio.2019.06.001
11. Yeung C-YC, Kadler KE. Chapter Eleven - Importance of the circadian clock in tendon development. In: Current Topics in Developmental Biology. (Olsen BR. ed.) Academic Press: 2019; pp. 309-342.
12. Provenzano PP, Vanderby R. Collagen fibril morphology and organization: Implications for force transmission in ligament and tendon. Matrix Biology 2006;25(2):71-84, doi:https://doi.org/10.1016/j.matbio.2005.09.005
13. Longo UG, Franceschi F, Ruzzini L, et al. Light microscopic histology of supraspinatus tendon ruptures. Knee Surgery, Sports Traumatology, Arthroscopy 2007;15(11):1390-1394, doi:10.1007/s00167-007-0395-8
14. Maffulli N, Longo UG, Franceschi F, et al. Movin and Bonar scores assess the same characteristics of tendon histology. Clin Orthop Relat Res 2008;466(7):1605-11, doi:10.1007/s11999-008-0261-0
15. Theodossiou SK, Murray JB, Schiele NR. Cell-cell junctions in developing and adult tendons. Tissue Barriers 2020;8(1):1695491, doi:10.1080/21688370.2019.1695491
16. Wall ME, Dyment NA, Bodle J, et al. Cell Signaling in Tenocytes: Response to Load and Ligands in Health and Disease. Adv Exp Med Biol 2016;920(79-95, doi:10.1007/978-3-319-33943-6_7

17. Johnson J, Von Stade D, Regan D, et al. Tendon midsubstance trauma as a means for the development of translatable chronic rotator cuff degeneration in an ovine model. Annals of Translational Medicine 2021;9(21):1616-1616, doi:10.21037/atm-21-2749
18. Johnson J, Von Stade D, Regan D, et al. Enthesis trauma as a means for the development of translatable chronic rotator cuff degeneration in an ovine model. Annals of Translational Medicine 2021;9(9):741-741, doi:10.21037/atm-21-354
19. Andarawis-Puri N, Flatow EL, Soslowsky LJ. Tendon basic science: Development, repair, regeneration, and healing. Journal of Orthopaedic Research 2015;33(6):780-784
20. Thorpe CT, Streeter I, Pinchbeck GL, et al. Aspartic Acid Racemization and Collagen Degradation Markers Reveal an Accumulation of Damage in Tendon Collagen That Is Enhanced with Aging. Journal of Biological Chemistry 2010;285(21):15674-15681, doi:10.1074/jbc.m109.077503
21. Franchi M, Ottani V, Stagni R, et al. Tendon and ligament fibrillar crimps give rise to left-handed helices of collagen fibrils in both planar and helical crimps. Journal of Anatomy 2010;216(3):301-309, doi:https://doi.org/10.1111/j.1469-7580.2009.01188.x
22. Ellingson AJ, Pancheri NM, Schiele NR. Regulators of collagen crosslinking in developing and adult tendons. Eur Cell Mater 2022;43(130-152, doi:10.22203/eCM.v043a11
23. Södersten F, Ekman S, Eloranta M-L, et al. Ultrastructural immunolocalization of cartilage oligomeric matrix protein (COMP) in relation to collagen fibrils in the equine tendon. Matrix Biology 2005;24(5):376-385, doi:https://doi.org/10.1016/j.matbio.2005.06.003
24. Silva Barreto I, Pierantoni M, Hammerman M, et al. Nanoscale characterization of collagen structural responses to in situ loading in rat Achilles tendons. Matrix Biology 2023;115(32-47, doi:https://doi.org/10.1016/j.matbio.2022.11.006
25. Benjamin M, McGonagle D. Entheses: tendon and ligament attachment sites. Scandinavian Journal of Medicine & Science in Sports 2009;19(4):520-527, doi:10.1111/j.1600-0838.2009.00906.x
26. Shaw HM, Benjamin M. Structure–function relationships of entheses in relation to mechanical load and exercise. Scandinavian Journal of Medicine & Science in Sports 2007;17(4):303-315, doi:https://doi.org/10.1111/j.1600-0838.2007.00689.x
27. Itoigawa Y, Suzuki O, Sano H, et al. The role of an octacalcium phosphate in the re-formation of infraspinatus tendon insertion. Journal of Shoulder and Elbow Surgery 2015;24(7):e175-e184, doi:https://doi.org/10.1016/j.jse.2015.01.011
28. Killian ML. Growth and mechanobiology of the tendon-bone enthesis. Seminars in Cell & Developmental Biology 2022;123(64-73, doi:https://doi.org/10.1016/j.semcdb.2021.07.015
29. Haraldsson BT, Aagaard P, Qvortrup K, et al. Lateral force transmission between human tendon fascicles. Matrix Biology 2008;27(2):86-95, doi:https://doi.org/10.1016/j.matbio.2007.09.001
30. Sharma P, Maffulli N. Biology of tendon injury: healing, modeling and remodeling. Journal of musculoskeletal and neuronal interactions 2006;6(2):181
31. Citro V, Clerici M, Boccaccini AR, et al. Tendon tissue engineering: An overview of biologics to promote tendon healing and repair. Journal of Tissue Engineering 2023;14(doi:10.1177/20417314231196275
32. Ackerman JE, Muscat SN, Adjei-Sowah E, et al. Identification of Periostin as a critical niche for myofibroblast dynamics and fibrosis during tendon healing. Matrix Biology 2024;125(59-72, doi:https://doi.org/10.1016/j.matbio.2023.12.004

33. Bautista CA, Srikumar A, Tichy ED, et al. CD206+ tendon resident macrophages and their potential crosstalk with fibroblasts and the ECM during tendon growth and maturation. Frontiers in Physiology 2023;14(doi:10.3389/fphys.2023.1122348
34. Wang JHC. Mechanobiology of tendon. Journal of Biomechanics 2006;39(9):1563-1582, doi:https://doi.org/10.1016/j.jbiomech.2005.05.011
35. Xin Ooi MW, Fenning L, Dhir V, et al. Rotator cuff assessment on imaging. J Clin Orthop Trauma 2021;18(121-135, doi:10.1016/j.jcot.2021.04.004
36. Newton JB, Fryhofer GW, Rodriguez AB, et al. Mechanical properties of the different rotator cuff tendons in the rat are similarly and adversely affected by age. J Biomech 2021;117(110249, doi:10.1016/j.jbiomech.2021.110249
37. Sunwoo JY, Eliasberg CD, Carballo CB, et al. The role of the macrophage in tendinopathy and tendon healing. Journal of Orthopaedic Research 2020;38(8):1666-1675, doi:10.1002/jor.24667
38. Darrieutort-Laffite C, Arnolfo P, Garraud T, et al. Rotator Cuff Tenocytes Differentiate into Hypertrophic Chondrocyte-Like Cells to Produce Calcium Deposits in an Alkaline Phosphatase-Dependent Manner. J Clin Med 2019;8(10), doi:10.3390/jcm8101544
39. Johnson J, von Stade D, Gadomski B, et al. Biomechanical and histological changes secondary to aging in the human rotator cuff: A preliminary analysis. Journal of Orthopaedic Research® 2023;
40. Gaytan F, Morales C, Reymundo C, et al. A novel RGB-trichrome staining method for routine histological analysis of musculoskeletal tissues. Scientific Reports 2020;10(1):16659, doi:10.1038/s41598-020-74031-x
41. Izu Y, Adams SM, Connizzo BK, et al. Collagen XII mediated cellular and extracellular mechanisms regulate establishment of tendon structure and function. Matrix Biology 2021;95(52-67, doi:https://doi.org/10.1016/j.matbio.2020.10.004
42. Closset L, Gultekin O, Salehi S, et al. The extracellular matrix – immune microenvironment crosstalk in cancer therapy: Challenges and opportunities. Matrix Biology 2023;121(217-228, doi:https://doi.org/10.1016/j.matbio.2023.07.003
43. Cretoiu D, Vannucchi MG, Bei Y, et al. Telocytes: new connecting devices in the stromal space of organs. Innovations in cell research and therapy 2020;1-25
44. Russo V, El Khatib M, Prencipe G, et al. Tendon Immune Regeneration: Insights on the Synergetic Role of Stem and Immune Cells during Tendon Regeneration. Cells 2022;11(3):434
45. Xu HT, Lee CW, Li MY, et al. The shift in macrophages polarisation after tendon injury: A systematic review. J Orthop Translat 2020;21(24-34, doi:10.1016/j.jot.2019.11.009
46. Chamberlain CS, Clements AEB, Kink JA, et al. Extracellular Vesicle-Educated Macrophages Promote Early Achilles Tendon Healing. Stem Cells 2019;37(5):652-662, doi:10.1002/stem.2988
47. Wang C, Zhang Y, Zhang G, et al. Adipose Stem Cell-Derived Exosomes Ameliorate Chronic Rotator Cuff Tendinopathy by Regulating Macrophage Polarization: From a Mouse Model to a Study in Human Tissue. Am J Sports Med 2021;49(9):2321-2331, doi:10.1177/03635465211020010
48. Liu Z-W, Zhang Y-M, Zhang L-Y, et al. Duality of Interactions Between TGF-β and TNF-α During Tumor Formation. Frontiers in Immunology 2022;12(doi:10.3389/fimmu.2021.810286
49. Chen J, Wang J, Hart DA, et al. Complement factor D as a predictor of Achilles tendon healing and long-term patient outcomes. The FASEB Journal 2022;36(6), doi:10.1096/fj.202200200rr

50. Ubil E, Caskey L, Holtzhausen A, et al. Tumor-secreted Pros1 inhibits macrophage M1 polarization to reduce antitumor immune response. J Clin Invest 2018;128(6):2356-2369, doi:10.1172/jci97354
51. Li H, Yang P, Wang J, et al. HLF regulates ferroptosis, development and chemoresistance of triple-negative breast cancer by activating tumor cell-macrophage crosstalk. Journal of Hematology & Oncology 2022;15(1):2, doi:10.1186/s13045-021-01223-x
52. Paye M, Nusgens B, Lapière CM. Factor XIII of blood coagulation decreases the susceptibility of collagen precursors to proteolysis. Biochimica et Biophysica Acta (BBA) - General Subjects 1991;1073(3):437-441, doi:https://doi.org/10.1016/0304-4165(91)90212-Y
53. Wang Y, Yan K, Lin J, et al. Macrophage M2 Co-expression Factors Correlate With the Immune Microenvironment and Predict Outcome of Renal Clear Cell Carcinoma. Frontiers in Genetics 2021;12(doi:10.3389/fgene.2021.615655
54. Riuzzi F, Beccafico S, Sagheddu R, et al. Levels of S100B protein drive the reparative process in acute muscle injury and muscular dystrophy. Scientific Reports 2017;7(1), doi:10.1038/s41598-017-12880-9
55. Hu M, Guo G, Huang Q, et al. The harsh microenvironment in infarcted heart accelerates transplanted bone marrow mesenchymal stem cells injury: the role of injured cardiomyocytes-derived exosomes. Cell Death & Disease 2018;9(3), doi:10.1038/s41419-018-0392-5
56. Rilla K, Mustonen A-M, Arasu UT, et al. Extracellular vesicles are integral and functional components of the extracellular matrix. Matrix Biology 2019;75-76(201-219, doi:https://doi.org/10.1016/j.matbio.2017.10.003
57. Von Stade D, Meyers M, Johnson J, et al. Exosome Cell Origin Affects In Vitro Markers of Tendon Repair in Ovine Macrophages and Tenocytes. Tissue Engineering Part A 2023;29(9-10):282-291, doi:10.1089/ten.tea.2022.0185
58. Durtschi M, Kim S, Li J, et al. Optimizing Tissue Engineering for Clinical Relevance in Rotator Cuff Repair. Tissue engineering 2024;
59. Qi J, Liu Q, Reisdorf RL, et al. Characterization of a purified exosome product and its effects on canine flexor tenocyte biology. Journal of Orthopaedic Research 2020;38(8):1845-1855, doi:10.1002/jor.24587
60. Kalluri R, LeBleu VS. The biology, function, and biomedical applications of exosomes. Science 2020;367(6478), doi:10.1126/science.aau6977
61. Hamzah RN, Alghazali KM, Biris AS, et al. Exosome Traceability and Cell Source Dependence on Composition and Cell-Cell Cross Talk. International Journal of Molecular Sciences 2021;22(10):5346, doi:10.3390/ijms22105346
62. Panagopoulou MS, Wark AW, Birch DJS, et al. Phenotypic analysis of extracellular vesicles: a review on the applications of fluorescence. Journal of Extracellular Vesicles 2020;9(1):1710020, doi:10.1080/20013078.2019.1710020
63. Doyle L, Wang M. Overview of Extracellular Vesicles, Their Origin, Composition, Purpose, and Methods for Exosome Isolation and Analysis. Cells 2019;8(7):727, doi:10.3390/cells8070727
64. Martins TS, Vaz M, Henriques AG. A review on comparative studies addressing exosome isolation methods from body fluids. Analytical and Bioanalytical Chemistry 2023;415(7):1239-1263, doi:10.1007/s00216-022-04174-5
65. Soo CY, Song Y, Zheng Y, et al. Nanoparticle tracking analysis monitors microvesicle and exosome secretion from immune cells. Immunology 2012;136(2):192-7, doi:10.1111/j.1365-2567.2012.03569.x

66. Géminard C, de Gassart A, Blanc L, et al. Degradation of AP2 During Reticulocyte Maturation Enhances Binding of Hsc70 and Alix to a Common Site on TfR for Sorting into Exosomes. Traffic 2004;5(3):181-193, doi:https://doi.org/10.1111/j.1600-0854.2004.0167.x
67. Rupp A-K, Rupp C, Keller S, et al. Loss of EpCAM expression in breast cancer derived serum exosomes: Role of proteolytic cleavage. Gynecologic Oncology 2011;122(2):437-446, doi:https://doi.org/10.1016/j.ygyno.2011.04.035
68. Tontanahal A, Arvidsson I, Karpman D. Annexin Induces Cellular Uptake of Extracellular Vesicles and Delays Disease in Escherichia coli O157:H7 Infection. Microorganisms 2021;9(6), doi:10.3390/microorganisms9061143
69. Meister M, Tikkanen R. Endocytic trafficking of membrane-bound cargo: a flotillin point of view. Membranes (Basel) 2014;4(3):356-71, doi:10.3390/membranes4030356
70. Jiang L, Shen Y, Guo D, et al. EpCAM-dependent extracellular vesicles from intestinal epithelial cells maintain intestinal tract immune balance. Nature Communications 2016;7(1):13045, doi:10.1038/ncomms13045
71. Xu T, Xu M, Bai J, et al. Tenocyte-derived exosomes induce the tenogenic differentiation of mesenchymal stem cells through TGF-β. Cytotechnology 2019;71(1):57-65, doi:10.1007/s10616-018-0264-y
72. Donoso-Quezada J, Ayala-Mar S, González-Valdez J. The role of lipids in exosome biology and intercellular communication: Function, analytics and applications. Traffic 2021;22(7):204-220, doi:10.1111/tra.12803
73. Hosseini-Beheshti E, Pham S, Adomat H, et al. Exosomes as Biomarker Enriched Microvesicles: Characterization of Exosomal Proteins Derived from a Panel of Prostate Cell Lines with Distinct AR Phenotypes. Molecular & Cellular Proteomics 2012;11(10):863-885, doi:https://doi.org/10.1074/mcp.M111.014845
74. Yáñez-Mó M, Siljander PRM, Andreu Z, et al. Biological properties of extracellular vesicles and their physiological functions. Journal of Extracellular Vesicles 2015;4(1):27066, doi:10.3402/jev.v4.27066
75. Zheng D, Huo M, Li B, et al. The Role of Exosomes and Exosomal MicroRNA in Cardiovascular Disease. Frontiers in Cell and Developmental Biology 2021;8(doi:10.3389/fcell.2020.616161
76. Zou M, Wang J, Shao Z. Therapeutic Potential of Exosomes in Tendon and Tendon–Bone Healing: A Systematic Review of Preclinical Studies. Journal of Functional Biomaterials 2023;14(6):299, doi:10.3390/jfb14060299
77. Verweij FJ, Balaj L, Boulanger CM, et al. The power of imaging to understand extracellular vesicle biology in vivo. Nat Methods 2021;18(9):1013-1026, doi:10.1038/s41592-021-01206-3
78. Durak-Kozica M, Baster Z, Kubat K, et al. 3D visualization of extracellular vesicle uptake by endothelial cells. Cellular & Molecular Biology Letters 2018;23(1), doi:10.1186/s11658-018-0123-z
79. Huber J, Griffin MF, Longaker MT, et al. Exosomes: A Tool for Bone Tissue Engineering. Tissue Engineering Part B: Reviews 2022;28(1):101-113
80. Aktas E, Chamberlain CS, Saether EE, et al. Immune modulation with primed mesenchymal stem cells delivered via biodegradable scaffold to repair an Achilles tendon segmental defect. J Orthop Res 2017;35(2):269-280, doi:10.1002/jor.23258
81. Chamberlain CS, Saether EE, Aktas E, et al. Mesenchymal Stem Cell Therapy on Tendon/Ligament Healing. J Cytokine Biol 2017;2(1):

82. Saether EE, Chamberlain CS, Aktas E, et al. Primed Mesenchymal Stem Cells Alter and Improve Rat Medial Collateral Ligament Healing. Stem Cell Reviews and Reports 2016;12(1):42-53, doi:10.1007/s12015-015-9633-5
83. Zhang M, Liu H, Cui Q, et al. Tendon stem cell-derived exosomes regulate inflammation and promote the high-quality healing of injured tendon. Stem Cell Research & Therapy 2020;11(1):402, doi:10.1186/s13287-020-01918-x
84. Connor DE, Paulus JA, Dabestani PJ, et al. Therapeutic potential of exosomes in rotator cuff tendon healing. Journal of Bone and Mineral Metabolism 2019;37(5):759-767, doi:10.1007/s00774-019-01013-z
85. Li Z, Li Q, Tong K, et al. BMSC-derived exosomes promote tendon-bone healing after anterior cruciate ligament reconstruction by regulating M1/M2 macrophage polarization in rats. Stem Cell Research & Therapy 2022;13(1), doi:10.1186/s13287-022-02975-0
86. Zhang G, Zhou X, Hu S, et al. Large animal models for the study of tendinopathy. Front Cell Dev Biol 2022;10(1031638, doi:10.3389/fcell.2022.1031638
87. Mathewson MA, Kwan A, Eng CM, et al. Comparison of rotator cuff muscle architecture between humans and other selected vertebrate species. J Exp Biol 2014;217(Pt 2):261-73, doi:10.1242/jeb.083923
88. Turner AS. Experiences with sheep as an animal model for shoulder surgery: Strengths and shortcomings. Journal of Shoulder and Elbow Surgery 2007;16(5, Supplement):S158-S163, doi:https://doi.org/10.1016/j.jse.2007.03.002
89. Quirke LD, Maclean PH, Haack NA, et al. Characterization of local and peripheral immune system in pregnant and nonpregnant ewes. Journal of Animal Science 2021;99(8), doi:10.1093/jas/skab208
90. Cisek R, Joseph A, Harvey M, et al. Polarization-Sensitive Second Harmonic Generation Microscopy for Investigations of Diseased Collagenous Tissues. Frontiers in Physics 2021;9(726996
91. Durgam S, Singh B, Brokken M, et al. Second Harmonic Generation (SHG) Imaging of Equine Flexor Tendon Fascicular Structure during Healing. Veterinary and Comparative Orthopaedics and Traumatology 2019;32(S 03):A3754
92. Durgam S, Singh B, Cole SL, et al. Quantitative assessment of tendon hierarchical structure by combined second harmonic generation and immunofluorescence microscopy. Tissue Engineering Part C: Methods 2020;26(5):253-262
93. Harrison AK, Flatow EL. Subacromial Impingement Syndrome. JAAOS - Journal of the American Academy of Orthopaedic Surgeons 2011;19(11):701-708
94. Leong NL, Kator JL, Clemens TL, et al. Tendon and Ligament Healing and Current Approaches to Tendon and Ligament Regeneration. J Orthop Res 2020;38(1):7-12, doi:10.1002/jor.24475
95. Sambandam SN. Rotator cuff tears: An evidence based approach. World Journal of Orthopedics 2015;6(11):902, doi:10.5312/wjo.v6.i11.902
96. Wall ME, Dyment NA, Bodle J, et al. Cell Signaling in Tenocytes: Response to Load and Ligands in Health and Disease. In: Springer International Publishing: 2016; pp. 79-95.
97. Friedl P, Gilmour D. Collective cell migration in morphogenesis, regeneration and cancer. Nature Reviews Molecular Cell Biology 2009;10(7):445-457, doi:10.1038/nrm2720
98. Galatz LM, Sandell LJ, Rothermich SY, et al. Characteristics of the rat supraspinatus tendon during tendon-to-bone healing after acute injury. Journal of Orthopaedic Research 2006;24(3):541-550, doi:10.1002/jor.20067

99. Wang C, Zhang Y, Zhang G, et al. Adipose Stem Cell–Derived Exosomes Ameliorate Chronic Rotator Cuff Tendinopathy by Regulating Macrophage Polarization: From a Mouse Model to a Study in Human Tissue. The American Journal of Sports Medicine 2021;49(9):2321-2331, doi:10.1177/03635465211020010
100. Saether EE, Chamberlain CS, Aktas E, et al. Primed Mesenchymal Stem Cells Alter and Improve Rat Medial Collateral Ligament Healing. Stem Cell Rev Rep 2016;12(1):42-53, doi:10.1007/s12015-015-9633-5
101. Zhang M, Liu H, Cui Q, et al. Tendon stem cell-derived exosomes regulate inflammation and promote the high-quality healing of injured tendon. Stem Cell Research & Therapy 2020;11(1), doi:10.1186/s13287-020-01918-x
102. Doornaert M, De Maere E, Colle J, et al. Xenogen-free isolation and culture of human adipose mesenchymal stem cells. Stem Cell Research 2019;40(101532
103. Bi Y, Ehirchiou D, Kilts TM, et al. Identification of tendon stem/progenitor cells and the role of the extracellular matrix in their niche. Nature Medicine 2007;13(10):1219-1227, doi:10.1038/nm1630
104. Yang J, Zhao Q, Wang K, et al. Isolation, culture and biological characteristics of multipotent porcine tendon-derived stem cells. International Journal of Molecular Medicine 2018;41(6):3611-3619
105. Yao L, Bestwick C, Bestwick LA, et al. Phenotypic drift in human tenocyte culture. Tissue engineering 2006;12(7):1843-1849
106. Davies JQ, Gordon S. Isolation and culture of human macrophages. In: Basic cell culture protocols. Springer: 2005; pp. 105-116.
107. Ying W, Cheruku PS, Bazer FW, et al. Investigation of Macrophage Polarization Using Bone Marrow Derived Macrophages. Journal of Visualized Experiments 2013;76), doi:10.3791/50323
108. Liu J, Rashid M, Wang J, et al. Theileria annulata transformation altered cell surface molecules expression and endocytic function of monocyte-derived dendritic cells. Ticks and tick-borne diseases 2020;11(3):101365
109. Kobelt D, Walther W, Stein US. Real-Time Cell Migration Monitoring to Analyze Drug Synergism in the Scratch Assay Using the IncuCyte System. In: Springer US: 2021; pp. 133-142.
110. Mathivanan S, Ji H, Simpson RJ. Exosomes: Extracellular organelles important in intercellular communication. Journal of Proteomics 2010;73(10):1907-1920, doi:https://doi.org/10.1016/j.jprot.2010.06.006
111. Willms E, Johansson HJ, Mäger I, et al. Cells release subpopulations of exosomes with distinct molecular and biological properties. Scientific Reports 2016;6(1):22519, doi:10.1038/srep22519
112. Tohyama H, Yasuda K, Uchida H, et al. The responses of extrinsic fibroblasts infiltrating the devitalised patellar tendon to IL-1β are different from those of normal tendon fibroblasts. The Journal of Bone and Joint Surgery British volume 2007;89-B(9):1261-1267, doi:10.1302/0301-620x.89b9.18053
113. Postlethwaite AE, Lachman LB, Kang AH. Induction of fibroblast proliferation by interleukin-1 derived from human monocytic leukemia cells. Arthritis & Rheumatism 1984;27(9):995-1001, doi:10.1002/art.1780270905
114. Artlett CM. The IL-1 family of cytokines. Do they have a role in scleroderma fibrosis? Immunology Letters 2018;195(30-37, doi:https://doi.org/10.1016/j.imlet.2017.11.012

115. Shen H, Yoneda S, Abu-Amer Y, et al. Stem cell-derived extracellular vesicles attenuate the early inflammatory response after tendon injury and repair. Journal of Orthopaedic Research 2020;38(1):117-127, doi:10.1002/jor.24406
116. Çıraklı A. Tranexamic acid has positive effect in early period of tendon healing by stimulating the tumor necrosis factor-alpha and matrix metalloproteinase-3 expression levels. Joint Diseases and Related Surgery 2020;31(3):463-469, doi:10.5606/ehc.2020.74265
117. Bian X, Liu T, Yang M, et al. The absence of oestrogen receptor beta disturbs collagen I type deposition during Achilles tendon healing by regulating the IRF5-CCL3 axis. Journal of Cellular and Molecular Medicine 2020;24(17):9925-9935, doi:10.1111/jcmm.15592
118. Stålman A, Bring D, Ackermann PW. Chemokine expression of CCL2, CCL3, CCL5 and CXCL10 during early inflammatory tendon healing precedes nerve regeneration: an immunohistochemical study in the rat. Knee Surgery, Sports Traumatology, Arthroscopy 2015;23(9):2682-2689, doi:10.1007/s00167-014-3010-9
119. Ackermann PW, Domeij-Arverud E, Leclerc P, et al. Anti-inflammatory cytokine profile in early human tendon repair. Knee surgery, sports traumatology, arthroscopy 2013;21(8):1801-1806
120. Lin TW, Cardenas L, Glaser DL, et al. Tendon healing in interleukin-4 and interleukin-6 knockout mice. Journal of Biomechanics 2006;39(1):61-69, doi:10.1016/j.jbiomech.2004.11.009
121. Panzer S, Madden M, Matsuki K. Interaction of IL-1β, IL-6 and tumour necrosis factor-alpha (TNF-α) in human T cells activated by murine antigens. Clinical & Experimental Immunology 1993;93(3):471-478, doi:10.1111/j.1365-2249.1993.tb08203.x
122. Millar NL, Akbar M, Campbell AL, et al. IL-17A mediates inflammatory and tissue remodelling events in early human tendinopathy. Scientific Reports 2016;6(1):27149, doi:10.1038/srep27149
123. Li LX, Xia YT, Sun XY, et al. CXCL-10/CXCR3 in macrophages regulates tissue repair by controlling the expression of Arg1, VEGFa and TNFα. J Biol Regul Homeost Agents 2020;34(3):987-999, doi:10.23812/20-59-a-65
124. Ricchetti ET, Reddy SC, Ansorge HL, et al. Effect of Interleukin-10 Overexpression on the Properties of Healing Tendon in a Murine Patellar Tendon Model. The Journal of Hand Surgery 2008;33(10):1843-1852, doi:10.1016/j.jhsa.2008.07.020
125. Dakin SG, Martinez FO, Yapp C, et al. Inflammation activation and resolution in human tendon disease. Science Translational Medicine 2015;7(311):311ra173-311ra1, doi:10.1126/scitranslmed.aac4269
126. Arvind V, Huang AH. Reparative and Maladaptive Inflammation in Tendon Healing. Frontiers in Bioengineering and Biotechnology 2021;9(625), doi:10.3389/fbioe.2021.719047
127. Deng G, Li K, Chen S, et al. Interleukin-10 promotes proliferation and migration, and inhibits tendon differentiation via the JAK/Stat3 pathway in tendon-derived stem cells in□vitro. Molecular Medicine Reports 2018, doi:10.3892/mmr.2018.9547
128. Ezura Y, Chakravarti S, Oldberg Å, et al. Differential Expression of Lumican and Fibromodulin Regulate Collagen Fibrillogenesis in Developing Mouse Tendons. Journal of Cell Biology 2000;151(4):779-788, doi:10.1083/jcb.151.4.779
129. Bridgewood C, Sharif K, Sherlock J, et al. Interleukin-23 pathway at the enthesis: The emerging story of enthesitis in spondyloarthropathy. Immunological Reviews 2020;294(1):27-47, doi:10.1111/imr.12840
130. Yang J, Yu X, Li Y, et al. Decreased HSP70 expression on serum exosomes contributes to cardiac fibrosis during senescence. Eur Rev Med Pharmacol Sci 2019;23(9):3993-4001

131. Sambandam SN, Khanna V, Gul A, et al. Rotator cuff tears: An evidence based approach. World J Orthop 2015;6(11):902-18, doi:10.5312/wjo.v6.i11.902
132. Howell KL, Kaji DA, Li TM, et al. Macrophage depletion impairs neonatal tendon regeneration. The FASEB Journal 2021;35(6), doi:10.1096/fj.202100049r
133. Ellis IM, Schnabel LV, Berglund AK. Defining the profile: Characterizing cytokines in tendon injury to improve clinical therapy. Journal of Immunology and Regenerative Medicine 2022;16(100059, doi:https://doi.org/10.1016/j.regen.2022.100059
134. Sarhadi VK, Daddali R, Seppänen-Kaijansinkko R. Mesenchymal Stem Cells and Extracellular Vesicles in Osteosarcoma Pathogenesis and Therapy. International Journal of Molecular Sciences 2021;22(20):11035
135. Johnson J, von Stade D, Gadomski B, et al. Biomechanical and histological changes secondary to aging in the human rotator cuff: A preliminary analysis. J Orthop Res 2023;41(10):2221-2231, doi:10.1002/jor.25529
136. Davies JQ, Gordon S. Isolation and culture of murine macrophages. Basic cell culture protocols 2005;91-103
137. Ying W, Cheruku PS, Bazer FW, et al. Investigation of macrophage polarization using bone marrow derived macrophages. J Vis Exp 2013;76), doi:10.3791/50323
138. Kobelt D, Walther W, Stein US. Real-Time Cell Migration Monitoring to Analyze Drug Synergism in the Scratch Assay Using the IncuCyte System. Methods Mol Biol 2021;2294(133-142, doi:10.1007/978-1-0716-1350-4_9
139. Yeruva S, Ramadori G, Raddatz D. NF-κB-dependent synergistic regulation of CXCL10 gene expression by IL-1β and IFN-γ in human intestinal epithelial cell lines. International Journal of Colorectal Disease 2008;23(3):305-317, doi:10.1007/s00384-007-0396-6
140. Kendal AR, Layton T, Al-Mossawi H, et al. Multi-omic single cell analysis resolves novel stromal cell populations in healthy and diseased human tendon. Scientific Reports 2020;10(1), doi:10.1038/s41598-020-70786-5
141. Best KT, Lee FK, Knapp E, et al. Deletion of NFKB1 enhances canonical NF-κB signaling and increases macrophage and myofibroblast content during tendon healing. Scientific Reports 2019;9(1), doi:10.1038/s41598-019-47461-5
142. Marsolais D, Côté CH, Frenette J. Pifithrin-α, an inhibitor of p53 transactivation, alters the inflammatory process and delays tendon healing following acute injury. American Journal of Physiology-Regulatory, Integrative and Comparative Physiology 2007;292(1):R321-R327, doi:10.1152/ajpregu.00411.2005
143. Xu Z, Yoshida T, Wu L, et al. Transcription Factor MEF2C Suppresses Endothelial Cell Inflammation via Regulation of NF-κB and KLF2. Journal of Cellular Physiology 2015;230(6):1310-1320, doi:10.1002/jcp.24870
144. Kim DH, Park JW, Jeong HO, et al. Novel Role of Lck in Leptin-Induced Inflammation and Implications for Renal Aging. Aging and disease 2019;10(6):1174, doi:10.14336/ad.2019.0218
145. Lv M, He F, Guo J, et al. Identification of hub genes correlated with tumor-associated M1-like macrophage infiltration in soft tissue sarcomas. Frontiers in Genetics 2022;13(doi:10.3389/fgene.2022.999966
146. Defour A, Medikayala S, Van Der Meulen JH, et al. Annexin A2 links poor myofiber repair with inflammation and adipogenic replacement of the injured muscle. Human Molecular Genetics 2017;26(11):1979-1991, doi:10.1093/hmg/ddx065

147. Fujii T, Murata K, Mun S-H, et al. MEF2C regulates osteoclastogenesis and pathologic bone resorption via c-FOS. Bone Research 2021;9(1), doi:10.1038/s41413-020-00120-2
148. Hasegawa T, Kikuta J, Sudo T, et al. Identification of a novel arthritis-associated osteoclast precursor macrophage regulated by FoxM1. Nature Immunology 2019;20(12):1631-1643, doi:10.1038/s41590-019-0526-7
149. Miao J, Yao H, Liu J, et al. Inhibition of KIF11 ameliorates osteoclastogenesis via regulating mTORC1-mediated NF-κB signaling. Biochemical Pharmacology 2023;217(115817, doi:https://doi.org/10.1016/j.bcp.2023.115817
150. Udagawa N, Takahashi N, Katagiri T, et al. Interleukin (IL)-6 induction of osteoclast differentiation depends on IL-6 receptors expressed on osteoblastic cells but not on osteoclast progenitors. The Journal of experimental medicine 1995;182(5):1461-1468, doi:10.1084/jem.182.5.1461
151. Yoshida S, Ikedo A, Yanagihara Y, et al. Bub1 suppresses inflammatory arthritis–associated bone loss in mice through inhibition of TNFα–mediated osteoclastogenesis. Journal of Bone and Mineral Research 2024, doi:10.1093/jbmr/zjae015
152. Muir AM, Ren Y, Butz DH, et al. Induced ablation of Bmp1 and Tll1 produces osteogenesis imperfecta in mice. Hum Mol Genet 2014;23(12):3085-101, doi:10.1093/hmg/ddu013
153. Wang J, Xue Y, Wang Y, et al. BMP-2 functional polypeptides relieve osteolysis via bi-regulating bone formation and resorption coupled with macrophage polarization. npj Regenerative Medicine 2023;8(1), doi:10.1038/s41536-023-00279-2
154. Wei F, Zhou Y, Wang J, et al. The Immunomodulatory Role of BMP-2 on Macrophages to Accelerate Osteogenesis. Tissue Engineering Part A 2018;24(7-8):584-594, doi:10.1089/ten.tea.2017.0232
155. Ramachandran A, Gong EM, Pelton K, et al. FosB Regulates Stretch-Induced Expression of Extracellular Matrix Proteins in Smooth Muscle. The American Journal of Pathology 2011;179(6):2977-2989, doi:10.1016/j.ajpath.2011.08.034
156. Kimura A, Kitajima M, Nishida K, et al. NQO1 inhibits the TLR-dependent production of selective cytokines by promoting IκB-ζ degradation. Journal of Experimental Medicine 2018;215(8):2197-2209, doi:10.1084/jem.20172024
157. Kobayashi EH, Suzuki T, Funayama R, et al. Nrf2 suppresses macrophage inflammatory response by blocking proinflammatory cytokine transcription. Nature Communications 2016;7(1):11624, doi:10.1038/ncomms11624
158. Lui PPY, Zhang X, Yao S, et al. Roles of Oxidative Stress in Acute Tendon Injury and Degenerative Tendinopathy—A Target for Intervention. International Journal of Molecular Sciences 2022;23(7):3571, doi:10.3390/ijms23073571
159. Ross D, Siegel D. The diverse functionality of NQO1 and its roles in redox control. Redox Biol 2021;41(101950, doi:10.1016/j.redox.2021.101950
160. Vriend J, Reiter RJ. The Keap1-Nrf2-antioxidant response element pathway: A review of its regulation by melatonin and the proteasome. Molecular and Cellular Endocrinology 2015;401(213-220, doi:https://doi.org/10.1016/j.mce.2014.12.013
161. Wang Y, Tang B, Li H, et al. A small-molecule inhibitor of Keap1-Nrf2 interaction attenuates sepsis by selectively augmenting the antibacterial defence of macrophages at infection sites. EBioMedicine 2023;90(104480, doi:10.1016/j.ebiom.2023.104480
162. Lee S-H, Kim T-S, Choi Y-W, et al. Osteoimmunology: cytokines and the skeletal system. BMB Reports 2008;41(7):495-510, doi:10.5483/bmbrep.2008.41.7.495

163. Fu S, Wang Y, Xia X, et al. Exosome engineering: Current progress in cargo loading and targeted delivery. NanoImpact 2020;20(100261
164. Alvarez-Erviti L, Seow Y, Yin H, et al. Delivery of siRNA to the mouse brain by systemic injection of targeted exosomes. Nature biotechnology 2011;29(4):341-345
165. Yu Y, Sun B, Wang Z, et al. Exosomes from M2 macrophage promote peritendinous fibrosis posterior tendon injury via the MiR-15b-5p/FGF-1/7/9 pathway by delivery of circRNA-Ep400. Frontiers in Cell and Developmental Biology 2021;9(595911
166. Blaser MC, Aikawa E. Differential miRNA Loading Underpins Dual Harmful and Protective Roles for Extracellular Vesicles in Atherogenesis. Circulation Research 2019;124(4):467-469, doi:10.1161/circresaha.119.314596
167. Cui J, Zhang Y-J, Li X, et al. Decellularized tendon scaffolds loaded with collagen targeted extracellular vesicles from tendon-derived stem cells facilitate tendon regeneration. Journal of Controlled Release 2023;360(842-857, doi:https://doi.org/10.1016/j.jconrel.2023.07.032
168. Johnson J, von Stade D, Regan D, et al. Enthesis trauma as a means for the development of translatable chronic rotator cuff degeneration in an ovine model. Ann Transl Med 2021;9(9):741, doi:10.21037/atm-21-354
169. Raposo G, Stoorvogel W. Extracellular vesicles: exosomes, microvesicles, and friends. J Cell Biol 2013;200(4):373-83, doi:10.1083/jcb.201211138
170. Abels ER, Breakefield XO. Introduction to Extracellular Vesicles: Biogenesis, RNA Cargo Selection, Content, Release, and Uptake. Cell Mol Neurobiol 2016;36(3):301-12, doi:10.1007/s10571-016-0366-z
171. van Niel G, D'Angelo G, Raposo G. Shedding light on the cell biology of extracellular vesicles. Nat Rev Mol Cell Biol 2018;19(4):213-228, doi:10.1038/nrm.2017.125
172. Zhang J, Li S, Li L, et al. Exosome and exosomal microRNA: trafficking, sorting, and function. Genomics Proteomics Bioinformatics 2015;13(1):17-24, doi:10.1016/j.gpb.2015.02.001
173. Tiruvayipati S, Wolfgeher D, Yue M, et al. Variability in protein cargo detection in technical and biological replicates of exosome-enriched extracellular vesicles. PLOS ONE 2020;15(3):e0228871, doi:10.1371/journal.pone.0228871
174. von Stade D, Meyers M, Johnson J, et al. Exosome Cell Origin Affects In Vitro Markers of Tendon Repair in Ovine Macrophages and Tenocytes. Tissue Eng Part A 2023, doi:10.1089/ten.TEA.2022.0185
175. Wang T, Larcher LM, Ma L, et al. Systematic Screening of Commonly Used Commercial Transfection Reagents towards Efficient Transfection of Single-Stranded Oligonucleotides. Molecules 2018;23(10), doi:10.3390/molecules23102564
176. Li Z, Li Q, Tong K, et al. BMSC-derived exosomes promote tendon-bone healing after anterior cruciate ligament reconstruction by regulating M1/M2 macrophage polarization in rats. Stem Cell Research & Therapy 2022;13(1):295, doi:10.1186/s13287-022-02975-0
177. Sung BH, von Lersner A, Guerrero J, et al. A live cell reporter of exosome secretion and uptake reveals pathfinding behavior of migrating cells. Nature Communications 2020;11(1):2092, doi:10.1038/s41467-020-15747-2
178. Luan X, Sansanaphongpricha K, Myers I, et al. Engineering exosomes as refined biological nanoplatforms for drug delivery. Acta Pharmacologica Sinica 2017;38(6):754-763, doi:10.1038/aps.2017.12
179. Lennaárd AJ, Mamand DR, Wiklander RJ, et al. Optimised Electroporation for Loading of Extracellular Vesicles with Doxorubicin. Pharmaceutics 2021;14(1):38, doi:10.3390/pharmaceutics14010038

180. Barile L, Vassalli G. Exosomes: Therapy delivery tools and biomarkers of diseases. Pharmacol Ther 2017;174(63-78, doi:10.1016/j.pharmthera.2017.02.020
181. Yamashita T, Takahashi Y, Takakura Y. Possibility of Exosome-Based Therapeutics and Challenges in Production of Exosomes Eligible for Therapeutic Application. Biol Pharm Bull 2018;41(6):835-842, doi:10.1248/bpb.b18-00133
182. Quesenberry PJ, Aliotta J, Deregibus MC, et al. Role of extracellular RNA-carrying vesicles in cell differentiation and reprogramming. Stem Cell Res Ther 2015;6(153, doi:10.1186/s13287-015-0150-x
183. Ohno S, Drummen GP, Kuroda M. Focus on Extracellular Vesicles: Development of Extracellular Vesicle-Based Therapeutic Systems. Int J Mol Sci 2016;17(2):172, doi:10.3390/ijms17020172
184. Zhang B, Yeo RW, Tan KH, et al. Focus on Extracellular Vesicles: Therapeutic Potential of Stem Cell-Derived Extracellular Vesicles. Int J Mol Sci 2016;17(2):174, doi:10.3390/ijms17020174
185. Rani S, Ryan AE, Griffin MD, et al. Mesenchymal Stem Cell-derived Extracellular Vesicles: Toward Cell-free Therapeutic Applications. Mol Ther 2015;23(5):812-823, doi:10.1038/mt.2015.44
186. Turner AS. Experiences with sheep as an animal model for shoulder surgery: strengths and shortcomings. J Shoulder Elbow Surg 2007;16(5 Suppl):S158-63, doi:10.1016/j.jse.2007.03.002
187. Jenner F, Wagner A, Gerner I, et al. Evaluation of the Potential of Umbilical Cord Mesenchymal Stromal Cell-Derived Small Extracellular Vesicles to Improve Rotator Cuff Healing: A Pilot Ovine Study. Am J Sports Med 2023;51(2):331-342, doi:10.1177/03635465221145958
188. Chamberlain CS, Kink JA, Wildenauer LA, et al. Exosome-educated macrophages and exosomes differentially improve ligament healing. Stem Cells 2021;39(1):55-61, doi:10.1002/stem.3291
189. Sloas C, Gill S, Klichinsky M. Engineered CAR-Macrophages as Adoptive Immunotherapies for Solid Tumors. Front Immunol 2021;12(783305, doi:10.3389/fimmu.2021.783305
190. Fang F, Lake SP. Experimental evaluation of multiscale tendon mechanics. Journal of Orthopaedic Research 2017;35(7):1353-1365, doi:10.1002/jor.23488
191. Lui PPY. Mesenchymal Stem Cell-Derived Extracellular Vesicles for the Promotion of Tendon Repair - an Update of Literature. Stem Cell Reviews and Reports 2021;17(2):379-389, doi:10.1007/s12015-020-10023-8
192. Tsuzaki M, Guyton G, Garrett W, et al. IL-1β induces COX2, MMP-1, -3 and -13, ADAMTS-4, IL-1β and IL-6 in human tendon cells. Journal of Orthopaedic Research 2003;21(2):256-264, doi:10.1016/s0736-0266(02)00141-9
193. Archambault J, Tsuzaki M, Herzog W, et al. Stretch and interleukin-1β induce matrix metalloproteinases in rabbit tendon cells in vitro. Journal of Orthopaedic Research 2002;20(1):36-39, doi:10.1016/s0736-0266(01)00075-4
194. Jo CH, Lim H-J, Yoon KS. Characterization of tendon-specific markers in various human tissues, tenocytes and mesenchymal stem cells. Tissue engineering and regenerative medicine 2019;16(2):151-159
195. Veldman-Jones MH, Brant R, Rooney C, et al. Evaluating Robustness and Sensitivity of the NanoString Technologies nCounter Platform to Enable Multiplexed Gene Expression Analysis

of Clinical Samples. Cancer Research 2015;75(13):2587-2593, doi:10.1158/0008-5472.can-15-0262
196. Keller LE, Fortier LA, Delco ML, et al. High-Plex RNA Expression Profiling of Formalin-Fixed Paraffin-Embedded Synovial Membrane Indicates Potential Mechanism of Mesenchymal Stromal Cells in the Mitigation of Posttraumatic Osteoarthritis. CARTILAGE 2021;13(2_suppl):1200S-1203S, doi:10.1177/1947603521993521
197. Eager JM, Warrender WJ, Deusenbery CB, et al. Distinct Gene Expression Profile in Patients With Poor Postoperative Outcomes After Rotator Cuff Repair: A Case-Control Study. The American Journal of Sports Medicine 2021;49(10):2760-2770, doi:10.1177/03635465211023212
198. Franchi M, Fini M, Quaranta M, et al. Crimp morphology in relaxed and stretched rat Achilles tendon. J Anat 2007;210(1):1-7, doi:10.1111/j.1469-7580.2006.00666.x
199. Zhu J, Zhang X, Ma Y, et al. Ultrastructural and Morphological Characteristics of Human Anterior Cruciate Ligament and Hamstring Tendons. The Anatomical Record: Advances in Integrative Anatomy and Evolutionary Biology 2012;295(9):1430-1436, doi:10.1002/ar.22527
200. Xu M, Liu J, Sun J, et al. Optical Microscopy and Electron Microscopy for the Morphological Evaluation of Tendons: A Mini Review. Orthopaedic Surgery 2020;12(2):366-371, doi:10.1111/os.12637
201. Maitland DJ, Walsh JT. Quantitative measurements of linear birefringence during heating of native collagen. Lasers in Surgery and Medicine 1997;20(3):310-318, doi:10.1002/(sici)1096-9101(1997)20:3<310::aid-lsm10>3.0.co;2-h
202. Blair MJ, Quinn KP. Single shot quantitative polarized light imaging system for rapid planar biaxial testing of soft tissues. Frontiers in Bioengineering and Biotechnology 2022;10(doi:10.3389/fbioe.2022.1010307
203. Shribak M. Polychromatic polarization microscope: bringing colors to a colorless world. Scientific reports 2015;5(1):1-10
204. Costantini I, Cicchi R, Silvestri L, et al. In-vivo and ex-vivo optical clearing methods for biological tissues: review. Biomedical Optics Express 2019;10(10):5251, doi:10.1364/boe.10.005251
205. Hohmann E, Keough N, Glatt V, et al. The mechanical properties of fresh versus fresh/frozen and preserved (Thiel and Formalin) long head of biceps tendons: a cadaveric investigation. Annals of Anatomy-Anatomischer Anzeiger 2019;221(186-191
206. Gerson CJ, Goldstein S, Heacox AE. Retained structural integrity of collagen and elastin within cryopreserved human heart valve tissue as detected by two-photon laser scanning confocal microscopy. Cryobiology 2009;59(2):171-179
207. ELZINGA PA, FRED E. Pump/Probe Spectroscopy by Asynchronous Optical Sampling. 1987;
208. Wang E, Specht KS, Chicco AJ, et al. High-Repetition-Rate Transient Absorption Spectroscopy of Respiratory Supercomplexes. The Journal of Physical Chemistry B 2022;126(7):1404-1412, doi:10.1021/acs.jpcb.1c08714
209. Theodossiou T, Thrasivoulou C, Ekwobi C, et al. Second harmonic generation confocal microscopy of collagen type I from rat tendon cryosections. BIOPHYS J 2006;91(12):4665-4677
210. Williams RM, Zipfel WR, Webb WW. Interpreting second-harmonic generation images of collagen I fibrils. Biophysical journal 2005;88(2):1377-1386
211. Lee W, Rahman H, Kersh ME, et al. Application of quantitative second-harmonic generation microscopy to posterior cruciate ligament for crimp analysis studies. Journal of biomedical optics 2017;22(4):046009-046009

212. Pang X, Wu JP, Allison GT, et al. Three dimensional microstructural network of elastin, collagen, and cells in Achilles tendons. Journal of Orthopaedic Research 2017;35(6):1203-1214, doi:10.1002/jor.23240
213. Li H, Yan M, Yu J, et al. In vivo identification of arteries and veins using two-photon excitation elastin autofluorescence. Journal of Anatomy 2020;236(1):171-179, doi:10.1111/joa.13080

APPENDIX

Supplemental Data

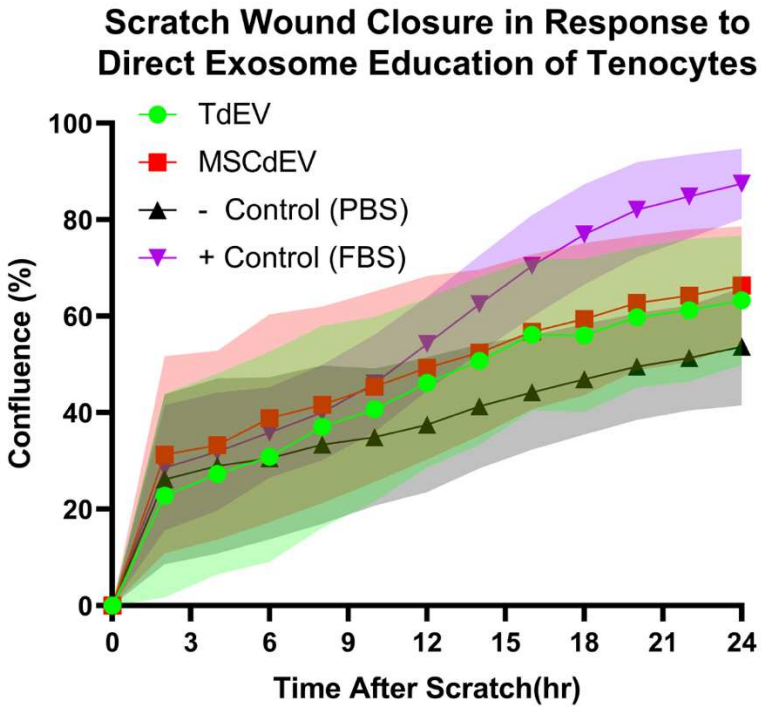

Supplemental Figure 1. Scratch wound closure over 24hours per treatment with Tenocytes treated directly with TdEVs, MSCdEVs, PBS negative control or 10%FBS positive control. There was no significant difference between experimental groups, though both EV treated groups demonstrated greater wound closure than the negative control and less than the positive control at the 15-24hour time points.